Lecture 12. Vertebrate genetic models and screens

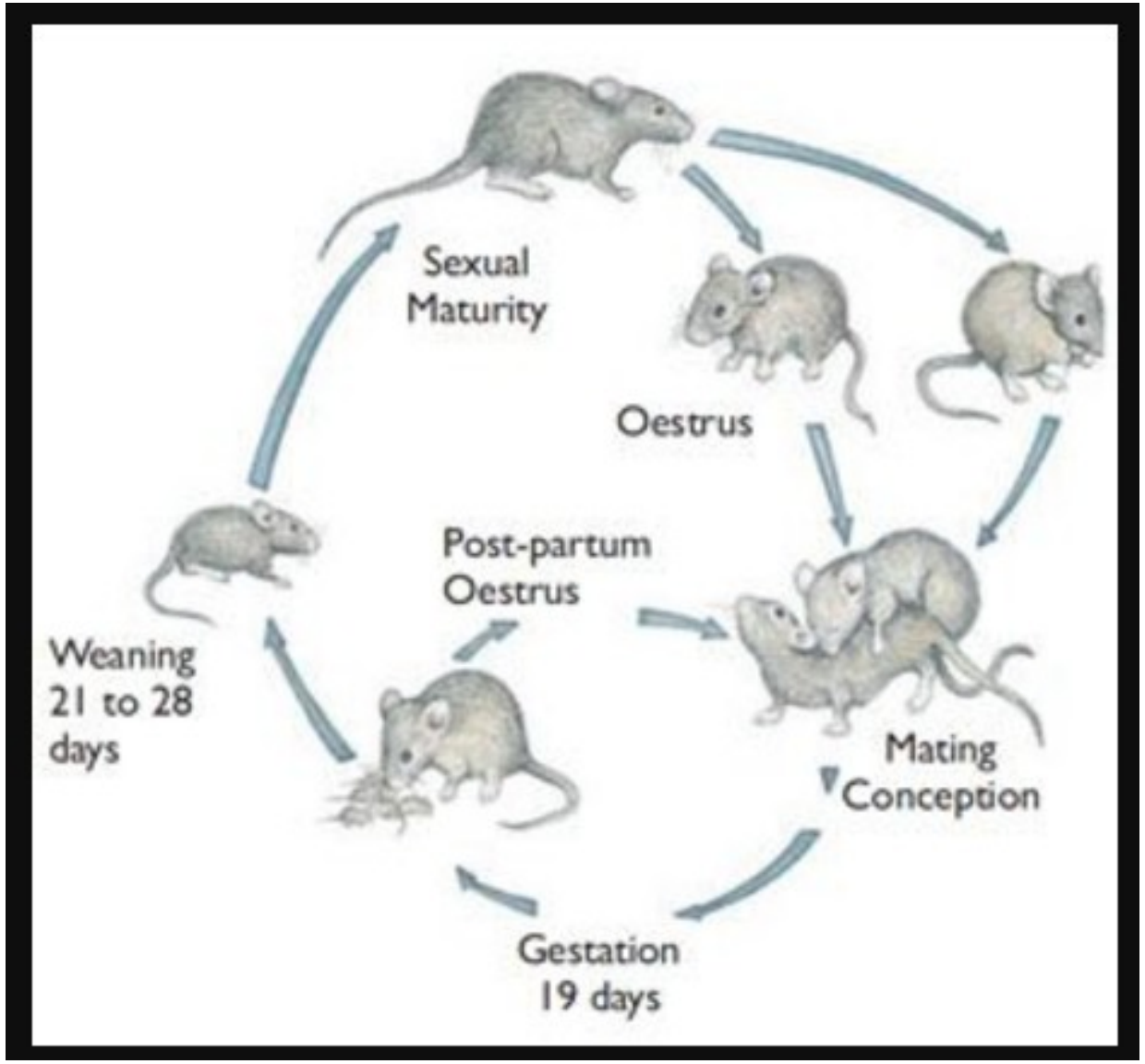

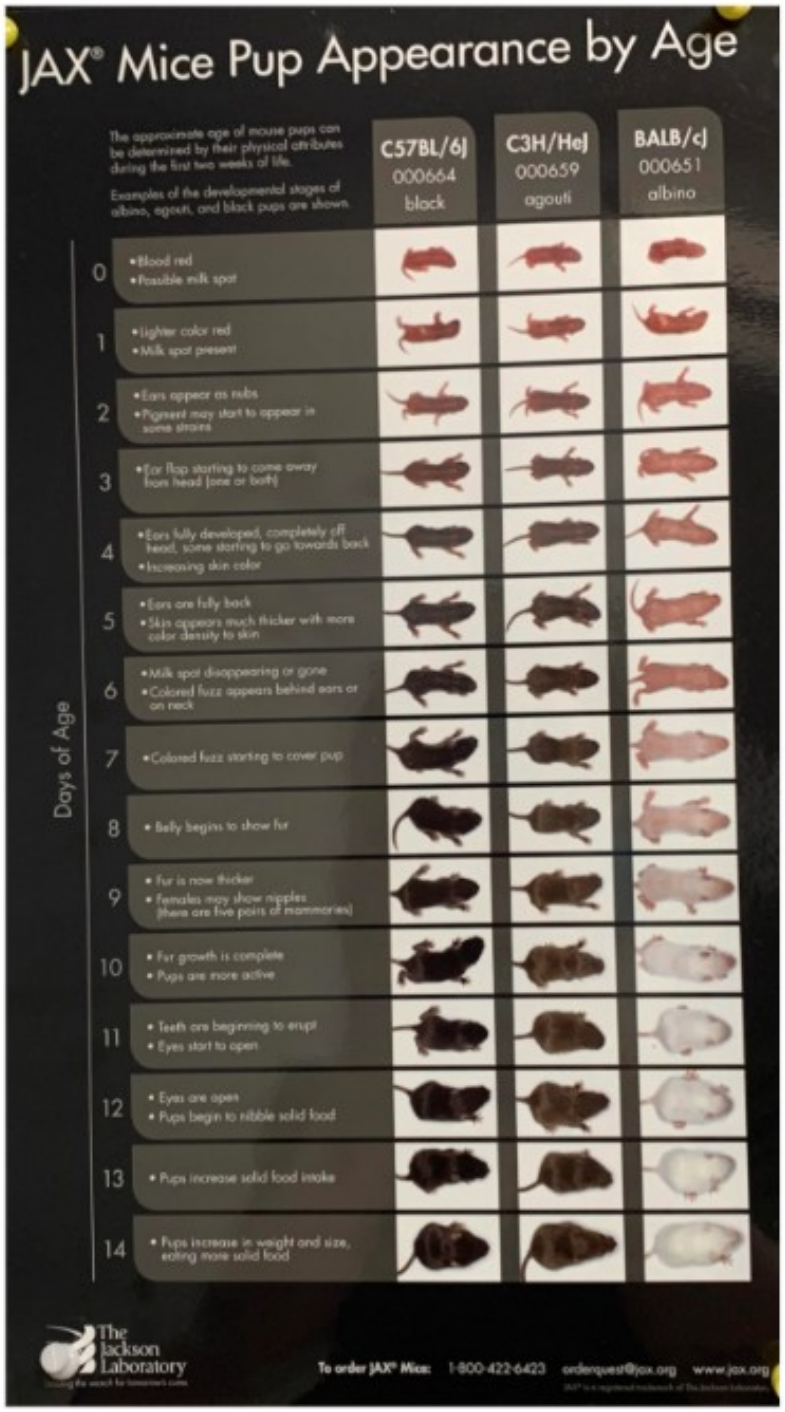

[Appearance of the vagina in proestrus]

Mate with
vasectomized male

[Vaginal plug]

Mouse Development

Embryonic Stages

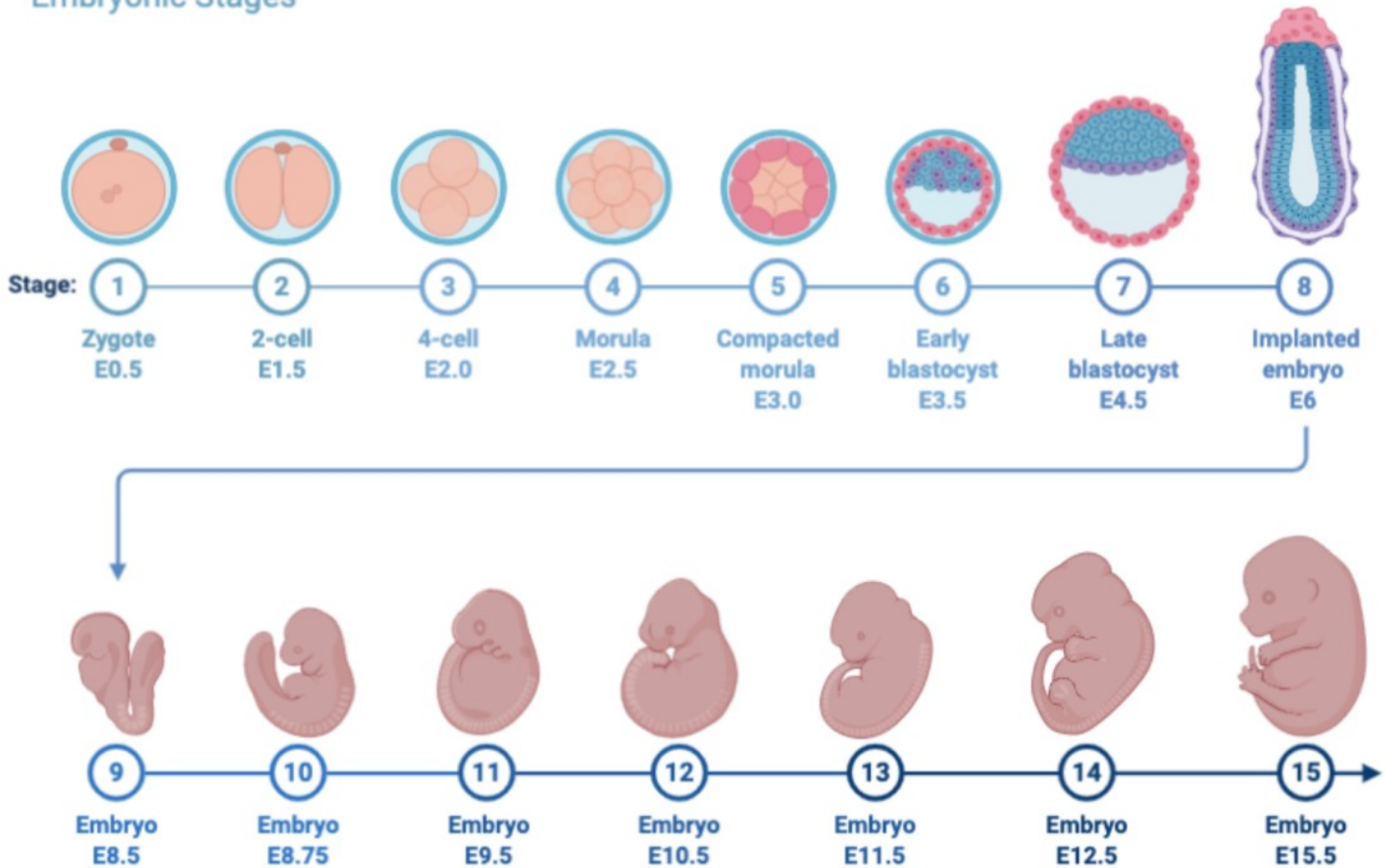

Zebrafish genetic model

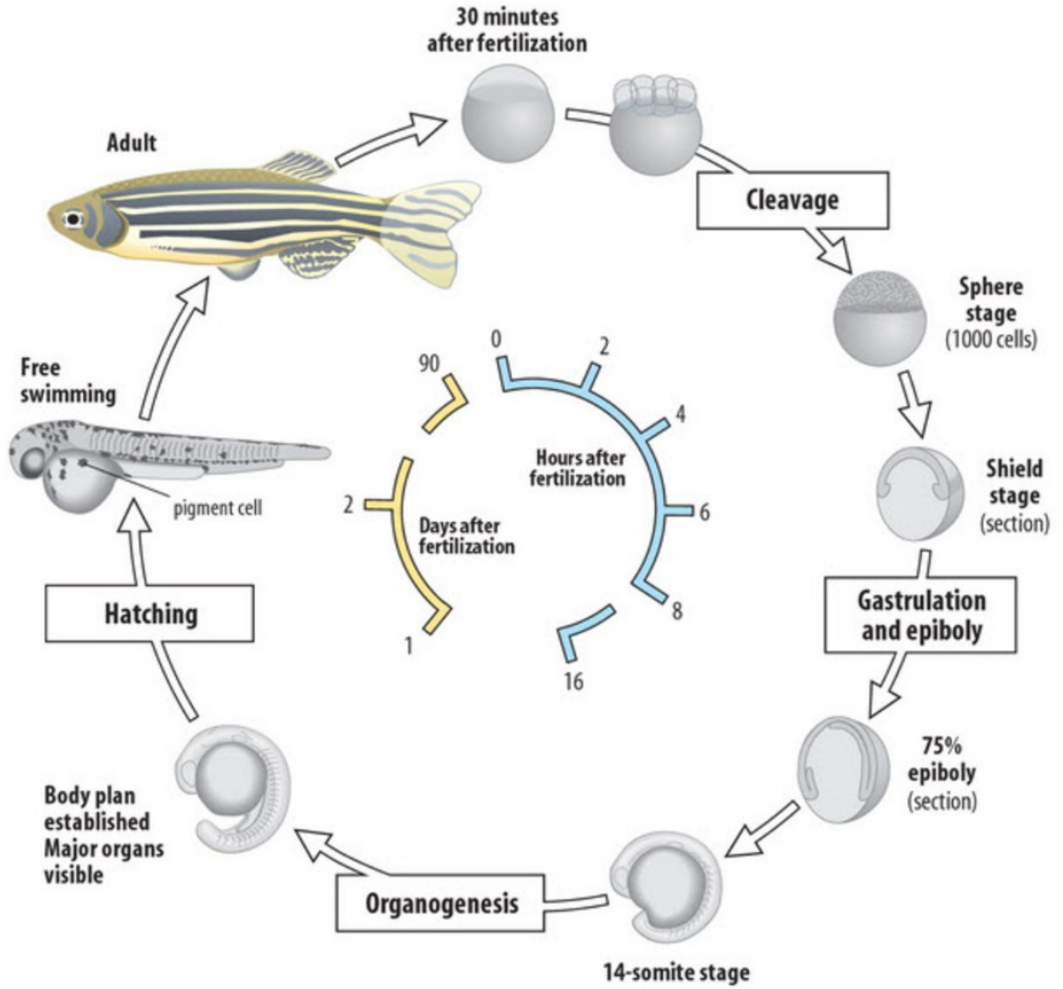

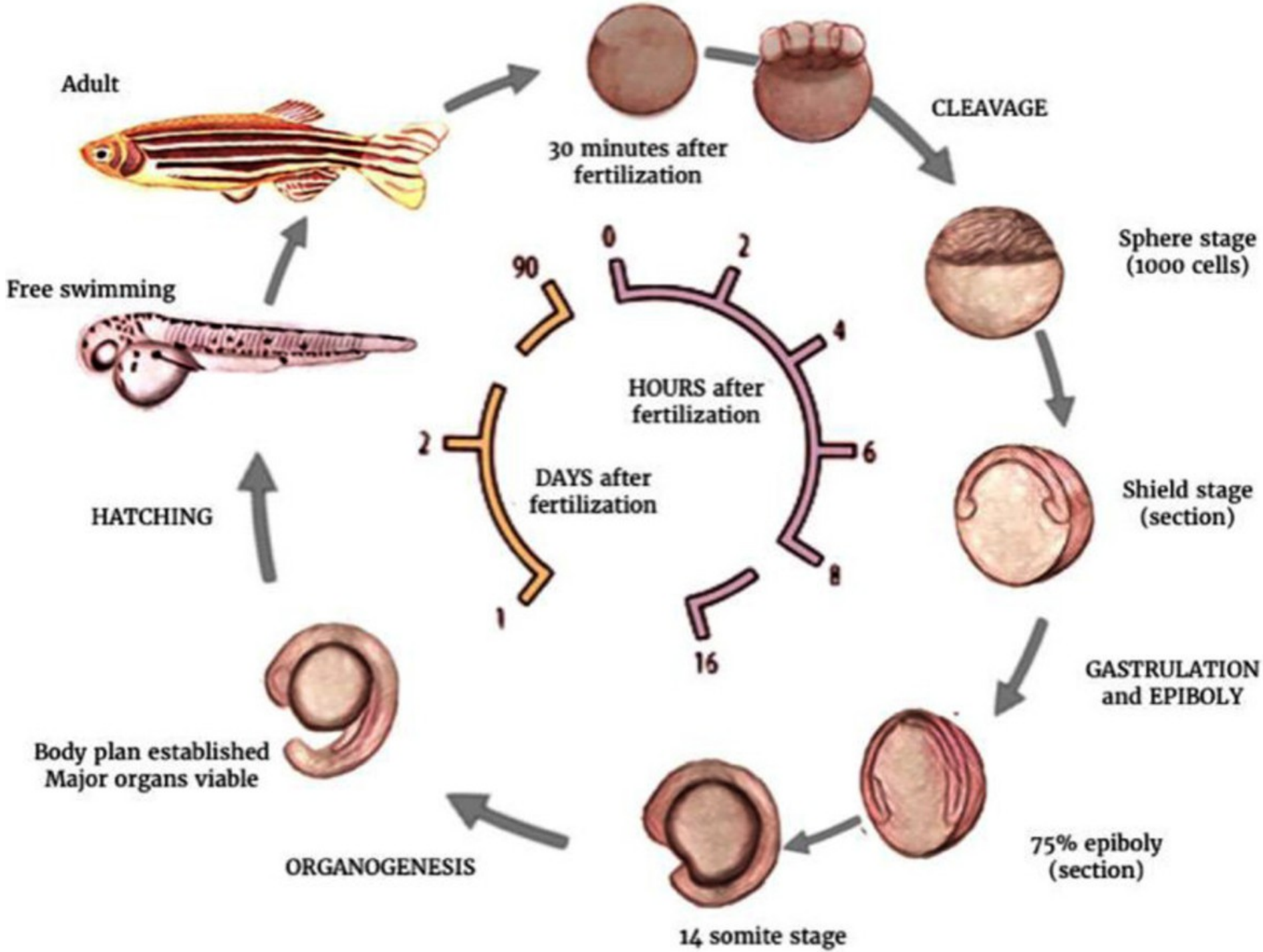
Adult
30 minutes after fertilization
CLEAVAGE
Sphere stage (1000 cells)
Shield stage (section)
GASTRULATION and EPIBOLY
75% epiboly (section)
14 somite stage
ORGANOGENESIS
Body plan established
Major organs viable
HATCHING
Free swimming
HOURS after fertilization
0
2
4
6
8
16
DAYS after fertilization
1
2
90

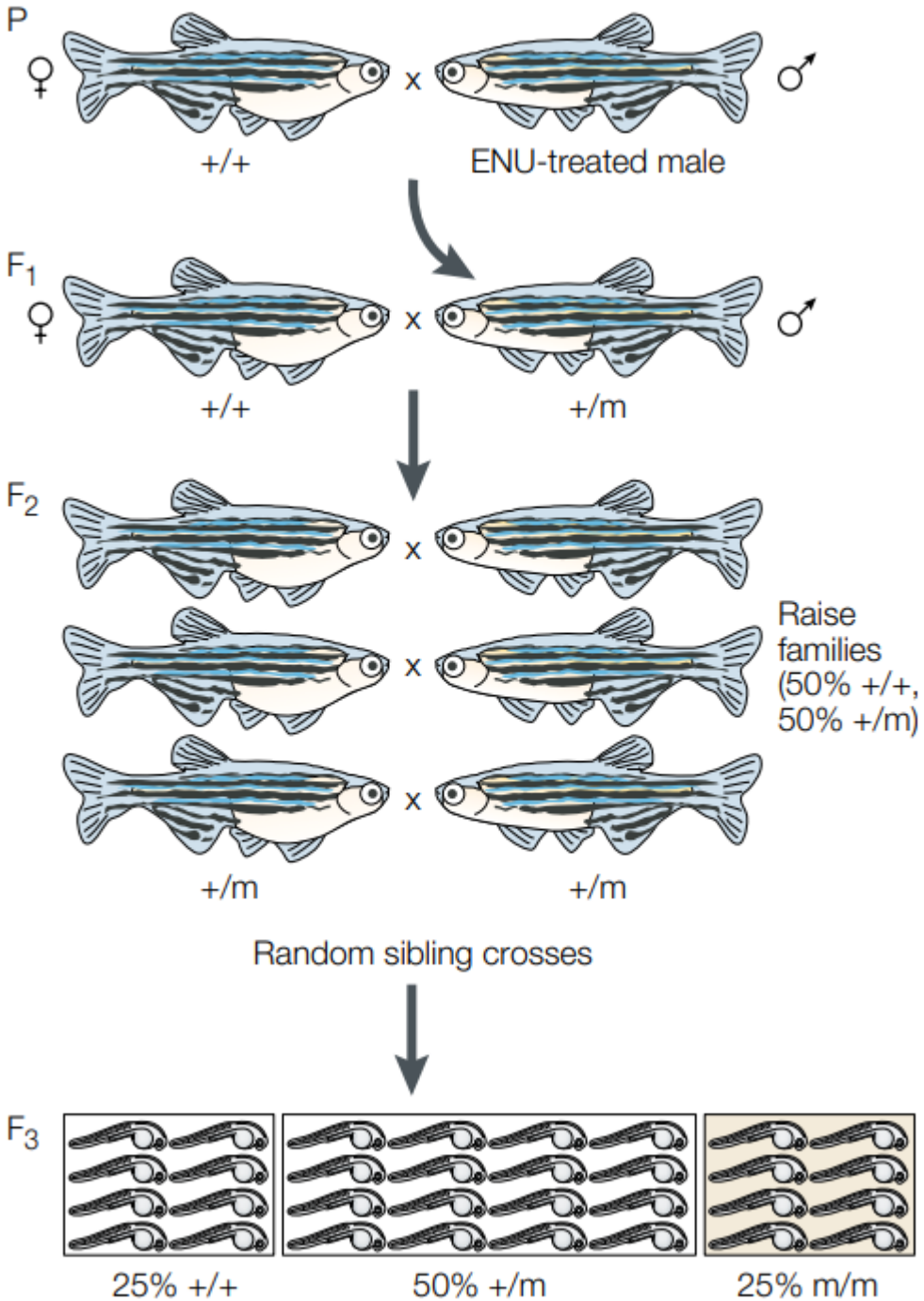

Figure 1 | **Outline of large-scale F_2 genetic screens.** In F_2 screens, a mutagen, such as ethylnitrosourea (ENU), is used to generate hundreds of point mutations in the male pre-meiotic germ cells (spermatogonia). ENU-treated males are crossed to wild-type females to produce the F_1 heterozygous progeny. F_1 fish are then crossed to siblings to create F_2 families, half of which are genotypically heterozygous for a specific mutation (m), whereas the other half are wild type. F_2 siblings are crossed, and the resulting F_3 progeny are 25% wild type (+/+), 50% heterozygous (+/m) and 25% homozygous (m/m) for a recessive mutation. Together, the Boston and Tübingen screens, starting from about 300 ENU founder males, involved raising more than 5,000 F_2 families, analysing more than 6,000 mutagenized genomes and selecting more than 2,000 new developmental mutants for characterization.

Fig. 2. Cover of The zebrafish issue of *Development* (December 1996), displaying the color pattern of the anal fins of several adult mutant fishes.

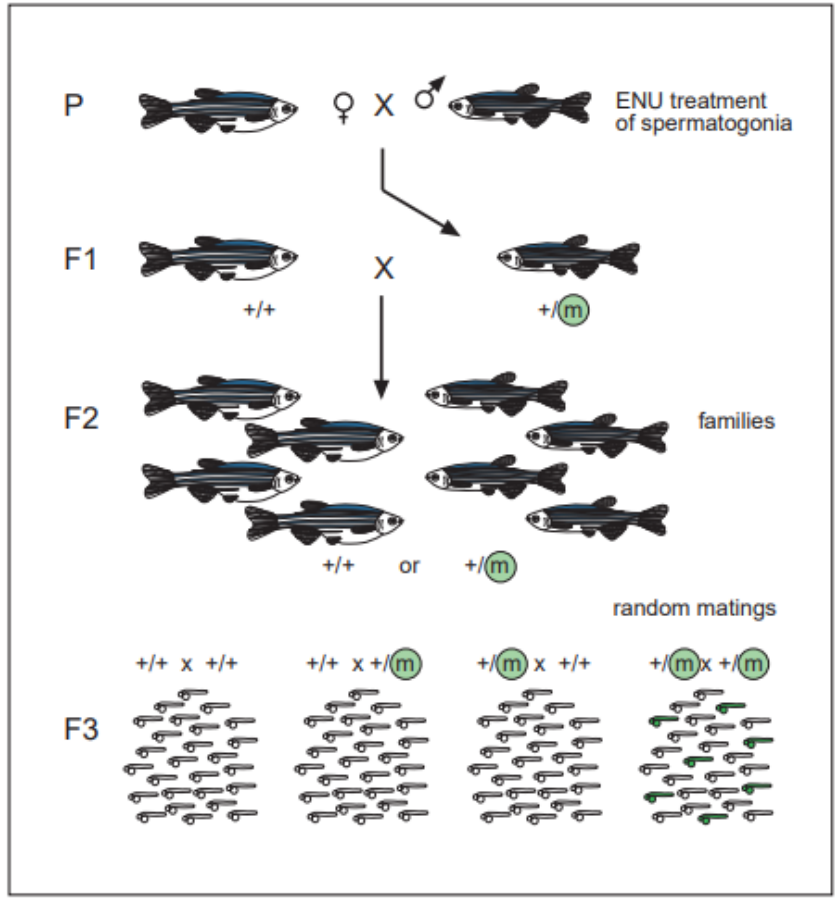

Fig. 3. Crossing scheme. Males mutagenized with ENU were mated to wild-type females. The F_1 progeny raised from matings 3 weeks after the mutagen treatment (resulting from treatment of spermatogonia) was heterozygous for one mutagenized genome. An F_2 generation was raised from sibling matings. A mutation **m** present in one of the F_1 parents was shared by 50% of the fish in the F_2 family. Eggs were collected from a number of matings between sibling fish. If both parents were heterozygous for **m,** expected in 1/4 of the crosses, 1/4 of the eggs will be homozygous and show the mutant phenotype. In this scheme, for simplicity, only one F_1 fish is heterozygous. In our experiment, both were heterozygous for a mutagenized genome. Therefore, the number of mutagenized genomes per family was two. The number of mutagenized genomes screened per family depends on the number of crosses (see legend to Table 1).

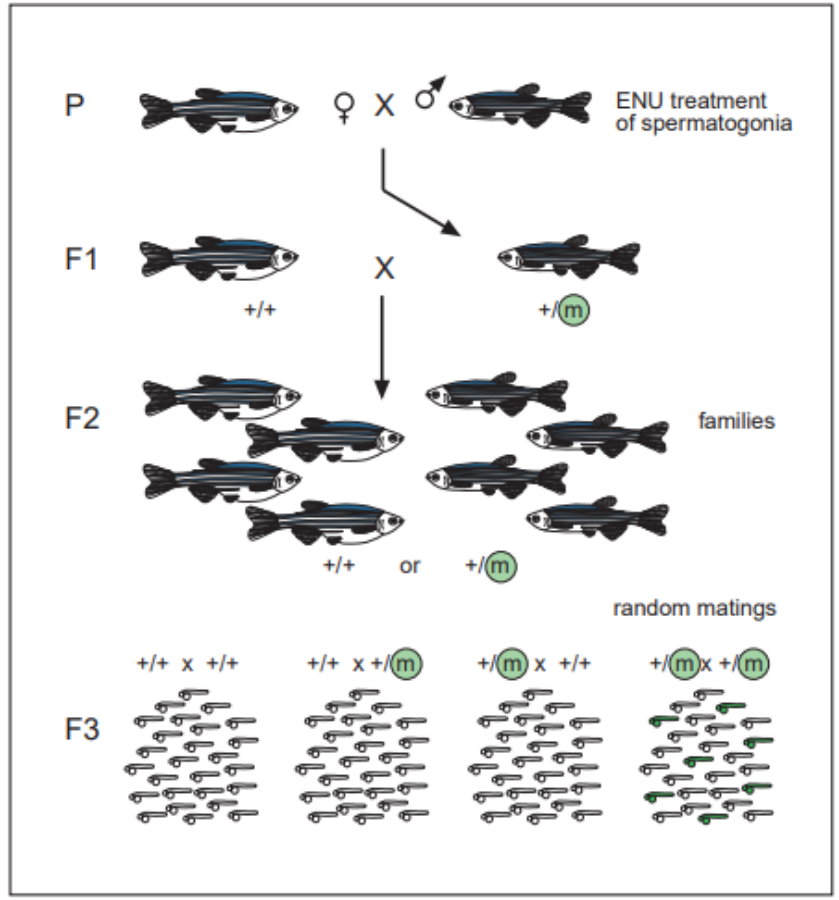

Fig. 3. Crossing scheme. Males mutagenized with ENU were mated to wild-type females. The F_1 progeny raised from matings 3 weeks after the mutagen treatment (resulting from treatment of spermatogonia) was heterozygous for one mutagenized genome. An F_2 generation was raised from sibling matings. A mutation **m** present in one of the F_1 parents was shared by 50% of the fish in the F_2 family. Eggs were collected from a number of matings between sibling fish. If both parents were heterozygous for **m,** expected in 1/4 of the crosses, 1/4 of the eggs will be homozygous and show the mutant phenotype. In this scheme, for simplicity, only one F_1 fish is heterozygous. In our experiment, both were heterozygous for a mutagenized genome. Therefore, the number of mutagenized genomes per family was two. The number of mutagenized genomes screened per family depends on the number of crosses (see legend to Table 1).

Development 123, 1-36
Printed in Great Britain © The Company of Biologists Limited 1996
DEV3343

The identification of genes with unique and essential functions in the development of the zebrafish, *Danio rerio*

Pascal Haffter, Michael Granato‡, Michael Brand†, Mary C. Mullins‡, Matthias Hammerschmidt§, Donald A. Kane¶, Jörg Odenthal, Fredericus J. M. van Eeden, Yun-Jin Jiang, Carl-Philipp Heisenberg, Robert N. Kelsh¶, Makoto Furutani-Seiki, Elisabeth Vogelsang, Dirk Beuchle††, Ursula Schach, Cosima Fabian and Christiane Nüsslein-Volhard***

Max-Planck-Institut für Entwicklungsbiologie, Abteilung Genetik, Spemannstrasse 35, 72076 Tübingen, Germany

†Present address: Institut für Neurobiologie, Universität Heidelberg, Im Neuenheimer Feld 364, 69120 Heidelberg, Germany
‡Present address: University of Pennsylvania, Department of Cell and Developmental Biology, 605 Stellar-Chance, Philadelphia, PA 19104-6058, USA
§Present address: Harvard University, Biolab, 16 Divinity Avenue, Cambridge, Massachusetts 02138, USA
¶Present address: University of Oregon, Institute of Neuroscience, Eugene, Oregon 97430, USA
**Present address: Institut für Genetik der Universität zu Köln, Weyertal 121, 50931 Köln, Germany
††Present address: Albert Einstein College of Medicine, 1300 Morris Park Avenue, Bronx, New York 10461, USA
*Author for correspondence (e-mail: cnv@fserv1.mpib-tuebingen.mpg.de)

SUMMARY

In a large-scale screen, we isolated mutants displaying a specific visible phenotype in embryos or early larvae of the zebrafish, *Danio rerio*. Males were mutagenized with ethylnitrosourea (ENU) and F_2 families of single pair matings between sibling F_1 fish, heterozygous for a mutagenized genome, were raised. Egg lays were obtained from several crosses between F_2 siblings, resulting in scoring of 3857 mutagenized genomes. F_3 progeny were scored at the second, third and sixth day of development, using a stereomicroscope. In a subsequent screen, fixed embryos were analyzed for correct retinotectal projection. A total of 4264 mutants were identified. Two thirds of the mutants displaying rather general abnormalities were eventually discarded. We kept and characterized 1163 mutants. In complementation crosses performed between mutants with similar phenotypes, 894 mutants have been assigned to 372 genes. The average allele frequency is 2.4. We identified genes involved in early development, notochord, brain, spinal cord, somites, muscles, heart, circulation, blood, skin, fin, eye, otic vesicle, jaw and branchial arches, pigment pattern, pigment formation, gut, liver, motility and touch response. Our collection contains alleles of almost all previously described zebrafish mutants. From the allele frequencies and other considerations we estimate that the 372 genes defined by the mutants probably represent more than half of all genes that could have been discovered using the criteria of our screen. Here we give an overview of the spectrum of mutant phenotypes obtained, and discuss the limits and the potentials of a genetic saturation screen in the zebrafish.

Key words: zebrafish, ENU mutagenesis, 'Tübingen' mutants', vertebrate development

INTRODUCTION

Multicellular organisms contain a large number of genes. The exact number is not known for any organism, nor can we say how many and which are absolutely required for survival, shape and pattern of the adult, juvenile or embryonic forms. Using modern methods of recombinant DNA technology, attempts are being made to clone and eventually sequence the genomes of several organisms such as *Caenorhabditis elegans, Drosophila melanogaster, Arabidopsis thaliana*, the mouse and *Homo sapiens*. Although it is likely that each gene has a function important for the organism, be it ever so subtle, from a large number of studies it emerged that in early pattern-forming processes and morphogenesis of the organism only a small fraction of the genes have indispensable and unique functions. The identification of these genes is a major issue in modern biological research.

Three types of information are most important to elucidate the function of a gene: the loss-of-function phenotype, the structure and biochemical properties of the protein product, and the distribution of the gene products within the organism. In vertebrates, a number of genes essential for development and pattern formation have been identified on the basis of their protein product or expression patterns. Mice mutants for any previously cloned gene can be created by homologous recombination in ES cells (Mansour et al., 1988), thus allowing in vivo analysis of gene function. This reverse genetic approach has the advantage that the gene corresponding to a mutant phenotype is already cloned, but a considerable disadvantage is that we cannot easily predict which genes have an indispensable function in the vertebrate embryo and thus will show a phenotype when mutant. So far, therefore, the most successful approach for identifying genes with indispensable functions in morphogenesis and pattern formation in the vertebrate

embryo is based on their surprising degree of homology to genes of invertebrates, i.e. *Drosophila melanogaster* and *Caenorhabditis elegans*. In invertebrates, a large collection of such genes have been identified by mutations.

Mutant searches have been carried out, with more or less systematic attempts at saturation, in a number of organisms for different phenotypic traits. Screens have been done for zygotic mutants showing a phenotype in the larval cuticle in *Drosophila melanogaster* (Jürgens et al., 1984; Nüsslein-Volhard and Wieschaus, 1980; Nüsslein-Volhard et al., 1984; Wieschaus et al., 1984), for various cell lineages in the post embryonic development of *Caenorhabditis elegans* (Brenner, 1974), for embryonic development in *Arabidopsis thaliana* (Mayer et al., 1991), and maternal mutants in *Drosophila* (Gans et al., 1975) and *C. elegans* (Kemphues et al., 1988). In these screens, a large number of lines originating from individuals treated with mutagenic agents were inbred for several generations. Homozyous progeny obtained were scored for the presence of morphological changes indicative of abnormal development. Using this approach, a large number of mutants with important functions in many developmental processes were identified. Groups of genes sharing particular phenotypic features helped to define pattern-forming pathways. For example, systematic searches for mutants affecting vulval development in *C. elegans* led to a detailed understanding of signaling processes and cellular interactions (Horvitz and Sulston, 1980). Mutants affecting axis determination and segmentation in the *Drosophila* embryo led to the elucidation of a small number of largely independent pattern-forming pathways (Nüsslein-Volhard and Wieschaus, 1980; St Johnston and Nüsslein-Volhard, 1992).

The advantage of mutagenesis is that it selects for the relatively small fraction of genes with unique and at least partially non-redundant functions. Their identification does not depend on preconceived ideas and models, although the ability to recognize a significant phenotype is dependent on the visibility of the structure affected, and is not always unbiased by models of interpretation. Genes with redundant functions go undetected, however (see Nüsslein-Volhard, 1994, for further discussion).

In vertebrates, systematic mutagenesis has been difficult so far because of long generation times, large space requirements, and laborious handling required in maintenance and breeding of these animals. Nevertheless, a small and valuable collection of mutants affecting early development in mice and zebrafish has accumulated. Because of the high degree of homology between genes of different vertebrates, a gene from one organism provides easy access to its homolog in another vertebrate. From gastrulation onwards, the early development of vertebrates is remarkably conserved. Therefore, the only essential requirement for the organism of choice is the possibility of doing large-scale mutagenesis. We have chosen to perform saturation mutagenesis screens in the zebrafish, *Danio rerio*, because of the many advantages it has as an embryological and genetical system (Streisinger et al., 1981). The most important property of the zebrafish is that the embryos are optically clear and are produced in large numbers. This allows screening for a large number of phenotypic traits by visibility with the dissecting microscope. For genetical analysis and stock keeping it is of advantage that eggs can be fertilized in vitro and sperm can be frozen. Furthermore, mutations can be induced with high efficiency. A random amplified polymorphic DNA map of the zebrafish genome has been constructed, on which a number of mutants and many cloned genes have already been mapped (Postlethwait et al., 1994).

Screens have been carried out before in the zebrafish, predominantly using X-rays as the mutagen. In these screens, the mutant embryos were detected in haploid progeny of females heterozygous for a mutagenized genome in part of the germline (Kimmel, 1989). Although elegant in principle, such screens have the disadvantage that specific phenotypes must be recognized against a high background of retarded and often abnormal development associated with haploidy (Streisinger et al., 1981). Frequently, the recovery of the mutant presents severe problems. We decided to screen diploids, although much more laborious, because the identification and recovery of mutants of many phenotypic classes can be performed with more consistency and reliability (Mullins et al., 1994).

In this paper we describe the isolation of 1163 mutants with defects in more than 372 genes of the zebrafish. The common feature of these genes is that they are indispensable for the development of a morphologically normal fish larva. Most of them display a specific and uniform visible phenotype in mutant embryos or larvae. The genes are required, as judged from the phenotypes, in a large number of processes in morphogenesis, pattern formation, organogenesis and differentiation. A preliminary account of the mutagenic treatment and the screening procedure has been published (Mullins et al., 1994). The genes and their properties are described in the accompanying papers (this issue).

MATERIALS AND METHODS

Fish strains

The wild-type strain used in mutagenesis was Tübingen. It originated from a local pet shop and was inbred for several generations. For outcrossing the mutant fish, the AB strain from the Oregon laboratory, a Tübingen:AB hybrid strain, and a strain homozygous for *leo*^{t1} and *lof*^{fd2} called TL, were also used. This latter strain was obtained from a dealer and kept by raising mixed eggs from different egg lays of particularly well-laying females. *leo*^{t1} is a recessive mutation causing spotting in adult fish, also known as *tup*, or *Brachydanio frankei*. *lof*^{fd2} is a dominant, homozygous viable mutation causing long fins. Both are described in more detail by Haffter et al. (1996).

Media

Embryo medium: (E3 medium) 5 mM NaCl, 0.17 mM KCl, 0.33 mM $CaCl_2$, 0.33 mM $MgSO_4$. To suppress growth of mold, the medium was supplemented with 10^{-5}% methylene blue. For anesthetizing, a 0.2% solution of 3-aminobenzoic acid ethyl ester (Sigma), containing Tris buffer, pH 7, was used (Westerfield, 1993).

Fish raising and keeping procedures; mutagenesis

The zebrafish breeding conditions and the mutagenesis protocol have been described by Mullins and Nüsslein-Volhard (1993). A detailed account of the keeping and raising methods has been described recently (Brand et al., 1995), and is available upon request. Adult male fish were mutagenized with 3 mM ENU by placing them into an aqueous solution for three 1 hour periods within 1 week. 3 weeks after the ENU treatment, males were crossed to wild-type females at weekly intervals and the progeny originating from mutagenized premeiotic germ cells obtained were raised. The progeny from each mutagenized male were kept separate such that the origin of individual mutations could be traced back to the founder male. Strings of

mutations originating from the same mutational event in the spermatogonia of the paternal founder fish have probably not been recovered, at least not in a significant number, since of the 59 genes with two alleles, in only five cases did both alleles come from the same founder male. The families were labeled with letters (ta-tz, ta200-tz200) corresponding to the founder male, and a consecutive number.

Screening procedure

For screening, about 15 pairs of fish per family, and about 100 families per week were set up for egg lay in one afternoon (Tuesday) of the week as described (Brand et al., 1995; Mullins et al., 1994). The following morning eggs from successful matings were collected using a tea strainer, and 2-3× 40 fertilized embryos were sorted within 6 hpf (hours postfertilization) into 60 mm Petri dishes in E3 medium. From about 300 families no successful matings were obtained, mainly because the fish showed an extreme sex ratio (mostly male families). The parents of successful matings were kept until the final evaluation of the retinotectal screen (Baier et al., 1996). Fish that had not laid on the first day were checked again on the second day after set up. The number and quality of the fish varied within the screen, and not all matings were successful. Fish of unsuccessful matings by the second day (40-80% of the crosses set up) were returned to their tank, and more crosses of their family, if necessary, were set up 2 weeks later. In general, not more than eight crosses of one family were evaluated with care, the average being 4.7. Table 1 summarizes the data of the mutagenesis experiment.

Embryos were scored at three successive time points (the second, third and sixth day after collection) corresponding to the pharyngula period, the hatching period, and the swimming larva (Kimmel et al., 1995), for abnormalities visible under a dissecting microscope at maximal 80× magnification. During the screening period, the egg lays were kept at 28°C. At each time point, after a general inspection, at least 12 embryos or larvae of each egg collection were aligned and inspected using a checklist (see Figs 1 and 2 for the structures on the checklist at various developmental stages). Embryos of the pharyngula period (24-48 hpf) were examined for abnormalities in the shape and morphology of the developing eyes, brain, notochord, spinal cord and somites. After hatching (third and sixth day screen), embryos were checked for motility (see below), and were then anesthetized before further scoring. In addition to the structures scored earlier, the development of the cardiovascular system and the fins were scored in embryos of the hatching period. At day 6 of development, particular attention was given to late developing organs such as the jaw and gill arches, the gut, the liver, the eyes, the otic vesicles, the pattern and

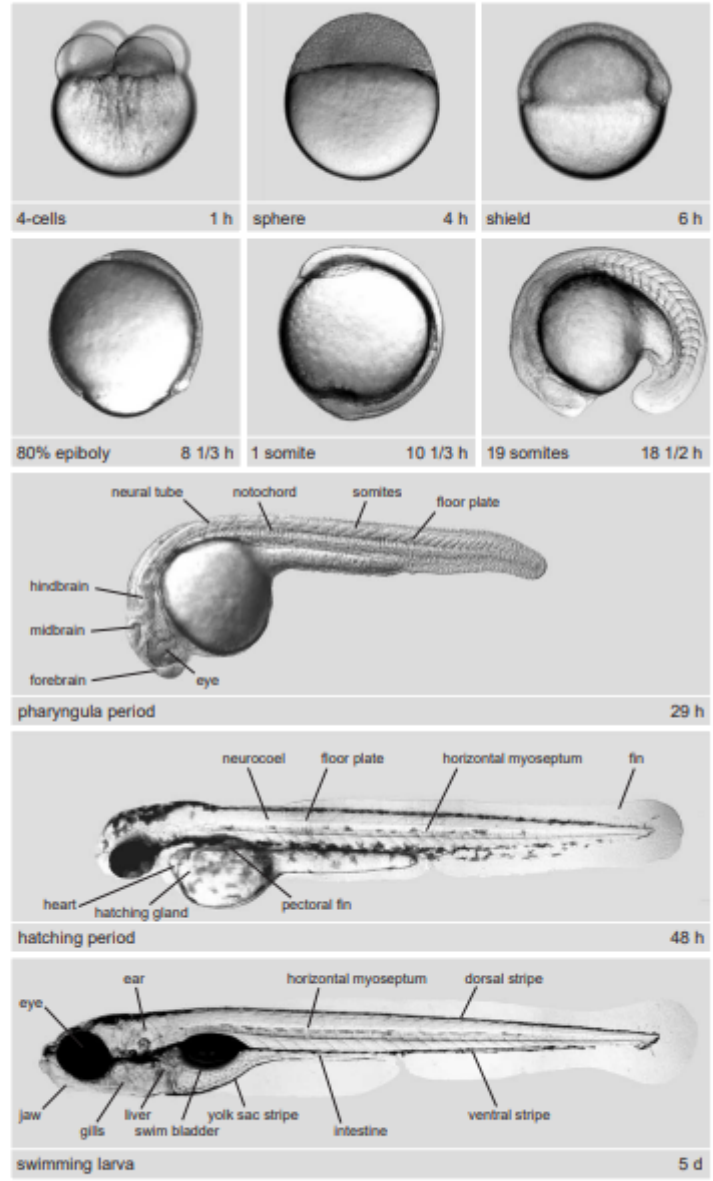

Fig. 1. Living embryos of relevant stages during the first 24 hours of development and of the approximate age during the three screening periods. The structures that were on the checklist are marked.

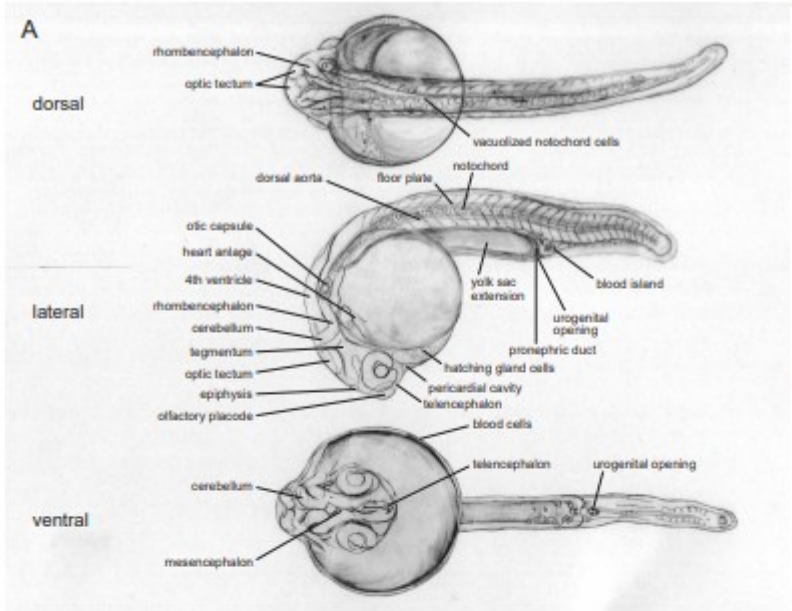

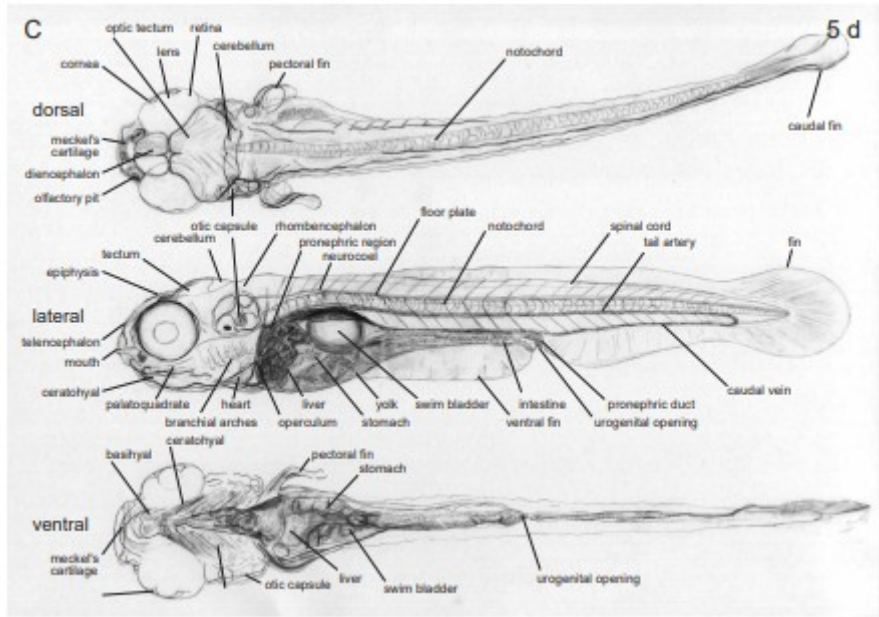

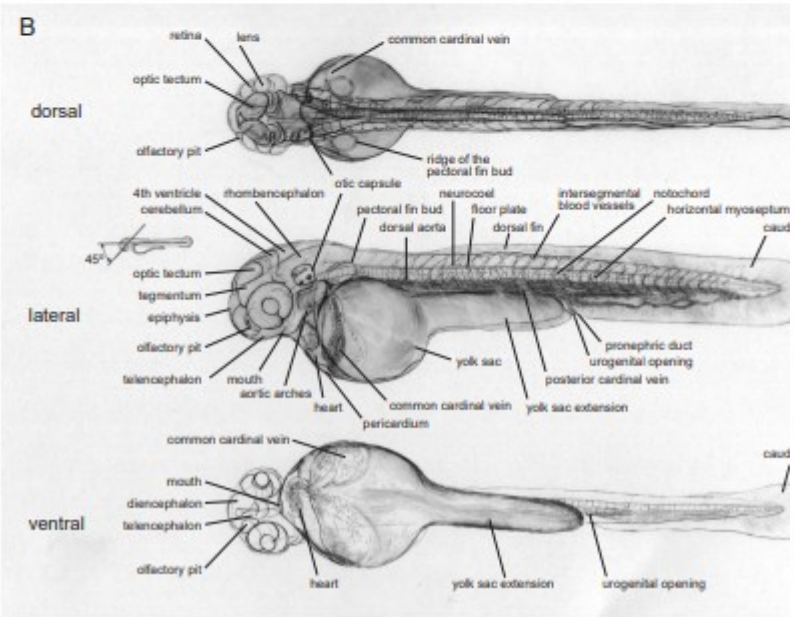

Fig.2a,b. For legend see p. 6.

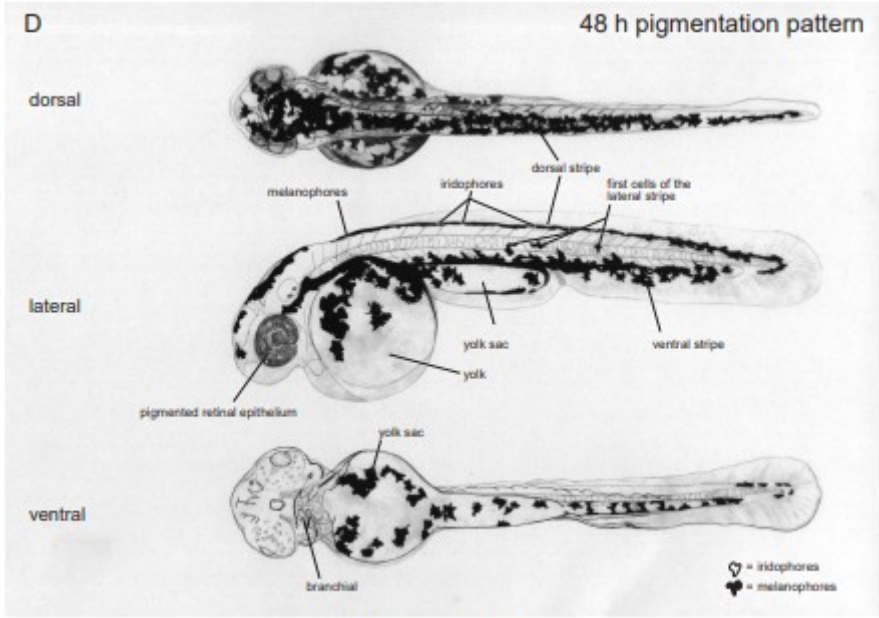

Fig.2c,d. For legend see p. 6.

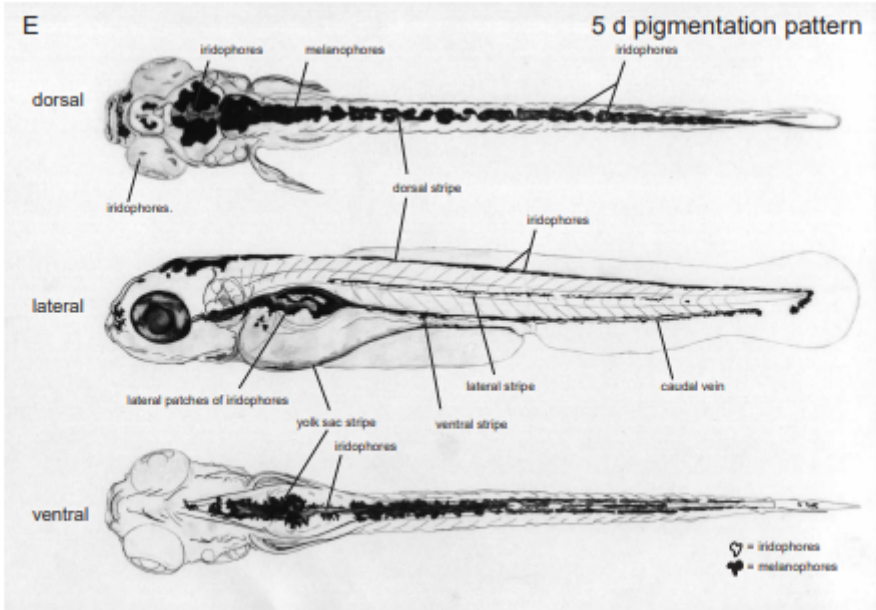

Fig. 2. Drawings of embryos at 24 hours (A), 48 hours (B,D), and 5 days (C,E) of development. For clarity, the melanophore pigmentation pattern is omitted from B and C. It is depicted in D and E. Most of the structures that can be seen in the living embryo with a compound microscope are marked.

size of the melanophores, and the intensity of pigmentation of xanthophores, melanophores and iridophores. We also checked whether the embryos had an air-filled swimbladder. The larvae were also inspected with incident light to examine iridophore pigmentation and muscle striation. To assay for motility, the larvae were swirled into the center of the dish and observed as they moved from the center. The response to touch was tested. During each screen, the general appearance of mutant embryos or larvae was noted, and it was recorded whether they showed signs of retardation (beady eyes, bent body, unconsumed yolk by day 5) or slow death (degeneration, edema, enlarged heart cavity).

The evaluations were recorded in a score sheet, and each phenotype recognized in a family was described separately. As expected, often a particular mutant phenotype occurred in more than one cross of a family. Often, more than one mutation was identified in different crosses within a family, and these were distinguished by consecutive letters added to the family name. In several cases two independent mutations occurred in one cross, and three different phenotypes were found (the singles and a double). In almost all such cases, the frequency of the doubles was 1/4 of that of the singles, as expected for independent segregation. In rare cases, the low frequency of singles indicated linkage between the two mutations. After the last screen, the larvae were fixed and subjected to a screen for mutations affecting the retinotectal projection (Baier et al., 1996).

Table 1. Mutagenesis of zebrafish

	Number (average)	Number (range)
Mutagenized males	49	
Families per male	63	0-181
Families raised	3075	
Families scored	2746	
Successful crosses	14357	20-60%
Crosses per family	4.7	0-18
Genomes screened*	3857	
Mutants identified	4264	
Mutants per family	1.4	0-8
Mutants per genome	1.1	

*Summarized over the numbers calculated for each family, starting from two heterozygous parental fish using the formula: $2x(1-0.75^n)$. n is the number of crosses scored per family.

Criteria for keeping mutants

On average 1.1 mutations with a recessive phenotype clearly visible in 25% of the embryos/larvae were found per mutagenized genome, confirming the result of a small-scale screen (Mullins et al., 1994). A total of 4264 mutants were tentatively identified by scoring 14357 successful crosses resulting from 2746 families (fish from 329 families did not give eggs) (Table1). Mutants were classified into one of four large classes of phenotypes. (A) general abnormality: degeneration, retardation, necrosis; (B) well defined specific deviation from normal morphology; (C) abnormal motility, or touch response; and (D) abnormal retinotectal projection.

Because of the large numbers, it was impossible for us to keep all identified mutants. Mutants with phenotypes characterized by rather general abnormalities (Class A) were therefore not kept. These mutants displayed any of four phenotypes, occurring with about equal frequency (Mullins et al., 1994): (1) degeneration of the entire embryo, observed during the hatching period-screen; (2) degeneration of the brain, usually followed by general necrosis of the entire body; (3) degeneration, associated with an enlarged heart cavity and reduced

circulation during the hatching period; (4) retardation, judged by underdevelopment of the jaw, the liver and gut, small eyes, and the presence of unconsumed yolk on day 6 of development. All these phenotypes affect the entire body of the fish and do not show any specific visible defects that are restricted to a limited set of body regions or organs. Furthermore, they comprise large numbers of mutants with similar phenotypes, which are difficult to distinguish. This makes it practically impossible to perform comprehensive complementation tests. Mutants with late phenotypes (affecting jaw and arches, liver, gut, eyes and ear, pigmentation of iridophores and xanthophores), were only kept if they did not show signs of severe retardation. Several phenotypes, especially those affecting late events, were difficult to detect or distinguish in a background of general degeneration or retardation. For instance, small eyes and small jaw and gill arches are features often associated with the general retardation phenotype, and we kept mutants with small eyes and arches only if other late features such as the development of the liver and gut appeared well advanced, or if associated with another specific phenotype such as pigmentation or fin defects. Mutants with fin necrosis were only kept if the embryos developed a swimbladder. This also applied to mutants that were morphologically normal but had expanded melanophores (black fish). Mutants with a curved body axis were kept only if the curvature was pronounced until day 6 of development. A number of egg lays showed variable abnormalities, notably anterior defects, which were rarely consistent and often occurred with frequencies deviating from the 25% expected for a zygotic mutant. In almost all such cases, in the rescreen, the egg lays were normal.

Rescreen, outcross and complementation

Parents of a total of 2092 independent mutant progeny were kept and subjected to a second screen. This included all mutants with distinct and specific phenotypes of classes B, C and D. In addition, we rescreened cases in which many embryos had lysed by the pharyngula period, which might be due to a mutation affecting the first 24 hours of development. We also rescreened mutants on which a clear decision could not be made.

In the rescreen, the embryos were scored during early somite stages, twice during the pharyngula period, and once at all subsequent days until the swimming larva period. Careful counts of mutant embryos were carried out and each screen was performed by at least two observers. Often, pictures of mutant embryos were taken as a permanent record and, if appropriate, the phenotype was described with the help of a compound microscope. After the rescreen, about 30% of the candidate mutants were discarded, and the mutants to be kept were classified using a three star system. The rescreen protocol was used for the subdivision of the mutants into phenotypic groups for further analysis. 22 mutants were lost before retesting. 513 mutants were either not confirmed or reassigned to class A, and discarded. 1474 mutants were confirmed during the rescreen, but 83 could not be rescreened because one of the parents had died, or because the pair did not produce eggs any more. The data are summarized in Table 2.

Table 2. Mutants recovered

Mutants	Number	Percentage
Total identified	4264	100
Kept for rescreen	2070	49
Not confirmed or lost in rescreen	513	12
F_3 raised	1557	35
Not confirmed in F_3	221	5
Lost in F_3	237	6
Newly discovered in F_3	102	2.5
Confirmed and characterized	1163	27
Mutants total	1163	=100
Assigned to genes	894	77
Unresolved	269	23

From these 1557 mutants, an F_3 generation was raised. In general one, and in particularly valuable mutants, both, of the parental fish were crossed to wild-type fish. Although the incidence of carrier fish in the F_3 generation would have been higher following the raising of viable fish from two heterozygous parents, in practice the viability and vigor of fish resulting from inbreeding was very much reduced compared to outbred fish. This was also true in the next generation, and therefore outcrossing to independent wild-type strains was usually performed. In the F_3 generation, heterozygous carrier fish were identified by sibling matings and used for further characterization of the mutant phenotype as well as for complementation crosses with other mutants. In the course of identification of carrier fish in the F_3, 121 previously unnoticed mutants were found, 102 of which were kept. About 221 mutants were lost, and 237 were classified as general abnormalities and discarded. In the end, 1163 mutants were kept (Table 2).

For the further analysis of mutant phenotypes, carrier fish were identified by scoring random crosses between siblings from the F_3 outcrosses. As a backup, sperm of mutant carriers was frozen as described by Westerfield (1993), with the modifications described by Driever et al. (1996). For the establishment of complementation groups, crosses were performed between mutants with similar phenotypes. The methods for the analysis of the mutant embryos are indicated in the individual papers in which the mutants are described in more detail.

RESULTS

Mutagenic treatment and screening

For large-scale mutagenesis, it is desirable to induce point mutations with a potent mutagen that mutagenizes genes on a random basis. For zebrafish, as for mice (Russell et al., 1979), ENU had the highest mutagenicity of the agents tested, inducing apparent point mutations at a rate of about one mutation causing a visible phenotype in the embryo or larva per treated haploid genome (Mullins et al., 1994). Alleles of previously known pigmentation mutants were induced at a rate of one to three per thousand treated genomes. Other mutagens such as X-rays, EMS, or insertion of DNA proved to be by one to several orders of magnitude less efficient at inducing recoverable mutations (Mullins et al., 1994; Solnica-Krezel et al., 1994, Gaiano et al., personal communication). The procedures used in the present screen have been described previously (Mullins et al., 1994; Materials and Methods section).

49 treated males provided the mutagenized genomes for inducing the 1163 mutants described in this issue (Fig. 3). Single pair matings were performed between F_1 fish and 40-70 F_2 progeny from each mating were raised. They constitute a family of sibling fish that share a gene pool of two mutagenized haploid genomes (one from each parent). In order to detect the induced mutations, crosses between F_2 siblings were carried out and the resulting embryos scored for the occurrence of mutant phenotypes. As only 50% of the fish in a family share a particular mutation, on average every fourth cross yields embryos homozygous for a mutation originating from one of the F_1 parents of that family. The probability of detecting such a mutation increases with the number of crosses. On average 4.7 crosses per family were evaluated from a total of 3075 families. This corresponds to 1.3 mutagenized haploid genomes on average screened per family, amounting to a total of 3857 mutagenized haploid genomes screened (Fig. 3; Table 1).

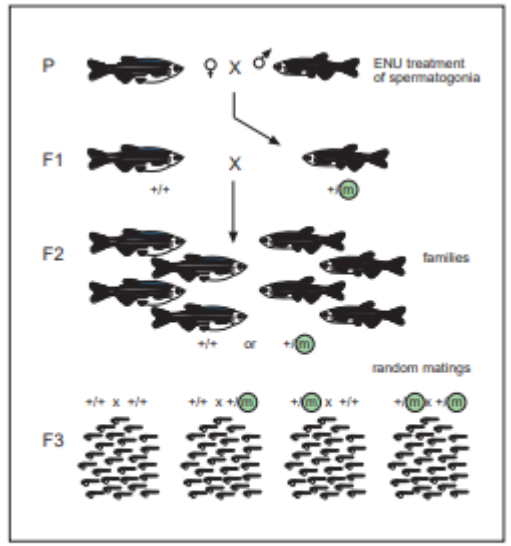

Fig. 3. Crossing scheme. Males mutagenized with ENU were mated to wild-type females. The F_1 progeny raised from matings 3 weeks after the mutagen treatment (resulting from treatment of spermatogonia) was heterozygous for one mutagenized genome. An F_2 generation was raised from sibling matings. A mutation **m** present in one of the F_1 parents was shared by 50% of the fish in the F_2 family. Eggs were collected from a number of matings between sibling fish. If both parents were heterozygous for **m,** expected in 1/4 of the crosses, 1/4 of the eggs will be homozygous and show the mutant phenotype. In this scheme, for simplicity, only one F_1 fish is heterozygous. In our experiment, both were heterozygous for a mutagenized genome. Therefore, the number of mutagenized genomes per family was two. The number of mutagenized genomes screened per family depends on the number of crosses (see legend to Table 1).

Complementation analysis

The mutants were assigned to one of several large groups according to the most prominent phenotypic feature. Within each group, several smaller subgroups were established in order to facilitate complementation tests among mutants. Several mutants were assigned to more than one group or subgroup, and a more careful analysis of phenotypic features was performed, depending on the phenotype. Crosses were performed between pairs of mutants with similar phenotypes. In general, not all possible complementation crosses within each group were done, and often only one or two members of one complementation group were tested against further mutants. In most cases, members of one complementation group showed the same or a very similar phenotype. In at least 40 complementation groups, alleles with different allelic strength could be identified. Many complementation groups have a unique phenotype, while in other cases a small number of genes share a similar or identical phenotype. In these cases, complementation testing presented no problem and the numbers of alleles per gene are reasonably high (see Table 5). Frequently, mutants display more than one phenotypic feature, often in seemingly unrelated traits, and therefore in several instances different alleles of genes were initially assigned to different groups. Examples are *chameleon* and *you too* (Brand et al., 1996b; van Eeden et al., 1996b), with a somite and a neural tube phenotype, *boxer* and *dackel* (Schilling et al., 1996; Trowe et al., 1996; van Eeden et al., 1996a), with a jaw, a pectoral fin, and a retinotectal pathfinding phenotype, and *bashful* (Odenthal et al., 1996a; Karlstrom et al., 1996) with a brain, a notochord and a retinotectal projection phenotype. For that reason we expect that in a few instances allelism will be assessed between what are now described as independent genes, following more extensive analysis and mapping. Difficulties were also encountered in cases where rather large numbers of mutants share similar phenotypes, with few clear cut and easily displayed criteria to distinguish between them, for example mutants with notochord degeneration (Odenthal et al., 1996a), circling behaviors (Granato et al., 1996), curly body (Brand et al., 1996b), and jaw defects (Piotrowski et al., 1996; Schilling et al., 1996). In many of these, it has not yet been possible to complete the complementation analysis.

Of the 1163 mutants isolated and kept from the screen, 894 (77%) have been tested in complementation with most other mutants with similar phenotypes. These mutants define a total of 372 genes, 150 of which have more than one allele. 222 of the genes are defined by only one allele. 269 mutants are yet to be characterized further (Table 3). They are listed as unresolved in the publications. The allele frequencies observed are not random (Table 4). While a small number of genes have high allele frequencies (11 genes with more than ten alleles, the maximum allele number being 34), many genes are represented by only one allele. The average allele frequency varies between 1 and 7.5 in different phenotypic groups (Table 5), with an overall average of 2.4.

Table 3. Allele frequencies: an overview

	Number	Percentage
Mutants kept in F_3	1163	100
Mutants assigned to genes	894	77
Mutants in unresolved groups	269	23
Mutants with more than one allele	672	75
Single mutants	222	25
		=100
Total number of genes	372	100
Complementation groups (>1 allele)	150	40
Genes with one allele only	222	60

Table 4. Allele frequencies: genes

n alleles	*n* genes	*n* mutants	*n* alleles	*n* genes	*n* mutants
1	222	222	11	3	33
2	61	122	12	2	24
3	28	84	13	0	0
4	15	60	14	1	14
5	12	60	15	1	15
6	9	54	16	0	0
7	7	49	17	1	17
8	3	24	22	1	22
9	3	27	23	1	23
10	1	10	34	1	34
Sum	361	712	Sum	11	182

Table 5. Genes identified in the Tübingen screen: phenotypic groups

Phenotypic group	Subgroup	Genes*	Genes (*n*)	Alleles (*n*)	Alleles/ gene	Un-resolved (*n*)	Reference
Early	Epiboly	*hab, ava, law, weg, (yob)*	4	4	1.0	0	Kane et al., 1996a
	Early arrest and necrosis	*zom, spb, spr, trl, kap, ban, ogr, plt, nrv, ghl, hrp*	11	18	1.6	0	Kane et al., 1996b
Body axes	Dorsalised	*swr, snh, pgy, laf, sbn, mfn*	6	19	3.2	5	Mullins et al., 1996
	Ventralised	*mes, din*	2	4	2.0	0	Hammerschmidt et al., 1996a
	Others	*ppt, spt, tri, bib, udu, kgg, sam, sch, ind, mpt*	10	17	1.7	2	Hammerschmidt et al., 1996b
	Prechordal plate, hatching	*dns, zja, oep*	4	4	1.0	3	Hammerschmidt et al., 1996b
Mesoderm	Notochord formation	*ffh, mom, doc, ntl, (din)*	4	9	2.3	0	Odenthal et al., 1996a
	Notochord differentiation	*hap, sny, dop, sly, gup, bal*	6	45	7.5	0	Odenthal et al., 1996a
	Undulated notochord	*qam, ctd, wat, ziz, kik*	5	13	2.6	0	Odenthal et al., 1996a
	Degenerating notochord, late notochord defects	*luc, blo, kon, (acc, beo, zim, tnt, sla, roc, baj, que, exp, pun, dtw)*	3	4	1.3	18	Odenthal et al., 1996a
	Somite formation	*fss, bea, ales, aei, (sap, wit)*	4	19	4.8	1	van Eeden et al., 1996b
	Somite patterning	*syu, you, yot, ubo, (ntl, mom, ffh, doc, con, cho)*	4	7	1.8	0	van Eeden et al., 1996b
CNS	Forebrain	*mbl, kas, slb, (cyc)*	3	4	1.3	1	Heisenberg et al., 1996
	Midbrain-hindbrain	*ace, noi*	2	7	3.5	0	Brand et al., 1996b
	Hindbrain, a. o.	*snk, pac, nat, wit, atl, ele, ott, ful, bid, vip, win, wis, sbd*	13	26	2.0	0	Jiang et al., 1996
	Brain degeneration†	*(rec, aoi, mur, awa, yug)† (brd, dfd, van, blc, wei, tin, ger, ivy, sll, bch, fla, dns, stu)*	0	0	0	32	Furutani-Seiki et al., 1996
	Spinal chord, a. o.	*con, cyc, sps, bad, dtr, sur, igu, agb, stb, slt, mol, smh, (yot)*	12	21	1.8	2	Brand et al., 1996a
	Curly tails	*spi, wir, cup, tig, lok, cos, sin, sic, vic, pir, hkn sen, snt*	13	58	4.4	31	Brand et al., 1996a
Organs	Blood	*mon, frs, weh, cha, ret, yqe, frx, zin, sau, cdy, cia, gre, mot, pnt, tbr, cab, ris*	17	32	1.9	2	Ransom et al., 1996
	Heart morphology	*sug, sco, cas, mil, fau, olp, san, loa, (nat)*	8	9	1.1	0	Chen et al., 1996
	Heart beat	*bre, tan, hip, plk, sth, sih, wea, web, tre, leg, quh, pip, str, sli, (hel,vip, hat, slp, jam, sky)*	14	18	1.3	4	Chen et al., 1996
	Circulation	*hyp, kus, (syu, you, yot, con)*	2	3	1.5	0	Chen et al., 1996
	Liver, gut, kidney	*flo, gam, tip, lum, trp, stf, (lok, noi)*	6	6	1.0	0	Chen et al., 1996
	Eye	*bum, rne, kor, sri, hez, mic, dre, lep, uki, (cco, blc, pio, blr, fad, mlk, sbl, coo, bch, fla, ivy, van, mir, fdv, dfd, sll, flo, sug, sah, era, ser, bab, fac, dul)*	9	12	1.3	10	Heisenberg et al., 1996
	Otoliths	*eis, kei, men, kst, wnp, sub, rst, bks, (clx, blc, cls, stw, nob)*	8	29	3.6	7	Whitfield et al., 1996
	Ear morphology and lateral line organ	*bge, hph, lau, lte, dog, eso, vgo, eps, spk, era, bxe, mic, hps, (ace, cls, puz, sah, box, ful, dak, snk, ott, clx, wei, lep, dre)*	13	19	1.5	4	Whitfield et al., 1996
	Fins	*frf, nag, rfl, pif, fra, fyd, bla, ika, dak, med, krm, tut, sto, (mes, sub, box, lep, dre, fls, ubo, mon)*	13	61	4.7	5	van Eeden et al., 1996a
	Skin	*gsp, ddf, pen, bob*	4	9	2.3	1	van Eeden et al., 1996a
Pigment cells	Pigment cell number and pattern	*cls, shd, uns, spa, cho, los, snp, pde, slk, (sal, pfe, mom, tig, ful, ffh, wit, mes, ubo, mon)*	9	32	3.6	1	Kelsh et al., 1996
	Melanin pigmentation	*goi, alb, sdy, mrd, bry, nkl, pew, led*	8	25	3.1	1	Kelsh et al., 1996
	Melanophore differentiation	*tdo, fad, lnd, sln, fdv, dfd, sah, (qam)*	7	21	3.0	5	Kelsh et al., 1996
	Melanophore shape	*sas, drp, ger, uni, obs, nir, zwa, mac, sum, tin, fam, pet, lak*	13	25	1.9	2	Kelsh et al., 1996
	Xanthophores	*pfe, kef, sal, esr, edi, yob, clx, til, bri, nob, qua, yoc, tof, fet, ric, tar, bst*	17	62	3.6	0	Odenthal et al., 1996b
	Iridophores	*lcl, tnd, hei, bed, dim, tod, mat*	7	8	1.1	1	Kelsh et al., 1996
	Two cell types affected	*cco, pio, pep, pup, pol, mlk, coo, ivy, pun, frk, van, mir, blr, cot*	14	40	2.9	10	Kelsh et al., 1996
	Three cell types affected	*wsh, blc, sbl, puz, bch, wei, sll, bli, stw, pch*	10	15	1.5	1	Kelsh et al., 1996
Jaw and gills	Flatheads, posterior arches	*fla, low, ser, bab, fac, dul, gap, (box, puz, pio, mlk, dak, pic, ger, sbl)*	7	11	1.6	32	Schilling et al., 1996
	Hammerheads, ant. arches	*hot, ham, hen, get, stu, jef, suc, dol, koi, hoo, pek, she, (sur, ppt, vgo, con, igu, yot, dtr, slb)*	12	22	1.8	22	Piotrowski et al., 1996
Motility	Reduced motility, muscle striation	*slo, fro, fub, tur, buf, fap, slw, sne, hem, dus, mah, slp, jam, sky, sap, sof, sml, ruz*	18	51	2.8	12	Granato et al., 1996
	Reduced motility, normal striation	*sop, nic, red, hat, hel, unp, sho, two, ali, far, mao, ste, cro, sla, slm, (ubo, syu, yot, ffh, wis, wir, box, nor, zwa, sum, tdo, clx, luc, kon, stb, cls)*	15	25	1.7	21	Granato et al., 1996
	Abnormal motility	*acc, zim, beo, dtw, que, baj, exp, spo, spc, twi, tnt, roc, way, her, (ntl, doc, mom, nev)*	14	35	2.5	17	Granato et al., 1996
Adults	Body shape	*lil, dml, stp, smf, (sps)*	4	4	1.0	0	Haffter et al., 1996
	Pigment pattern	*leo, obe, ase, (sal, pfe, spa)*	3	8	2.7	1	Haffter et al., 1996
	Eyes	*(bum, fdv, kor, rne, yob)*				0	Haffter et al., 1996
	Fins	*alf, lof, wan, fls, (frf, krm, mes, pif)*	4	4	1.0	0	Haffter et al., 1996
	Pigmentation	*(alb, bry, bum, drp, gol, mrd, obs, sdy, shd, tar, brs)*				0	Haffter et al., 1996
Retinotectal	Pathfinding	*ast, bel, blw, uml, (bal, esr, box, yot, con, til, dtr, igu, tof, gup, pic, sly, dak, cyc)*	4	7	1.8	0	Karlstrom et al., 1996
	Mapping	*box, nev, pic, blu, mio, woe, brd, (dfd, esr, noi, dak, ace, mao, til)*	7	23	3.3	14	Trowe et al., 1995
Total			372	894	2.4	269	

*Genes in brackets are dealt with in more detail in a paper describing a different class of mutants.
†This class of mutants was not kept systematically (Furutani-Seiki et al., 1996).

also isolated a small number of mutations affecting other internal organs such as the liver and the kidney (Chen et al., 1996).

Many mutants affect the outer morphology of the body of the fish larva or adult. At least 13 genes were identified that are required for the formation of the larval fins (van Eeden et al., 1996a). The pectoral fins are reduced in mutants in at least four genes such as *ikarus* (van Eeden et al., 1996a). With the exception of the pectoral fins, the adult fins are quite different from the larval fins in morphology and pigmentation, appearing only in the third week. Nevertheless a number of mutants with altered adult fin morphology were fortuitously isolated, such as *wanda*, *stein und bein* and *finless* (Haffter et al., 1996; van Eeden et al., 1996a). Often, mutants showing altered larval fin morphology are viable and the adults show no or only very mild mutant phenotypes (Haffter et al., 1996).

Dominant mutations causing visible phenotypes in the adult fish have also been identified (Haffter et al., 1996). Several lead to a short body and some show severe skeletal defects. Other dominant mutations cause alterations in the striped pigmentation pattern of the adult. Broader stripes are formed in heterozygous and homozygous fish mutant in the genes *asterix* and *obelix*. The stripes are interrupted in heterozygotes, and spotted in the homozygous mutants *leopard*, *salz* and *pfeffer* (Haffter et al., 1996). *salz* and *pfeffer* homozygous larvae lack xanthophores (Odenthal et al., 1996b; Kelsh et al., 1996). In several instances, mutants showing a pale pigmentation in the larvae reveal a related phenotype in homozygous adults, such as those affecting melanin production. These may be useful marker mutations (Haffter et al., 1996; Kelsh et al., 1996).

About 100 mutants were isolated with specific defects in the motility of the larva (Granato et al., 1996). Mutant larvae fail to respond to touch properly, or show reduced or abnormal spontaneous swimming or escaping behavior. The phenotype of 18 of these genes is associated with muscular defects visible with incident illumination, and in several cases (*sloth, buzz-off*) muscle abnormalities could be detected in sections. In another 29 mutants, no obvious morphological abnormality in the musculature could be found. The phenotypes show reduced or no motility (*sofa potato*), spastic and circling behavior (*techno trousers*), as well as defects in reciprocal inhibition of muscle contractions (*'accordion'* group, 7 genes). In a small number of mutants, defects in the outgrowth of motor neurons have been detected (*unplugged, diwanka*; Granato et al., 1996).

About 100 mutations affecting the establishment of the retinotectal projection were isolated in a screen performed on larvae fixed after day 5 of development (Baier et al., 1996). A number of genes were identified that affect the pathfinding of the retinal axons to the tectum (Karlstrom et al., 1996), and several others which are involved in the mapping on the tectum were characterized (Trowe et al., 1996). Although many of these mutants were isolated on the basis of the axonal pathfinding phenotype, in both groups the majority of mutants have additional visible phenotypes and many are also described in other contexts, such as *bashful, boxer* and *dackel*, and *esrom* (Odenthal et al., 1996a,b; Schilling et al., 1996). In two cases, a motility defect is associated with a retinotectal phenotype *(never mind, macho)* (Granato et al., 1996; Trowe et al., 1996).

Viability

In several mutants, homozygous embryos develop a swim-bladder. These were classified as embryonic viable. In many cases, these could grow up to adults, which frequently, but not always, displayed a visible phenotype. Mutations in 79 genes are homozygous viable, and 19 semiviable (Haffter et al., 1996). Seven of the lethal genes also have viable alleles, indicating that the viable alleles are weak or hypomorphic. Mutations in 38 of the adult viable genes cause a recessive adult phenotype, while mutants in the remainder look normal as adults. Not all viable alleles have been tested for fertility, but one maternal effect mutant (*yobo*) was identified. Homozygous *yobo* larvae derived from heterozygous parents have

Development 123, 37-46
Printed in Great Britain © The Company of Biologists Limited 1996
DEV3351

A genetic screen for mutations affecting embryogenesis in zebrafish

W. Driever*, L. Solnica-Krezel, A. F. Schier, S. C. F. Neuhauss, J. Malicki, D. L. Stemple, D. Y. R. Stainier†, F. Zwartkruis‡, S. Abdelilah, Z. Rangini§, J. Belak and C. Boggs

Cardiovascular Research Center, Massachusetts General Hospital and Harvard Medical School, 149 13th Street, Charlestown, MA 02129, USA

*Author for correspondence (e-mail: Driever@Helix.MGH.Harvard.EDU or: Driever@ruf.uni-freiburg.de)
†Present address: Department of Biochemistry and Biophysics, School of Medicine, UCSF, San Francisco, CA 94143-0554, USA
‡Present address: Laboratory for Physiological Chemistry, Utrecht University, Universiteitsweg 100, 3584 CG Utrecht, The Netherlands
§Present address: Department of Oncology, Sharett Institute, Hadassah Hospital, Jerusalem 91120, Israel

SUMMARY

Systematic genome-wide mutagenesis screens for embryonic phenotypes have been instrumental in the understanding of invertebrate and plant development. Here, we report the results from the first application of such a large-scale genetic screening to vertebrate development.

Male zebrafish were mutagenized with N-ethyl N-nitrosourea to induce mutations in spermatogonial cells at an average specific locus rate of one in 651 mutagenized genomes. Mutations were transmitted to the F_1 generation, and 2205 F_2 families were raised. F_3 embryos from sibling crosses within the F_2 families were screened for developmental abnormalities. A total of 2337 mutagenized genomes were analyzed, and 2383 mutations resulting in abnormal embryonic and early larval phenotypes were identified. The phenotypes of 695 mutants indicated involvement of the identified loci in specific aspects of embryogenesis. These mutations were maintained for further characterization and were classified into categories according to their phenotypes. The analyses and genetic complementation of mutations from several categories are reported in separate manuscripts. Mutations affecting pigmentation, motility, muscle and body shape have not been extensively analyzed and are listed here. A total of 331 mutations were tested for allelism within their respective categories. This defined 220 genetic loci with on average 1.5 alleles per locus. For about two-thirds of all loci only one allele was isolated. Therefore it is not possible to give a reliable estimate on the degree of saturation reached in our screen; however, the number of genes that can mutate to visible embryonic and early larval phenotypes in zebrafish is expected to be several-fold larger than the one for which we have observed mutant alleles during the screen. This screen demonstrates that mutations affecting a variety of developmental processes can be efficiently recovered from zebrafish.

Key words: zebrafish *Danio rerio*, mutagenesis, genetic control, embryogenesis

INTRODUCTION

Genetic analysis of vertebrates, especially mice, has traditionally focused on traits that are expressed postnatally, and do not lead to embryonic lethality (Lyon and Searle, 1989). Zygotic-effect mutations leading to intrauterine embryonic lethality are difficult both to identify and to analyze in mammals. Therefore, there have been few mutations found to interfere with the establishment of the body plan and early steps of organogenesis. This situation has changed since targeted gene disruption makes it possible to follow the segregation of mutant alleles using molecular analysis, and to determine whether a given embryo is homozygous for the induced mutation (Capecchi, 1989). This technology has made a tremendous impact on our understanding of vertebrate development (McMahon and Bradley, 1990; Thomas and Capecchi, 1990; Joyner et al., 1991; Carpenter et al., 1993; Urbanek et al., 1994; Wurst et al., 1994). Two important approaches remain very difficult in mice. First, forward genetics to identify novel genes involved in embryogenesis is prohibitively expensive. Second, experimental and embryological studies of mutations acting early in embryogenesis are greatly inhibited by the intrauterine mode of development.

It is exactly the combination of the last two approaches that has been the experimental basis for the current detailed understanding of invertebrate and plant development. Large scale, systematic genetic screens led to the characterization of genetic pathways that pattern the *C. elegans*, *Drosophila* and *Arabidopsis* embryos (Hirsh and Vanderslice, 1976; Nüsslein-Volhard and Wieschaus, 1980; Mayer et al., 1991).

Zebrafish (*Danio rerio*), a small tropical freshwater teleost, was recognized as a genetic system in which similar approaches would be feasible (Streisinger et al., 1981). The high fecundity, short generation time and rapid development of the externally fertilized, translucent embryos make it an excellent vertebrate genetic model system (reviewed by Driever et al., 1994). Devel-

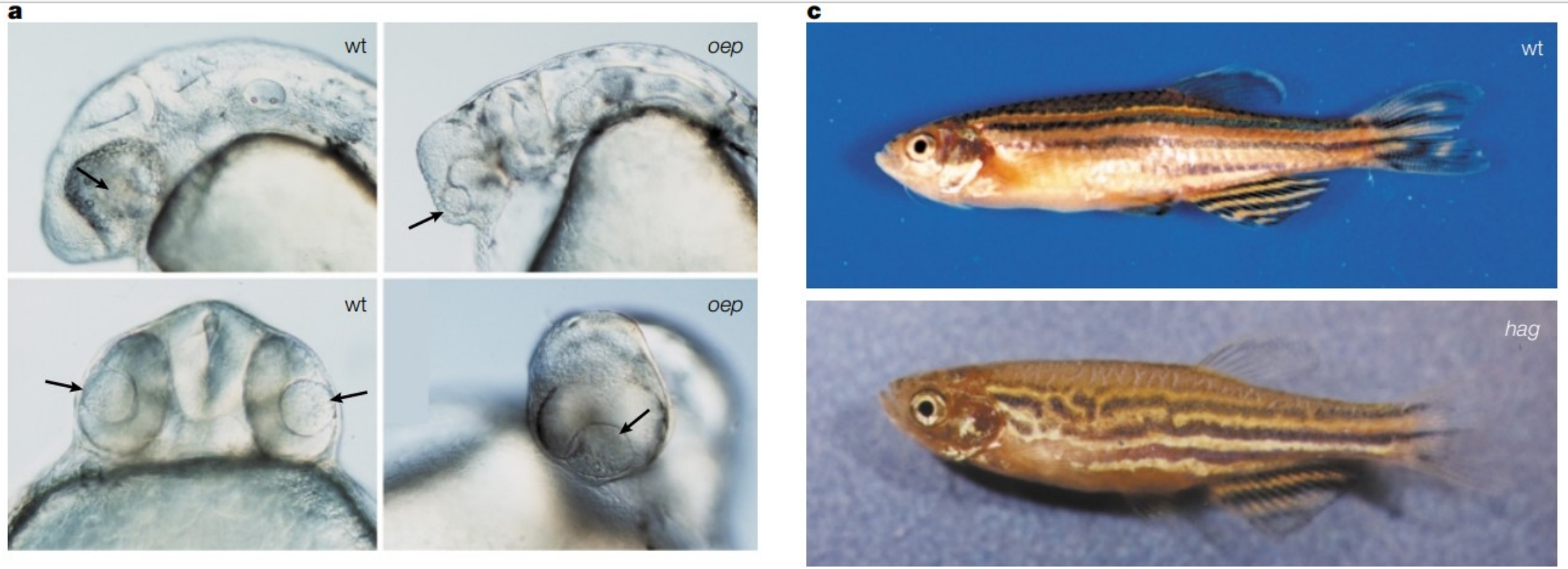

Figure 2 | **Examples of mutants identified in zebrafish large-scale screening efforts. a** | Mutants for *one-eyed pinhead* (*oep*), which encodes a member of the Nodal signalling pathway, lack endoderm, prechordal plate and ventral neuroectoderm, which results in severe cyclopia (arrows denote lens position) among other defects. Lateral (top panels) and anterior–ventral (bottom panels) view of wild type (wt) and *oep* mutants. Reproduced with permission from REF. 78 © (1996) Company of Biologists Ltd. **b** | The recessive embryonic-lethal mutation *weissherbst* (*weh*) results in hypochromic blood with decreasing blood cell counts. Staining of 2-day-old embryos with O-dianisidine to visualize haemoglobin (arrows) shows reduced levels of haemoglobin in the *weh* mutant. Reproduced with permission from REF. 15 © (1996) Company of Biologists Ltd. **c** | A dominant mutation, *hagoramo* (*hag*), which results in a disrupted stripe pattern of adult fish and encodes a protein with a possible role in proteolysis, was generated by insertional mutagenesis. Reproduced with permission from REF. 37 © (2000) Elsevier Science.

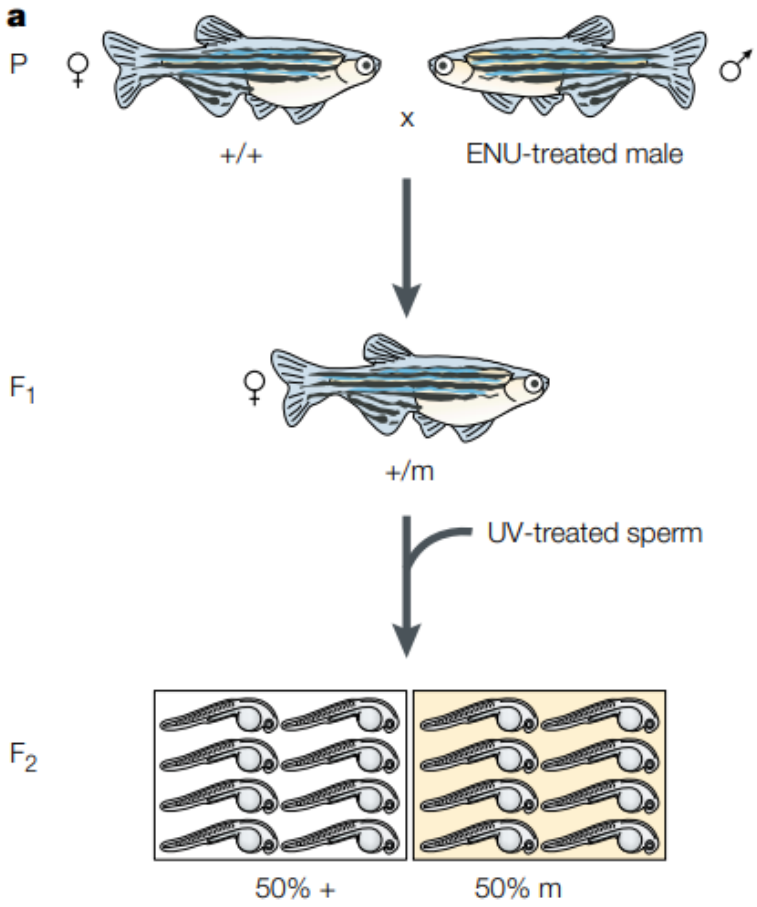
a
P
+/+
x
ENU-treated male
F1
+/m
UV-treated sperm
F2
50% +
50% m

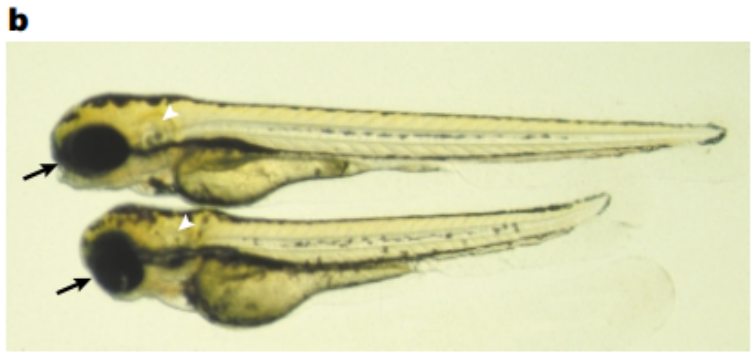
b

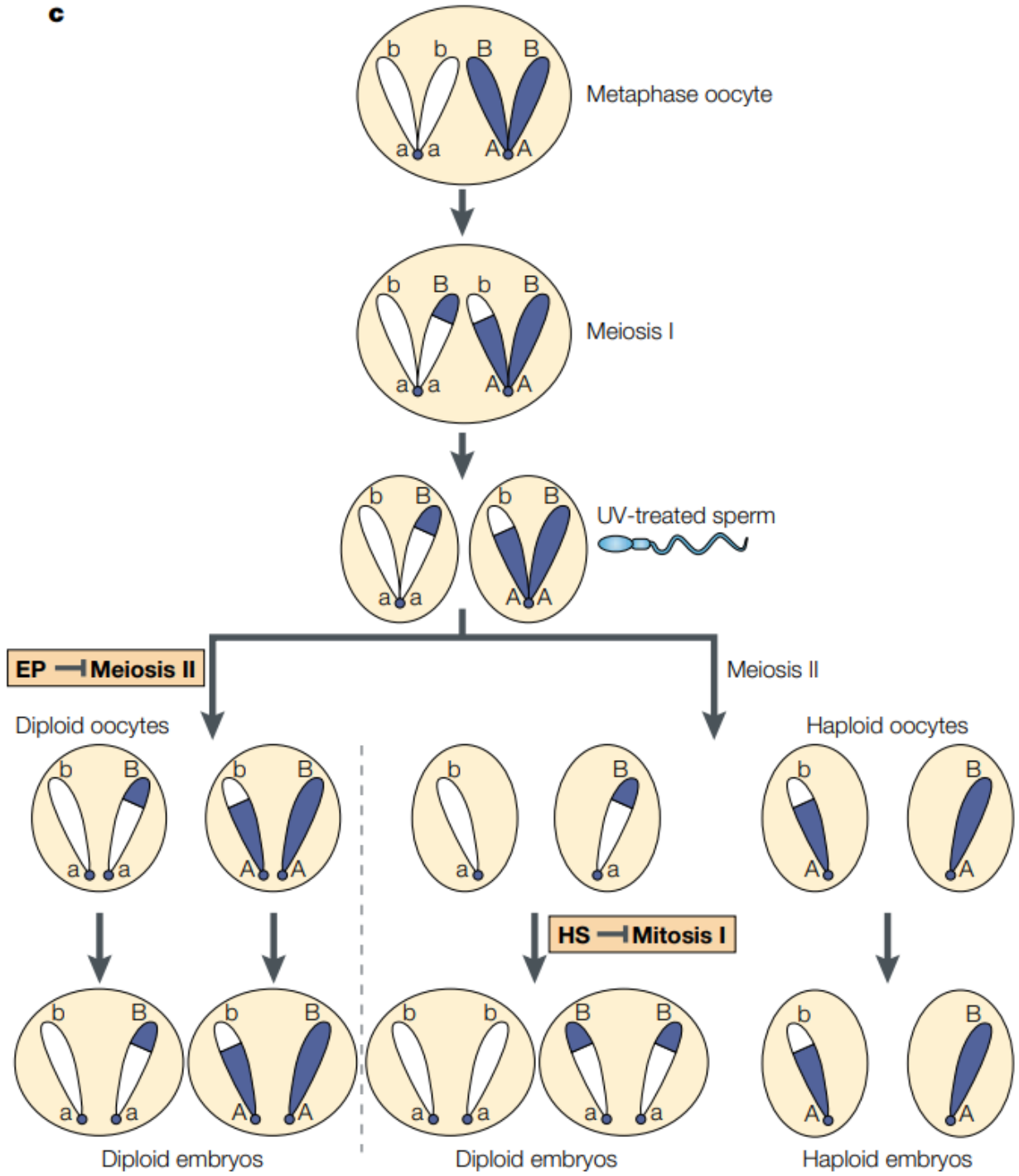
c
Metaphase oocyte
Meiosis I
UV-treated sperm
EP
Meiosis II
Meiosis II
Diploid oocytes
Haploid oocytes
HS
Mitosis I
Diploid embryos
Diploid embryos
Haploid embryos

Box 1 | **Haploid and homozygous diploid screens**

To avoid the cumbersome step of screening thousands of progeny for recessive mutations in conventional F_2 screens (FIG. 1), methods have been devised to uncover recessive alleles in a single generation by exploiting the ability to create haploid or homozygous diploid embryos.

Haploid screens

Recessive mutations can be revealed more quickly in zebrafish by taking advantage of their ability to survive for several days as haploid organisms[77]. In a haploid screen (**a**), female F_1 fish (derived from the cross between a wild-type female and an ethylnitrosourea (ENU)-mutagenized male) are squeezed gently to release their eggs, which are then fertilized with ultraviolet (UV)-treated sperm to generate haploid embryos. UV treatment destroys the parental DNA, without affecting its ability to activate the egg. A haploid clutch derived from a heterozygous female will contain 50% mutant and 50% wild-type embryos. Panel **b** shows 3-day-old diploid (top) and haploid (bottom) zebrafish embryos. Note that diploid and haploid embryos share a similar overall morphology, but haploid embryos are visibly shorter with abnormal eye (arrow) and otic vesicle (arrowhead) development.

Homozygous diploid screens: methods to induce gynogenesis

Eggs extracted from a female have completed meiosis I (the separation of homologous chromosomes) during ovulation, and initiate meiosis II (the separation of sister chromatids) on fertilization[24]. Early pressure (EP) applied to embryos during the first few minutes post-fertilization breaks down the meiotic spindle, and the egg maintains both sister chromatids (**c**, left). Subsequently, eggs undergo their first mitosis as diploids, with two sets of maternal chromosomes. By contrast, heat-shock treatment (HS; **c**, right) inhibits the first mitotic division, and eggs activated with UV-treated sperm enter the first mitotic division as haploids, abort mitosis and directly enter the second mitotic division as diploids. In meiosis, recombination and CHIASMA INTERFERENCE occur between homologous chromosomes when aligned as tetrads, so that there is, on average, a single crossover event per chromosome arm. Therefore, embryos that are derived from EP treatment will be homozygous for loci that are proximal to the crossover event that occurred at meiosis I (allele 'a' in the figure) and heterozygous for loci that are distal to it. Similar to haploid clutches, a gynogenetic diploid clutch that is derived from a heterozygous female and generated by HS will contain 50% mutant and 50% wild-type embryos. As embryos generated by HS are homozygous at all loci, they would be preferable to embryos generated by EP for use in genetic screens, except for their reportedly poor viability (10–20%).

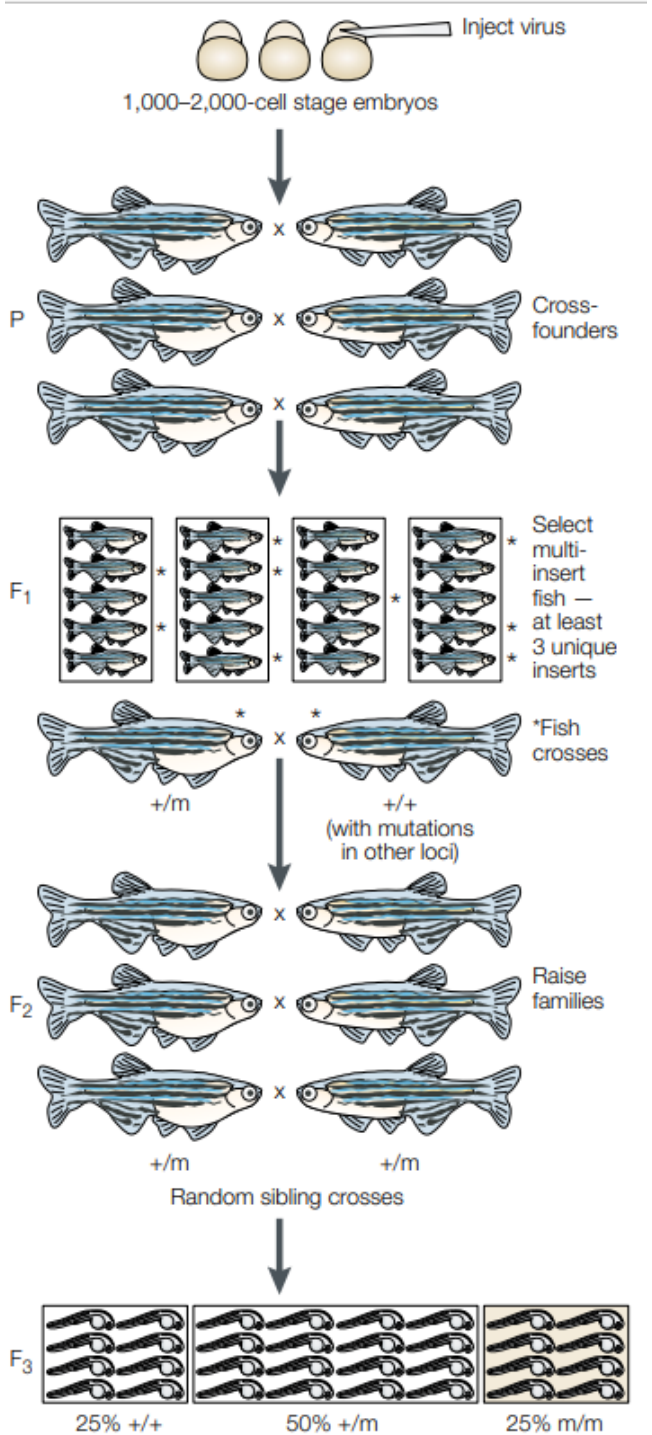

Figure 3 | **Outline of insertional mutagenesis screen.** The goal of the Cambridge screen is to identify ~1,000 genes involved in embryogenesis[36]. The protocol for large-scale insertional mutagenesis screening involves injecting virus into 250,000 embryos at the 1,000–2,000-cell stage[36]. The virus infects many cells, several times, among them the primordial germ cells. Approximately 36,000 embryos are raised (the founder fish; P), mated and several insertions transmitted to the F_1 generations. More than 10,000 F_1 families are raised, and multi-insert F_1 fish are selected by carrying out real-time PCR and Southern blot analysis of DNA isolated from tail biopsies. Multi-insert F_1 fish are crossed to each other and 10,000 F_2 families are raised. More than six sibling matings for each F_2 family are carried out to identify ~1,000 homozygous mutations in the F_3 generation. m, mutagenized chromosome.

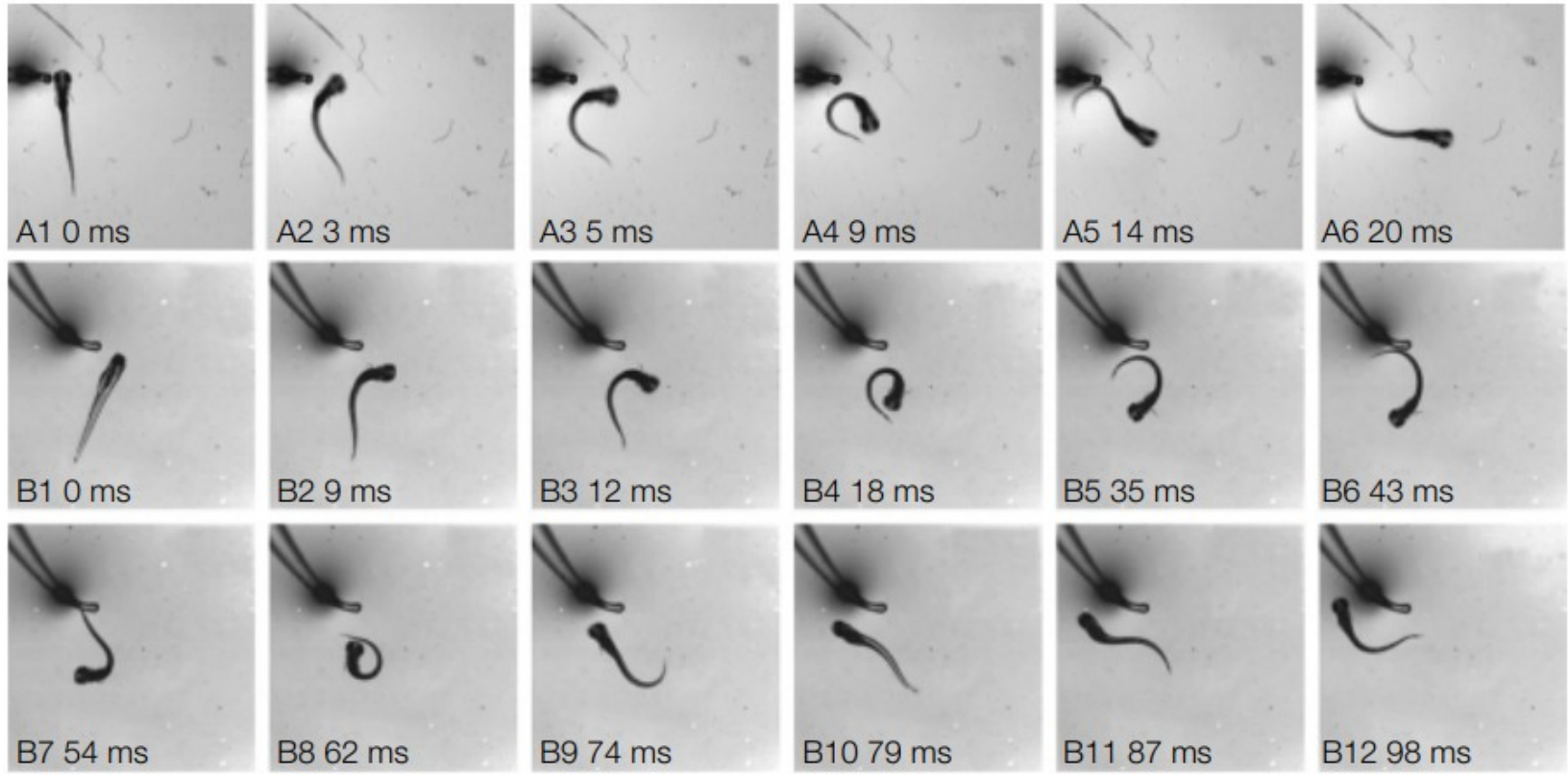

Figure 5 | **The *space cadet* locomotion mutant.** The *space cadet* mutant shows abnormal swimming behaviours during a stimulus-induced escape response. High-speed camera images capture the C-shaped bend of a wild-type larva as it rapidly moves its head away from the stimulus source (A1–A4; the timing of each frame is given, in milliseconds (ms)). The larva then makes a less powerful counterturn (A5, A6), before rapidly swimming away from the source (not shown). In response to a stimulus, the *space cadet* larva makes a C-shaped bend away from the stimulus in a similar manner to wild-type larvae (B1–B4), but has a poor counterturn (B5, B6). It then initiates a second turn towards the same side (B7–B9), before swimming away using a series of fast, bilateral tail flexures. A movie of the swimming defects of *space cadet* can be viewed at http://dev.biologists.org/cgi/content/full/128/11/2131/DC1 and http://www.nature.com/nsu/010607/010607-1.html. Modified with permission from REF. 47 © (2001) Company of Biologists Ltd.

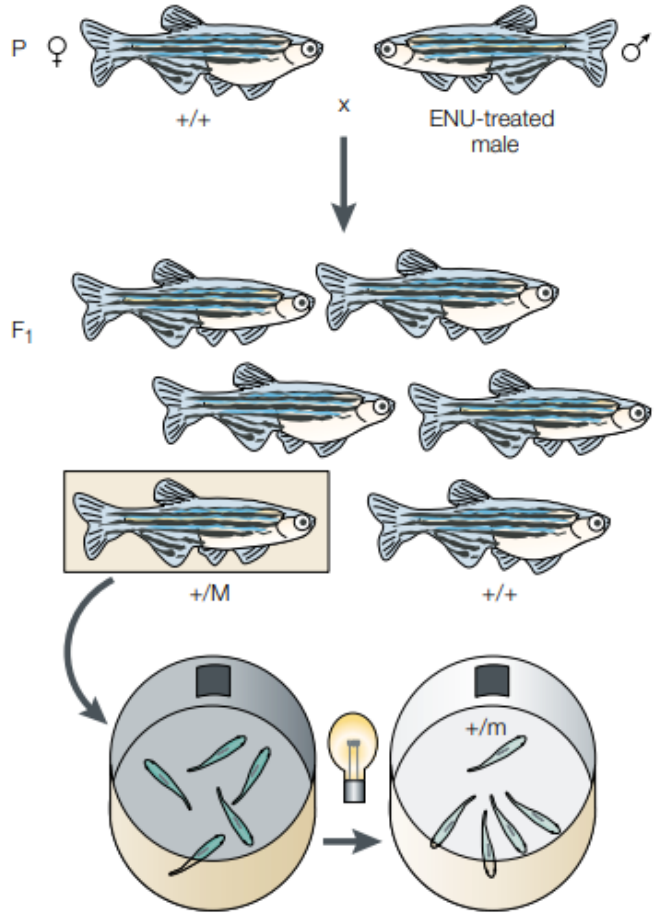

Figure 6 | **Behaviour screens: visual adaptation mutants.** A behavioural test can be a measure of visual sensitivity and be used to screen for subtle, eye-specific mutations in adult zebrafish. Adult F_1-generation fish derived from ethylnitrosourea (ENU)-mutagenized founders are placed in a transparent container that is surrounded by a rotating drum marked with a black square that represents a threatening object[49,50]. After initial dark adaptation, normal zebrafish rapidly 'escape' the threatening object in light above (but not below) their visual threshold (right drum). By contrast, fish that are heterozygous for the mutation *night blindness b* show the escape response at a visual threshold that is 2–3 log units above the average[50]. M, dominant mutation on an ENU-mutagenized chromosome.

Development 123, 117-128
Printed in Great Britain © The Company of Biologists Limited 1996
DEV3340

Mutations affecting development of the notochord in zebrafish

Derek L. Stemple*, Lilianna Solnica-Krezel*, Fried Zwartkruis[1], Stephan C. F. Neuhauss, Alexander F. Schier[2], Jarema Malicki, Didier Y. R. Stainier[3], Salim Abdelilah, Zehava Rangini[4], Elizabeth Mountcastle-Shah and Wolfgang Driever†

Cardiovascular Research Center, Massachusetts General Hospital and Harvard Medical School, 149 13th Street, 4th Floor, Charlestown, MA 02129, USA

*Contributed equally to the work
[1]Present address: Laboratory for Physiological Chemistry, Utrecht University, 3584 CG Utrecht, The Netherlands
[2]Present address: Skirball Institute of Biomolecular Medicine, New York University Medical Center, 550 First Avenue, New York, NY 10016, USA
[3]Present address: Department of Biochemistry and Biophysics, University of California San Francisco, San Francisco, CA 94143-0554, USA
[4]Present address: Department of Oncology, Sharett Institute, Hadassah Hospital, Jerusalem 91120, Israel
†Author for correspondence (e-mail: driever@helix.mgh.harvard.edu)

SUMMARY

The notochord is critical for the normal development of vertebrate embryos. It serves both as the major skeletal element of the embryo and as a signaling source for the establishment of pattern within the neurectoderm, the paraxial mesoderm and other tissues. In a large-scale systematic screen of mutations affecting embryogenesis in zebrafish we identified 65 mutations that fall into 29 complementation groups, each leading to a defect in the formation and/or maintenance of the notochord. These mutations produce phenotypic abnormalities at numerous stages of notochord development, thereby establishing a phenotypic pathway, which in turn suggests a genetic pathway for the development of the notochord. Perturbations within adjacent tissues in mutant embryos further indicate the importance of notochord-derived signals for patterning within the embryo and suggest that these mutations will yield additional insight into the cues that regulate these patterning processes.

Key words: zebrafish, notochord, floor plate, mesoderm, embryogenesis

INTRODUCTION

The notochord is a structure common to all members of the phylum Chordata. It serves as the major skeletal element for lower chordates and as such provides an important mechanical element for the locomotion of the individual. In lower vertebrates at larval stages of development the notochord plays a similar role serving as the major skeletal element in the body apparently necessary for coordinated movement. Perhaps more importantly, in all vertebrates, the notochord is required for the proper patterning of adjacent tissues, including the neurectoderm, paraxial mesoderm and the heart. In the neurectoderm, the notochord functions to signal the formation of the floor plate, and, independently, can signal the formation of motoneurons (Placzek et al., 1993; van Straaten et al., 1988; Yamada et al., 1993). In addition to specifying ventral fates the notochord suppresses the expression of dorsal fates in the neurectoderm (Bovolenta and Dodd, 1991; Goulding et al., 1993). The notochord appears to play several roles in the patterning of somitic tissue. First, based on experimental manipulation of avians as well as analysis of several mouse mutations, the notochord is responsible for the specification and maintenance of ventral, i.e. sclerotome, fates in the somite (Dietrich et al., 1993; Pourquie et al., 1993). The notochord is also involved in dermomyotome patterning. In avian experiments, notochord extirpation leads to a complete loss of epaxial muscles, i.e. deep back muscles, whereas hypaxial muscles, i.e. limb and ventrolateral body wall muscles, are unaffected (Christ et al., 1992; Rong et al., 1992). Muscle specification occurs in the absence of notochord, but a notochord derived signal is required to maintain the epaxial muscle fate (Bober et al., 1994). Mosaic analysis of the zebrafish mutation *no tail* (*ntl*), a mutation in a gene homologous to the mouse *Brachyury* gene, indicates that differentiated notochord is also required for the proper patterning of muscle pioneers in the developing myotome (Halpern et al., 1993; Herrmann et al., 1990; Schulte-Merker et al., 1992). Interestingly, mutants of the *ntl* locus form a floor plate (Halpern et al., 1993), suggesting that not all of the notochord signaling activities are disrupted by the mutation. In addition to its role in patterning the CNS and somites, the notochord may also serve to specify other tissues such as sympathoadrenal progenitors (Stern et al., 1991), the left-right asymmetry of the heart tube (Danos and Yost, 1995), and the differentiation of certain gut derivatives (Wiertz-Hoessels et al., 1987). There is evidence that specification of the floor plate and patterning of the somite are both mediated at least in part by *Sonic hedgehog* (*shh*) (Fan et al., 1995; Fan and Tessier-Lavigne, 1994;

Table 1. Complementation groups of mutations affecting notochord development

Locus name	Alleles	Category**	Phenotype	Other defects	Refs
Group I					
bozozok (*boz*)*	*m168*	A, B	No chordamesoderm	Reduced floor plate, cyclopia	a
floating head (*flh*)*	*m614*	B, C	No chordamesoderm	Reduced floor plate	b
Group II					
no tail (*ntl*)*	*m147, m550*	B, C	Notochord fails to vacuolate	Posterior segments not specified	c, d, e
gno (*gno*)	*m622*	B, C	Notochord fails to vacuolate		
Group III					
sleepy (*sly*)*	*m86, m91, m99, m152, m253, m388, m466, m515, m516, m707*	A, C	Notochord fails to vacuolate	Brain defects, eye defects	f
bashful (*bal*)*	*m102, m113, m190, m255, m268, m277, m290, m296, m430, m473, m373*	A, C	Notochord fails to vacuolate	Brain defects, eye defects	f
grumpy (*gup*)*	*m135, m189, m217, m726, m753*	A, C	Notochord fails to vacuolate	Brain defects, eye defects	f
Group IV					
dopey (*dop*)*	*m341, m475*	B, C	Notochord fails to vacuolate	d2 embryo degeneration	
sneezy (*sny*)*	*m456*	B, C	Notochord fails to vacuolate	d2 embryo degeneration	
mikry (*mik*)	*m218*	A, B, C	Notochord fails to vacuolate	d3 embryo degeneration	
nototod (*not*)	*m128*	B	d2 notochord degeneration	d2 somite degeneration	
Group V					
snow white (*snw*)	*m454*	B	d3 notochord shortened, d1 spherical notochord cells	Melanophores lightly pigmented	
changeling (*chg*)	*m275*	B	d2 spherical notochord cells	Not fully penetrant	
maggot (*mgt*)	*m350, m503, m635*	A, B, D	d1 spherical notochord cells, d2 notochord shorter	Head smaller, jaw/arch defects	
mind bomb (*mib*)	*m132, m178*	A, D	d1 sperical notochord cells, d2 notochord thinner	CNS neurogenesis defects	f
Group VI					
gitolo (*git*)	*m342*	B	d3 notochord shortened	Not fully penetrant	
drobny (*drb*)	*m759*	B	d3 notochord shortened	Viable	
snorri (*sno*)	*m563, m672*	B	d3 notochord shortened		
proteus (*pro*)	*m642*	B	Notochord breaks	Not fully penetrant	
Group VII					
gulliver (*gul*)	*m208*	A, B	d1 folded notchord	Head small	
leviathan (*lev*)	*m531*	B	Folded notochord	Partially dominant	
trilobite (*tri*)*	*m144, m209, m747, m778*	A, B	Notochord folded in tail	Slowed convergence	a
knypek (*kny*)	*m119*	A, B	Notochord folded in tail	Slowed convergence	a
heads up (*hup*)	*m438, m420, m568*	B, D	Notochord thinner	Head small, uncoordinated body movements	
Group VIII					
one-eyed pinhead (*oep*)*	*m134*	A	Notochord curved ventrally	d1 reduced floor plate, cyclopia	a, f
cyclops (*cyc*)*	*m101, m122, m294*	A	Persistent *col2a1* expression	d1 reduced floor plate, cyclopia	g, h
uncle freddy (*unf*)	*m768*	A	Notochord curved ventrally, breaks in sheath	Reduced floor plate d1, mild cyclopia	f
Group IX					
falisty (*fal*)	*m371*	A	Notochord curved	Reduced neurocoel	
falowany (*flw*)	*m735*	A	Notochord curved	Reduced neurocoel, ear malformations	

*Complementation testing has been preformed between these loci and the Tübingen group loci of the same name.

**Category: four different groups of loci (A, B, C, D) were tested for complementation. For example all loci listed as category A were mutually tested and constitute distinct complementation groups.

a, Solnica-Krezel et al. (1996); b, Talbot et al. (1995); c, Schulte-Merker et al. (1994); d, Schulte-Merker et al. (1992); e, Halpern (1993); f, Schier et al. (1996); g, Hatta et al. (1991b); h, Yan et al. (1995).

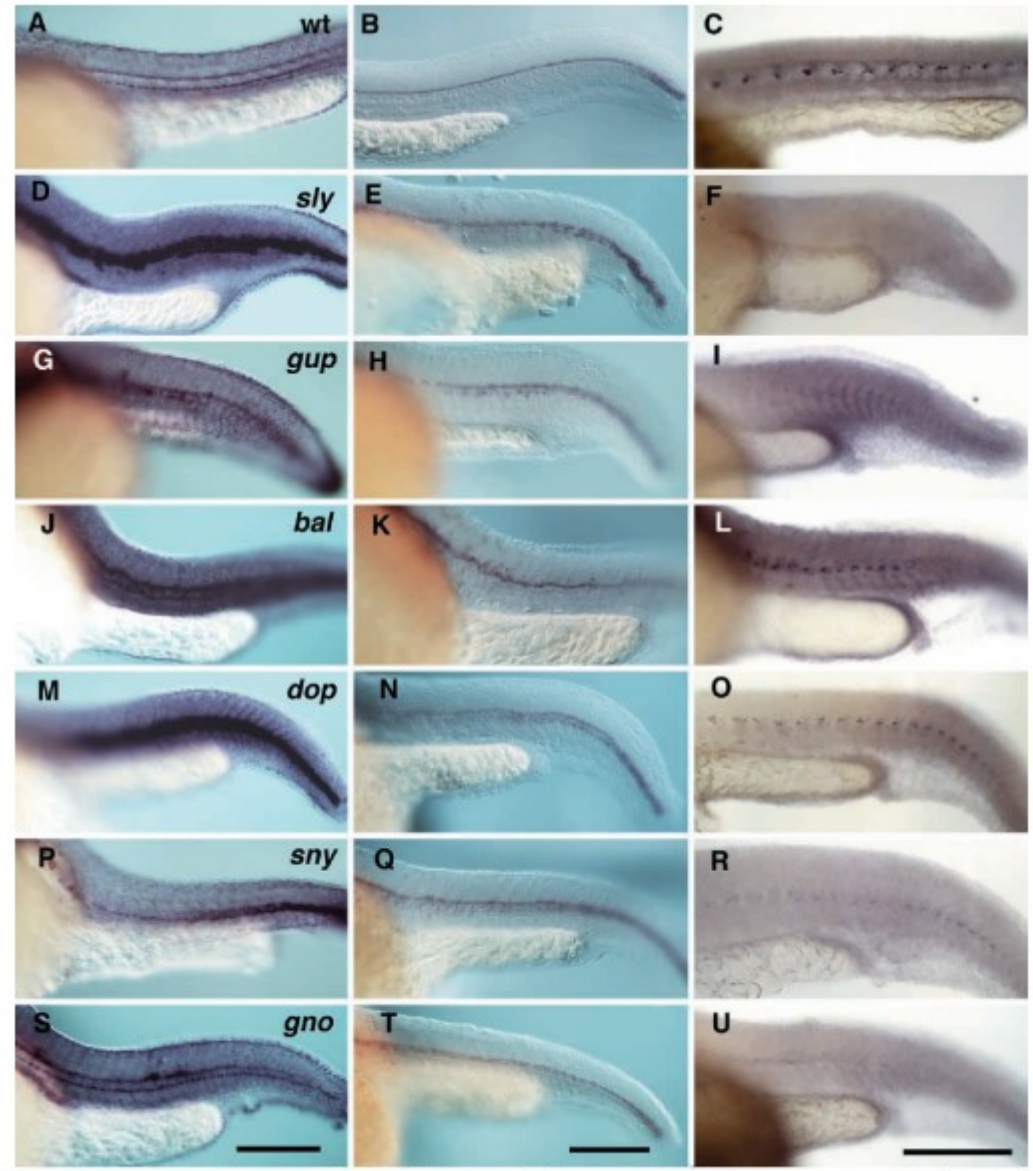

Fig. 5. *col2a1*, *shh*, and Engrailed expression in mutants in the *sly*, *gup*, *bal*, *dop*, *sny*, and *gno* loci. Shown are DIC micrographs of (A-C) wild-type embryos, and (D-F) sly^{m466}, (G-I) gup^{m189}, (J-L) bal^{m190}, (M-O) dop^{m341}, (P-R) sny^{m456}, and (S-U) gno^{m622} mutant embryos stained by in situ hybridization with anti-sense zebrafish *col2a1* (A,D,G,J,M,P,S), *shh* (B,E,H,K,N,Q,T) RNA or with monoclonal anti-Engrailed antibody 4D9 (C,F,I,L,O,R,U). Embryos stained for *col2a1* are at 32 hpf and embryos stained for *shh* or Engrailed are at 24 hpf. Scale bars, 250 μm.

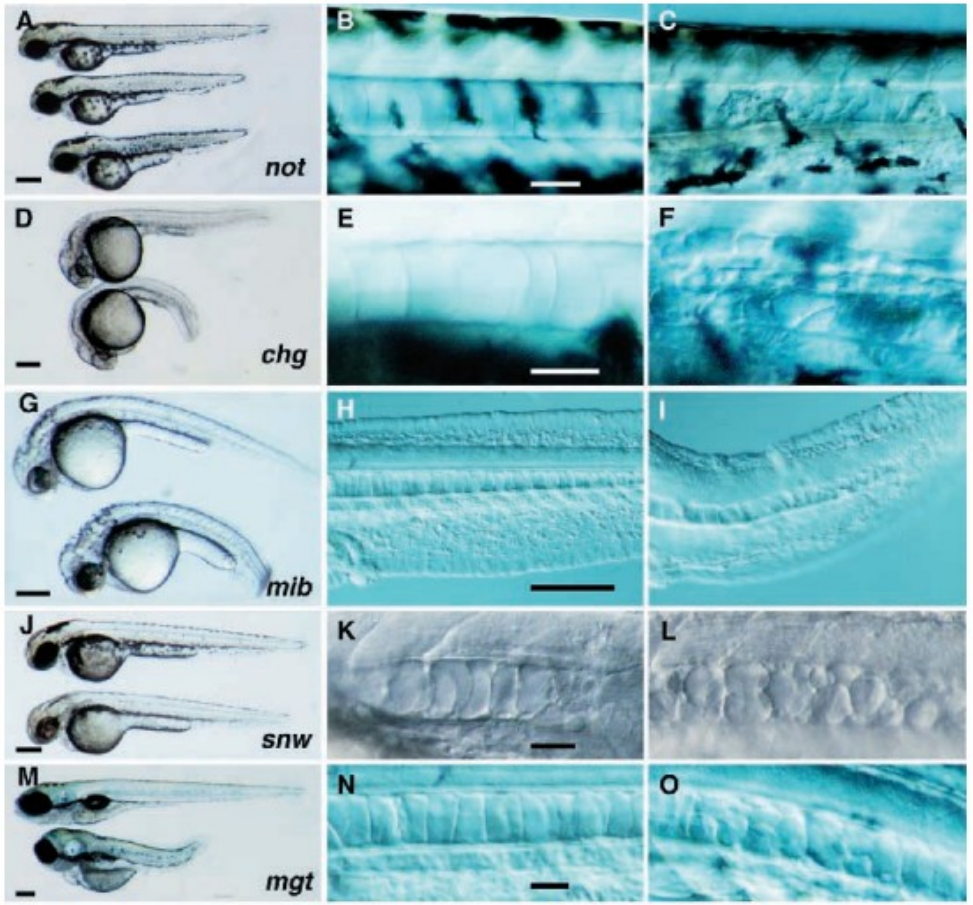

Fig. 6. Notochord phenotype of mutants in the *not, chg, mib, snw,* and *mgt* loci (A) The not^{m128} phenotype first becomes apparent at 48 hpf, manifest as regions of degeneration in the notochord (middle) or the notochord and muscle (lower). (B) Wild-type 48 hour notochord under DIC optics and (C) a not^{m128} mutant notchord displays abnormal cellular morphology and regions of degeneration. (D) The phenotype of chg^{m275} mutants becomes apparent by 24 hpf. By 48 hpf the notochord cellular morphology is abnormal throughout the axis. Shown is an anterior notochord from a 48 hpf wild-type embryo (E) and a corresponding region of a chg^{m275} mutant notochord (F). (G) Shown is a mib^{m132} mutant (lower) and a wild-type sibling (upper) at 24 hpf. (H) A 24 hpf wild-type tail and (I) mib^{m132} mutant tail show abnormal morphology of cells in the mutant notochord. The mutation snw^{m454} combines two phenotypes, regions of disrupted notochord with an overall failure to form melanophores properly. (J) In a 48 hpf snw^{m454} mutant (lower) the lack of melanophores is especially apparent on the yolk sac and in the head. The xanthophores and iridophores and the retinal pigmented epithelium are apparently unaffected. (K) A wild-type 28 hpf notochord displays the normal scalloped notochord cell morphology. (L) Regions of the notochord in *snw* mutants display an unusual phenotype in which rounded cells are present instead of the normally scalloped vacuolated notochord cells. (M) By 120 hpf mgt^{m635} mutant embryos (lower) are severly shorter than wild-type. Additionally, the mutants have abnormal craniofacial development including reduced branchial arch development. (N) A 32 hpf wild-type notochord and (O) a mgt^{m635} notochord with morphologically abnormal spherical cells. Scale bars, 250 µm (A,D,G,H,J,M); 50 µm (B,E,K,N).

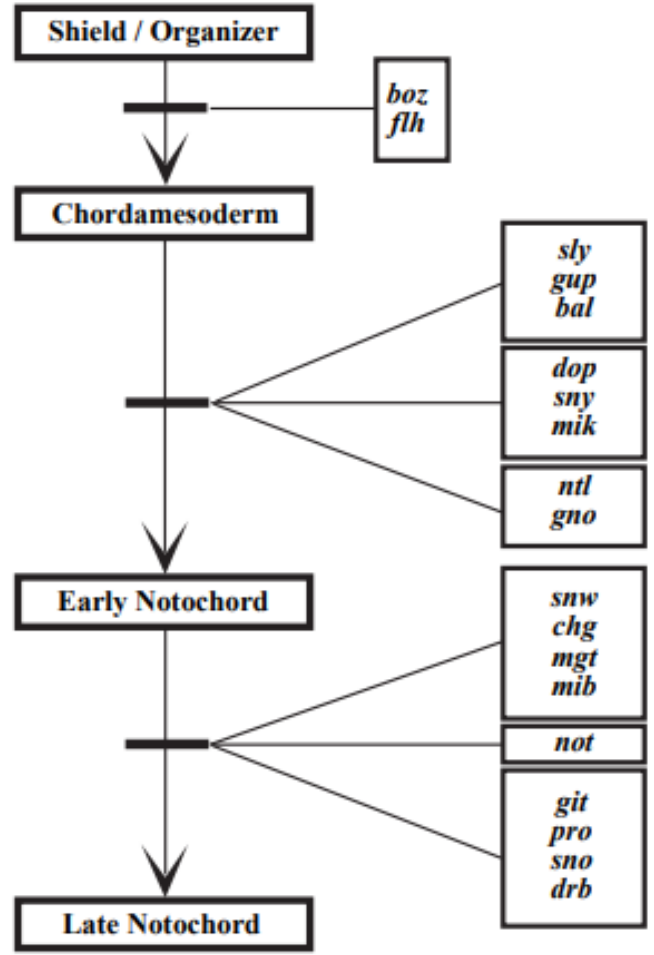

Fig. 9. Model of notochord formation and maintenance: A phenotypic pathway. Tissues at various stages of development are represented by the horizontal boxes. Heavy black arrows between tissues represent a progenitor-product relationship between the tissues. Mutations thought to act in a given process are listed in boxes with thin lines connecting them to heavy horizontal bars that, in turn, denote the place or developmental stage at which the associated mutations seem to act primarily.

Molecular Genetics of Axis Formation in Zebrafish

Alexander F. Schier[1] and William S. Talbot[2]

[1]Developmental Genetics Program, Skirball Institute of Biomolecular Medicine, Department of Cell Biology, New York University School of Medicine, New York, NY 10016-6497; email: schier@saturn.med.nyu.edu; present address: Department of Molecular and Cellular Biology, Harvard University, Cambridge, Massachusetts 02138

[2]Department of Developmental Biology, Stanford University School of Medicine, Stanford, California 94305; email: talbot@cmgm.stanford.edu

Annu. Rev. Genet.
2005. 39:561–613

First published online as a Review in Advance on August 9, 2005

The *Annual Review of Genetics* is online at genet.annualreviews.org

doi: 10.1146/annurev.genet.37.110801.143752

0066-4197/05/1215-0561$20.00

Key Words

gastrulation, mesoderm, endoderm, ectoderm, Nodal, Bmp, FGF, Wnt, retinoic acid

Abstract

The basic vertebrate body plan of the zebrafish embryo is established in the first 10 hours of development. This period is characterized by the formation of the anterior-posterior and dorsal-ventral axes, the development of the three germ layers, the specification of organ progenitors, and the complex morphogenetic movements of cells. During the past 10 years a combination of genetic, embryological, and molecular analyses has provided detailed insights into the mechanisms underlying this process. Maternal determinants control the expression of transcription factors and the location of signaling centers that pattern the blastula and gastrula. Bmp, Nodal, FGF, canonical Wnt, and retinoic acid signals generate positional information that leads to the restricted expression of transcription factors that control cell type specification. Noncanonical Wnt signaling is required for the morphogenetic movements during gastrulation. We review how the coordinated interplay of these molecules determines the fate and movement of embryonic cells.

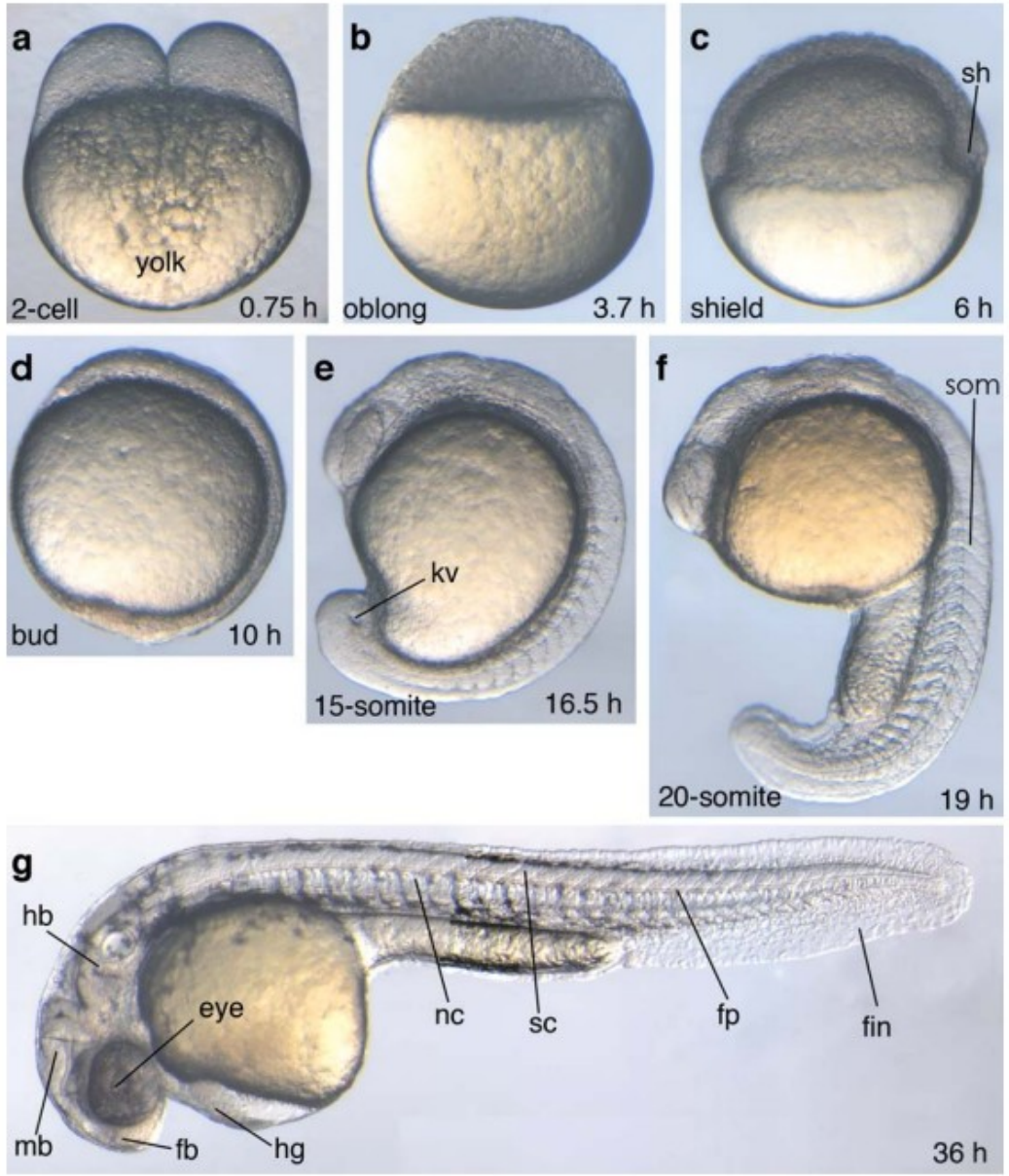

Figure 1

Zebrafish embryogenesis. Living zebrafish embryos are shown at the indicated developmental stages. Approximate developmental ages in hours postfertilization (h) are shown. Embryos are oriented: (*a*,*b*) animal pole to top; (*c*) animal pole to top, dorsal to the right; (*d–f*) anterior to the top, dorsal to the right; (*g*) anterior to the left, dorsal to the top. Abbreviations: sh, embryonic shield; kv, Kupffer's vesicle; som, somite; hg, hatching gland; fb, forebrain; mb, midbrain; hb, hindbrain; nc, notochord; sc, spinal cord; fp, floor plate. For further details see Reference 155.

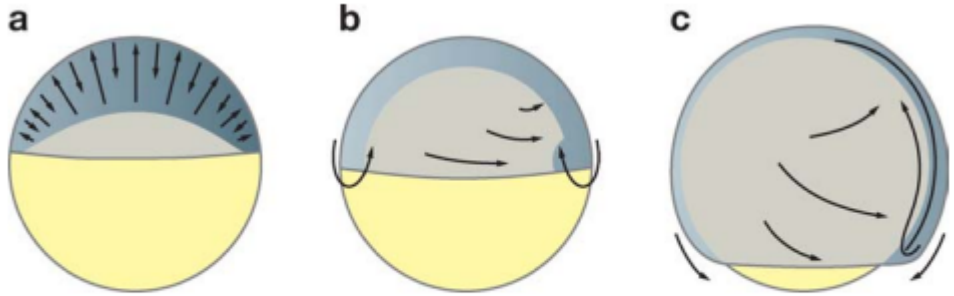

Figure 2

Gastrulation movements. (*a*) Dome stage. Cells intercalate radially, contributing to epiboly. (*b*) Shield stage. Cells at the margin internalize and migrate toward the animal pole. Cells converge dorsally, with lateral mesodermal cells starting convergence at later stages than cells closer to the shield (282). (*c*) 90% epiboly stage. Epiboly, internalization, convergence and extension continue. Modified from Reference 138.

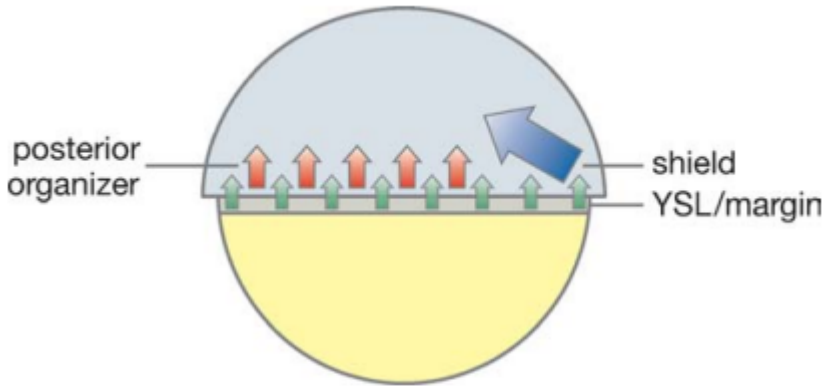

Figure 4

Zebrafish organizing centers. Lateral view, dorsal to the right, animal pole to the top. Yolk syncytial layer (YSL) can induce mesendodermal fates upon transplantation (*green arrows*). Posterior organizer is located at the ventral and lateral margin and can induce tail, posterior trunk, and hindbrain tissue upon transplantation (*red arrows*). Shield corresponds to Spemann-Mangold organizer and can induce dorsal and anterior structures upon transplantation (*blue arrow*).

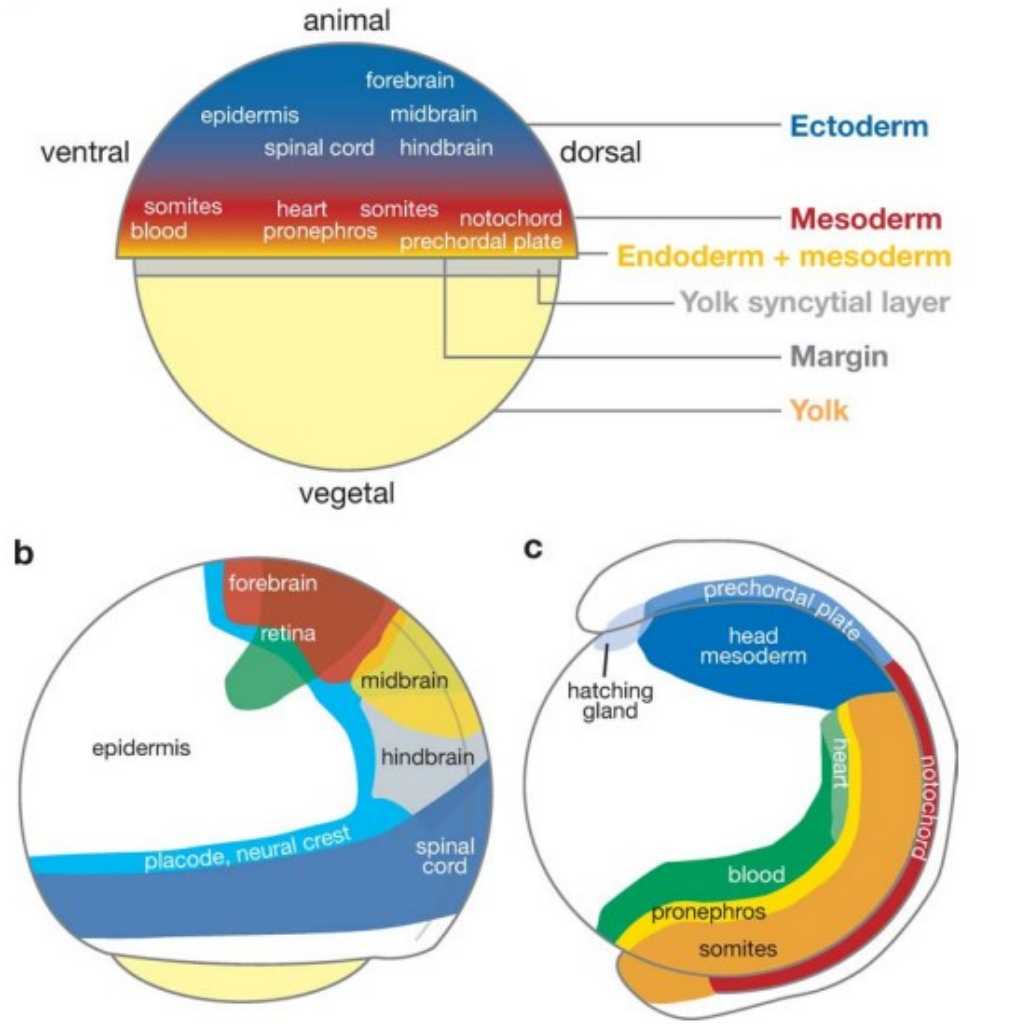

Figure 3

Zebrafish fate maps. (*a*) Fate map at 50% epiboly stage, the onset of gastrulation. Lateral view, dorsal to the right, animal pole to the top. Germ layers are arranged along the animal-vegetal axis. Different mesodermal and ectodermal fates are arranged along the dorsal-ventral axis. For details see References 66, 101, 145, 161, 345. For distribution of endodermal fates see Reference 334. No precise boundaries are depicted because cell fates are often intermingled. Modified from Reference 267. (*b*) Fate map of ectoderm at 90% epiboly. Lateral view, dorsal to the right, animal pole and anterior to the top. Modified from Reference 345; position of spinal cord territory is inferred from Reference 172. (*c*) Model fate map of mesoderm at early somite stage. Lateral view, dorsal to the right, animal pole and anterior to the top. Note that no precise fate map has been established at this stage. Therefore, regions shown here are approximations derived in part from the expression patterns of marker genes (ZFIN.org). The posterior region of the tail bud will continue to extend and give rise to different mesodermal and ectodermal fates. Modified from Reference 138.

Eddy De Robertis proposed an Urbilaterian shared ancestor. Ur = original

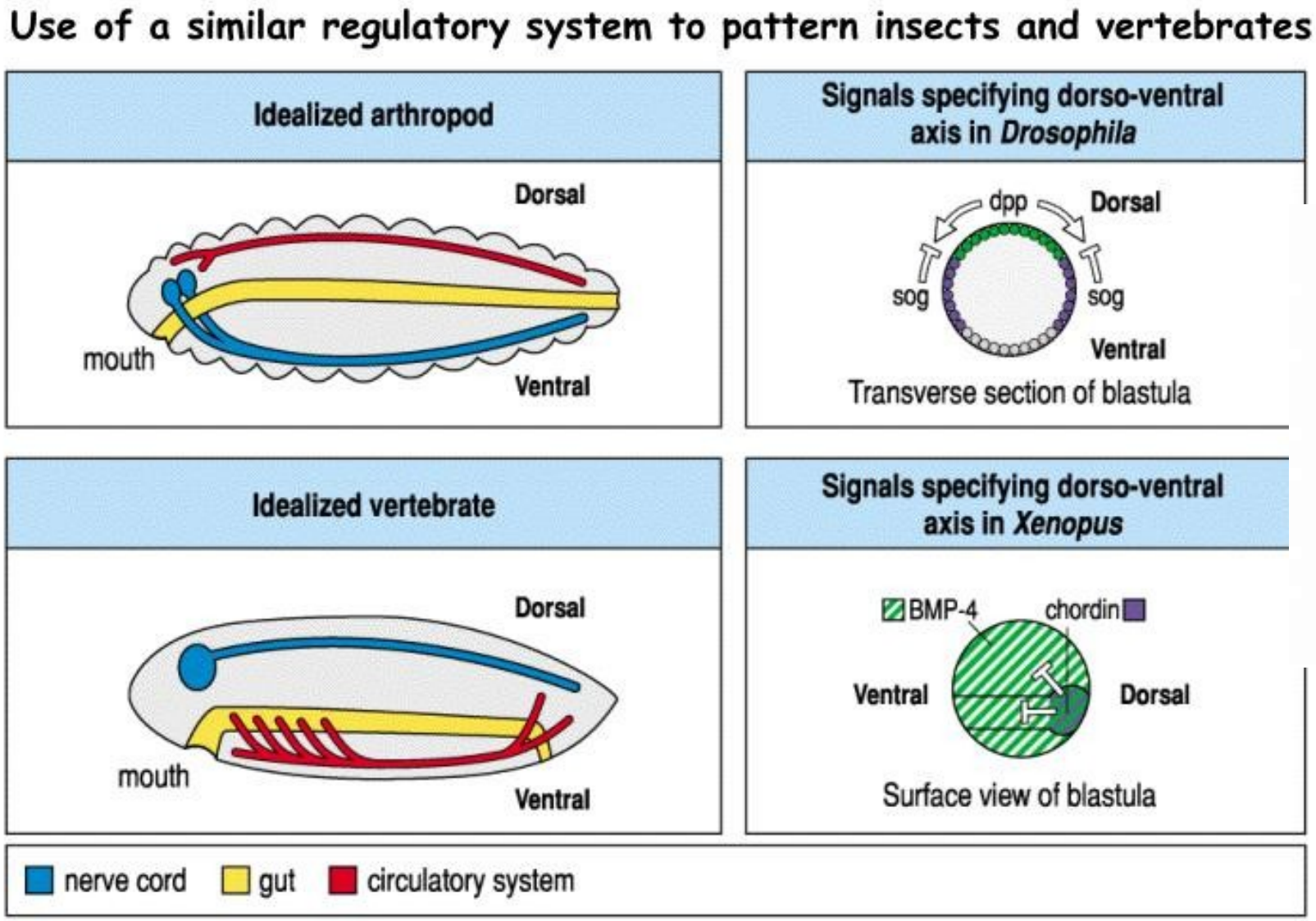

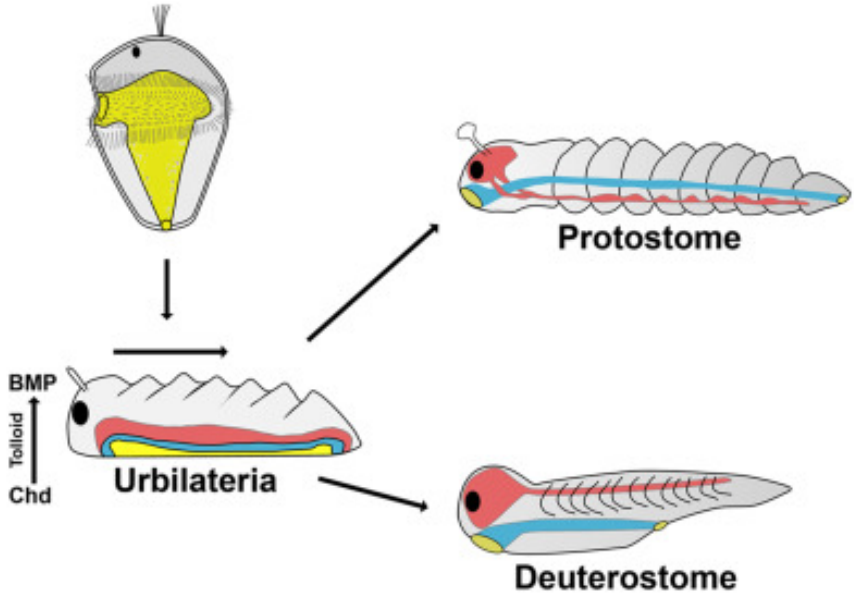

Download: Download high-res image (181KB)

Download: Download full-size image

Fig.8. Urbilateria was the last common ancestor of the deuterostomes and protostomes, and we propose that it had a primary larval form for dispersing in plankton before settling in the sea bottom for adult life. In the diagram shown here the digestive tract of this crawling creature is shown as open lengthwise extending form mouth and to anus (in yellow). This type of gastrulation is called amphistomy, to distinguish it from protostomy (mouth-first) and deuterostomy (mouth-second) type of gastrulation. The CNS is shown in red and is induced in the vicinity of the blastopore. When the ectoderm closes the elongated blastopore ventrally to form a gut tube (in blue), the protostome the nerve cord adopts a ventral subepidermal position, while the brain forms a supraesophageal ganglion that is traversed by the gut in the protostomes. In the deuterostomes a new mouth is formed ventrally and the CNS is not traversed by the gut.

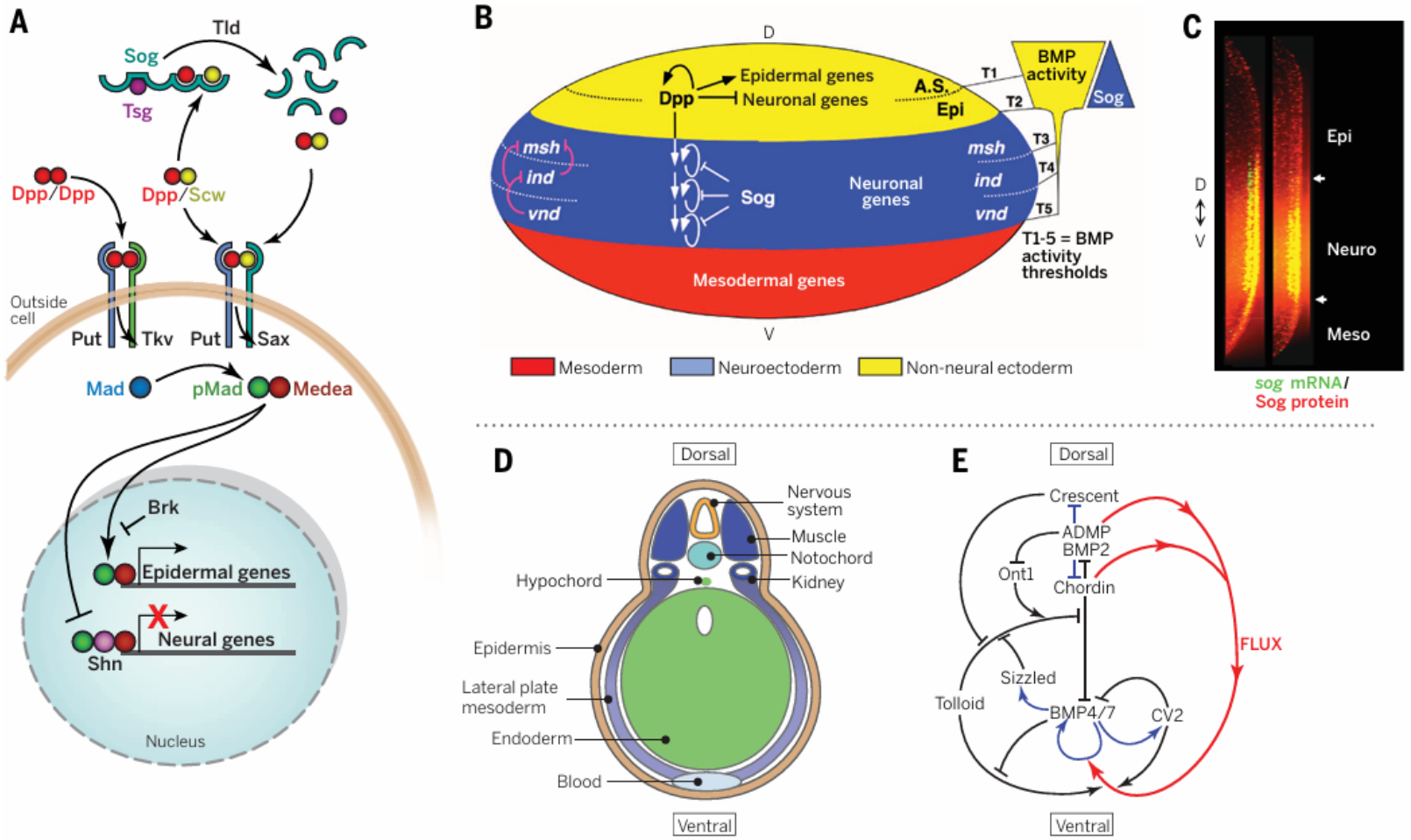

Fig. 2. BMP patterning during neural induction in *Drosophila* and *Xenopus*. (**A**) Diagram of BMP signaling components in *Drosophila*. See text for details. (**B**) Diagram of an early blastoderm-stage *Drosophila* embryo showing subdivision of the DV axis into mesoderm, neuroectoderm, and epidermis. (Right) A high-level BMP activity gradient in dorsal Dpp-expressing cells is created in response to an inverse Sog gradient (emanating from the neuroectoderm) that subdivides the epidermal region into amnioserosa and epidermis proper (thresholds T1 and T2, respectively). A low-level BMP gradient in the neuroectoderm helps partition this region into the three domains expressing the neural identity genes *msh*, *ind*, and *vnd* (thresholds T3 to T5, respectively). (Left) The neural identity genes engage in ventral-dominant repression wherein Vnd inhibits *ind* and *msh* and Ind inhibits *msh*. (**C**) Sog protein gradient viewed in cross section at two successive stages in the blastoderm embryo (left, when Sog protein is first expressed; right, 15 min later). (**D**) Stereotypical DV tissue types of the vertebrate body plan. (**E**) BMP activity along the DV axis results from a series of direct protein-protein interactions between Chordin and other partners (black arrows), transcriptional regulation (blue arrows), and protein flux (red arrows). The entire embryo participates in forming the BMP gradient, which results from the dueling activities of the dorsal and ventral signaling centers. (**F**) Diagram of a sagittal section of a *Xenopus* gastrula (as proposed by P. Nieuwkoop). Brachet's cleft is the narrow cavity that separates the mesendoderm from the ectoderm, encircling the entire DV axis (arrows). (**G**) The Chordin protein gradient spans the entire DV axis. (**H**) Distribution of Fibronectin protein in a comparable embryo is uniform. (**I**) Chordin mRNA is transcribed only on the dorsal side. (**J**) Protein quantification along the DV Brachet's cleft; the gradient forms over 2 mm. (**K**) Chordin fluorescence in radial tracings along the numbered arrows indicated in (G). [Credits: (C) figure 1, b′ and b″, of (*22*); (E to K) from (*40*)]

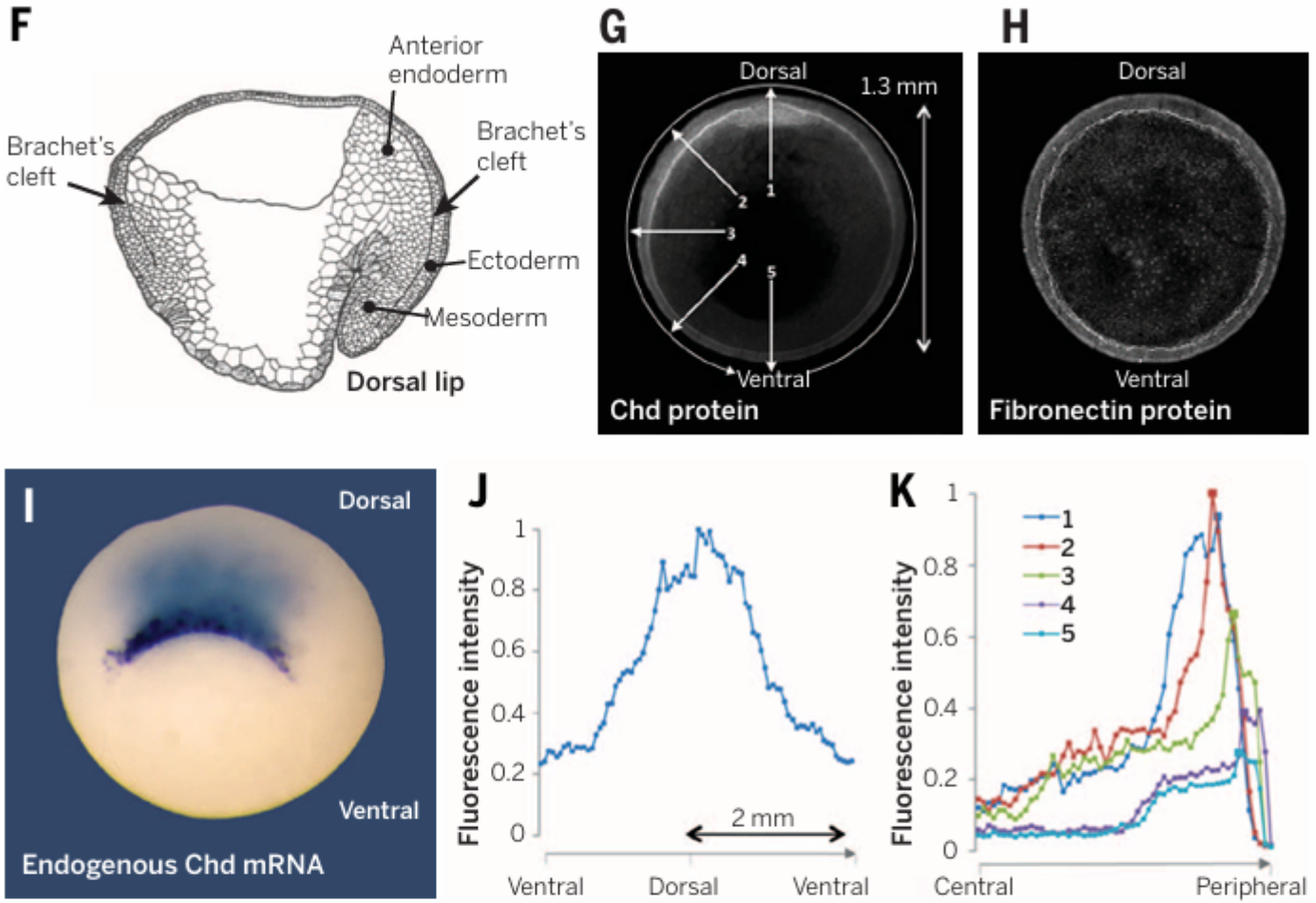

Fig. 2. BMP patterning during neural induction in *Drosophila* and *Xenopus*. (**A**) Diagram of BMP signaling components in *Drosophila*. See text for details. (**B**) Diagram of an early blastoderm-stage *Drosophila* embryo showing subdivision of the DV axis into mesoderm, neuroectoderm, and epidermis. (Right) A high-level BMP activity gradient in dorsal Dpp-expressing cells is created in response to an inverse Sog gradient (emanating from the neuroectoderm) that subdivides the epidermal region into amnioserosa and epidermis proper (thresholds T1 and T2, respectively). A low-level BMP gradient in the neuroectoderm helps partition this region into the three domains expressing the neural identity genes *msh*, *ind*, and *vnd* (thresholds T3 to T5, respectively). (Left) The neural identity genes engage in ventral-dominant repression wherein Vnd inhibits *ind* and *msh* and Ind inhibits *msh*. (**C**) Sog protein gradient viewed in cross section at two successive stages in the blastoderm embryo (left, when Sog protein is first expressed; right, 15 min later). (**D**) Stereotypical DV tissue types of the vertebrate body plan. (**E**) BMP activity along the DV axis results from a series of direct protein-protein interactions between Chordin and other partners (black arrows), transcriptional regulation (blue arrows), and protein flux (red arrows). The entire embryo participates in forming the BMP gradient, which results from the dueling activities of the dorsal and ventral signaling centers. (**F**) Diagram of a sagittal section of a *Xenopus* gastrula (as proposed by P. Nieuwkoop). Brachet's cleft is the narrow cavity that separates the mesendoderm from the ectoderm, encircling the entire DV axis (arrows). (**G**) The Chordin protein gradient spans the entire DV axis. (**H**) Distribution of Fibronectin protein in a comparable embryo is uniform. (**I**) Chordin mRNA is transcribed only on the dorsal side. (**J**) Protein quantification along the DV Brachet's cleft; the gradient forms over 2 mm. (**K**) Chordin fluorescence in radial tracings along the numbered arrows indicated in (G). [Credits: (C) figure 1, b′ and b″, of (*22*); (E to K) from (*40*)]

Table 1 Genes essential for zebrafish axis formation and patterning

Mutation	Gene product	Function	Phenotype	Reference
Bmp signaling				
swirl	Bmp2b	Bmp signal	Severely dorsalized	(162)
snailbouse	Bmp7	Bmp signal	Severely dorsalized	(60, 272)
lost-a-fin	Alk8	Type I Bmp receptor	Severely dorsalized	(22, 209)
somitabun	Smad5	Transcription factor	Weakly (zyg.) or strongly (mat.) dorsalized	(124)
morpholino	Twisted Gastrulation	Bmp agonist	Dorsalized	(186, 350)
minifin	Tolloid	Metalloprotease for Chordin	Weakly dorsalized	(49)
chordino	Chordin	Bmp inhibitor	Ventralized	(277)
ogon	Sizzled	Bmp inhibitor	Ventralized	(199, 351)
morpholino	Radar/Gdf6a	Bmp signal	Dorsalized	(293)
dominant negative	Kheper	Zinc finger/homeodomain	Reduced neuroectoderm	(220)
morpholino	ΔNp63	Transcriptional repressor	Reduced ventral ectoderm	(16, 177)
morpholino	ADMP	Divergent Bmp signal	Dorsalized	(180, 341)
Canonical Wnt signaling				
wnt8	Wnt8	Wnt signal	No ventral and posterior structures	(72, 179)
masterblind	Axin	Scaffolding protein	No eyes and telencephalon	(117)
headless	Tcf3	Transcription factor	No forebrain and midbrain	(153)
morpholino	Tlc SFRP	Wnt antagonist	Reduced telencephalon	(127)
ichabod	?	β-catenin localization?	Variably ventralized	(147)
tokkaebi	?	β-catenin stability?	Variably ventralized	(228)
morpholino	Sp5 and Sp5-like	SP1 Zn Finger	Anteriorized and dorsalized	(337)
Nodal signaling				
cyclops	Cyc (Nodal)	Nodal signal	Cyclopia	(115, 252, 265)
squint	Sqt (Nodal)	Nodal signal	Cyclopia, dorsal mesoderm defects	(79)
morpholino	Southpaw (Nodal)	Nodal signal	Loss or randomization of LR asymmetry	(191)
cyclops;squint			No endoderm and head/trunk mesoderm	(79)
one-eyed pinhead	EGF-CFC	Nodal co-receptor	No endoderm and head/trunk mesoderm	(102)
schmalspur	FAST1/FoxH1	Transcription factor	Dorsal mesoderm defects	(243, 295)
bonnie and clyde	Mix homeodomain	Transcription factor	Reduced endoderm	(151)
morpholino	Lefty1 and Lefty2	Antagonist of Nodal signaling	Increased mesoderm and endoderm	(3)
morpholino	Dapper2	Antagonist of Nodal signaling	Increased mesoderm and endoderm	(362)
morpholino	Charon	Antagonist of Nodal signaling	Loss of LR asymmetry	(114)
FGF signaling				
acerebellar	Fgf8	FGF signal	Ventralized with loss of chordin	(87, 253)
morpholino	Fgf24	FGF signal	Loss of posterior structures with loss of fgf8	(67)
morpholino	Sef	Antagonist of FGF signaling	Dorsalized	(84, 323)
morpholino	Sprouty2	Antagonist of FGF signaling	Dorsalized	(87)
morpholino	MKP3	Antagonist of FGF signaling	Dorsalized	(324)
Retinoic acid signaling				
neckless	Raldh2	RA synthesis pathway	Anterior spinal cord reduced, myocardial progenitors increased	(24, 144)
giraffe	Cyp26a1	RA degradation	Anterior spinal cord expanded	(70, 172)
Transcription factors				
bozozok	Boz homeodomain	Transcriptional repressor	Variable loss of dorsal mesoderm and forebrain	(75)
vox/vent	Vox, Vent homeodomain	Transcriptional repressor	Severely dorsalized in double mutants	(131)
morpholino	Ved homeodomain	Transcriptional repressor	Severely dorsalized with *vox/vent*	(290)
kugelig	Cdx4 homeodomain	Transcription factor	Reduced tail and blood	(56)
morpholino	Prdm1/Blimp1	Transcriptional repressor	Dorsalized	(342)
dominant negative	Iro3	Transcriptional repressor	Reduced dorsal mesoderm	(171)
spiel ohne grenzen	Pou2/Oct4	Transcription factor	Strongly reduced endoderm in maternal-zygotic mutants	(193, 254)
faust	Gata5 Zinc finger	Transcription factor	Reduced endoderm and heart	(255)
casanaova	HMG domain	Transcription factor	Strongly reduced endoderm	(61, 150)
morpholino	Mezzo homeodomain	Transcription factor	Reduced dorsal mesoderm and endoderm with *bon*	(245)
no tail	Ntl T-box	Transcription factor	Loss of notochord and tail	(106, 278)
floating head	Flh homeodomain	Transcription factor	Loss of notochord	(312)
spadetail	Spt T-box	Transcription factor	Loss of paraxial and lateral mesoderm	(99, 156)
Epiboly				
half-baked	E-cadherin	Cell adhesion	Strongly reduced epiboly	(137)
dominant negative	Eomesodermin T-box	Transcriptional activator	Strongly reduced epiboly	(32)
morpholino	Mtx2 homeodomain	Transcription factor	Disrupted epiboly during gastrulation	(32)
Stat3 pathway				
morpholino	Stat3	Transcription factor	Reduced prechordal plate migration and CE	(354)
morpholino	Liv1	Zinc transporter	Reduced prechordal plate migration and CE	(355)
morpholino	Snail1	Zinc-finger transcription factor	Reduced prechordal plate migration	(355)
Planar cell polarity signaling				
silberblick	Wnt11	Wnt signal	Reduced CE	(119)
pipetail	Wnt5	Wnt signal	Reduced CE	(249)
knypek	Glypican4	Wnt co-receptor?	Reduced CE	(320)
trilobite	Strabismus	Transmembrane protein	Reduced CE	(132)

(*Continued*)

Table 1 (*Continued*)

Mutation	Gene product	Function	Phenotype	Reference
morpholino	Frizzled2	Wnt receptor	Reduced CE	(236, 309)
morpholino	Flamingo1a and 1b	7TM protocadherin	Reduced CE	(82)
morpholino	Prickle1	Regulates Fz/Dsh	Reduced CE	(37)
morpholino	Diversin	Ankyrin repeat protein	Reduced CE	(279)
Others				
morpholino	Gα12/13	G protein subunit	Reduced CE	(184)
morpholino	Quattro	Rho GEF	Abnormal prechordal plate migration and CE	(51)
morpholino	CAP1	Regulates actin distribution	Abnormal prechordal plate migration and CE	(51)
dominant negative	Rok2	Kinase	Reduced CE	(197)
dominant negative	Rac1	Small GTPase	Reduced CE	(17)
inhibitor	Phosphoinosite 3-kinase	Kinase	Abnormal prechordal plate migration and CE	(216)
morpholino	Hyaluronan synthase 2	Polysaccharide synthesis	Reduced CE	(17)
landlocked	Scribble1	LRR/PDZ domain protein	Reduced CE	(329)

Abbreviations: LR, left-right; CE, convergence and extension; TM, transmembrane; for more extensive references see text.

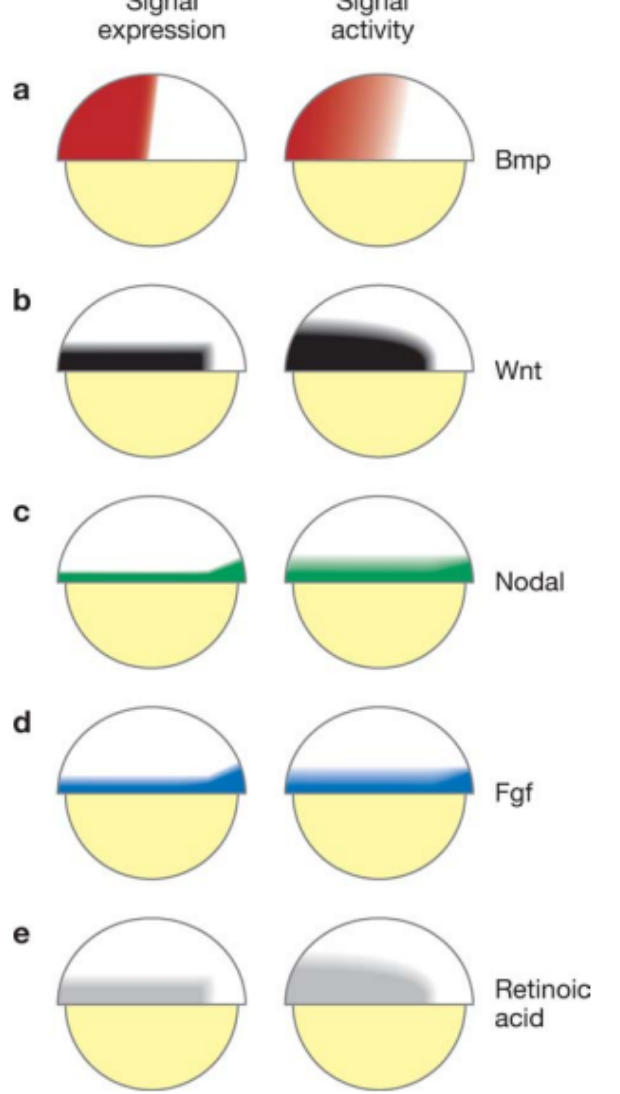

Figure 6

Signals patterning the embryo. Late-blastula stage, lateral view, dorsal to the right, animal pole to the top. Signal expression is based on published reports, but signaling activities are speculative and based on the potential range of signals and the expression pattern and range of antagonists. For example, Bmp signaling activity is inhibited dorsally by antagonists such as Chordin and Noggin. Wnt signaling activity is inhibited by antagonists such as Dickkopf1. Retinoic acid distribution indicates the site of synthesis by RALDH, and activity is inhibited by Cyp26-mediated hydrolysis of retinoic acid dorsally and at the animal pole. Nodal and FGF signals are concentrated on the dorsal side soon after the mid-blastula transition (not shown), but these signals are more uniform across the dorsal-ventral axis by the late-blastula stage that is represented in the figure.

Reading

THE ART AND DESIGN OF GENETIC SCREENS: ZEBRAFISH

E. Elizabeth Patton and Leonard I. Zon

Inventive genetic screens in zebrafish are revealing new genetic pathways that control vertebrate development, disease and behaviour. By exploiting the versatility of zebrafish, biological processes that had been previously obscured can be visualized and many of the responsible genes can be isolated. Coupled with gene knockdown and overexpression technologies, and small-molecule-induced phenotypes, genetic screens in zebrafish provide a powerful system by which to dissect vertebrate gene function and gene networks.

GYNOGENESIS
Development of an organism derived from the genetic material of the female gamete.

Howard Hughes Medical Institute, Children's Hospital of Boston, 300 Longwood Avenue, Enders 750, Boston, Massachusetts 02115, USA. Correspondence to L.I.Z. e-mails: epatton@enders.tch.harvard.edu; zon@enders.tch.harvard.edu

Twenty years ago, George Streisinger's pioneering research revealed the potential of the zebrafish as a vertebrate organism that was suitable for forward genetic screening[1]. A relatively small fish (3–4 cm long as an adult), zebrafish can be easily managed in large numbers in the laboratory environment. The ability to combine embryological and genetic methodology has established the zebrafish as a powerful research tool. External development of transparent embryos allows fundamental vertebrate developmental processes — from gastrulation to organogenesis — to be visualized and studied; in addition, the heart beats and blood circulation of the embryo are readily observed. Touch, sight and behavioural responses can also be monitored in live embryos under the dissecting microscope. Several features, such as a short generation time of 3–4 months, mean that zebrafish are particularly suitable for genetic studies. In addition, mutations can be induced with high frequency in zebrafish, and recessive mutations can be recovered within two generations[2,3]. Large progeny sizes (females lay about 100–200 eggs) facilitate large-scale genetic screening and mutation analysis in a Mendelian fashion.

Here, we review the methods of genetic screening in zebrafish, and include some examples of the resulting mutants and genes discovered from diploid, haploid and GYNOGENETIC diploid screens. We follow with a sampling of the recent, resourceful genetic screening techniques now carried out in zebrafish to show the potential and versatility of the zebrafish genetic system.

First large-scale vertebrate genetic screens

Systematic genome-wide screens for mutations in worms, flies and plants have successfully identified many genes that define embryological pathways. Smaller collections of mammalian mutants provide valuable insights into developmental processes. However, identifying large numbers of mutations in the mammalian system is problematic because of intrauterine development and expensive supporting laboratory facilities. The remarkable characteristics of the zebrafish, along with the initial success of the first zebrafish genetic screens[4], inspired two groups of scientists in Boston[5] and Tübingen[6] to undertake the first large-scale genetic screens in a vertebrate organism. The Boston and Tübingen screens identified mutant embryonic phenotypes in the F_3 generation (FIG. 1). Some of the ~2,000 mutated developmental genes that were identified in these two screens have been cloned, which assists in the dissection of the gene networks that control early development. For example, the genes that are mutated in the endoderm mutants *casanova* (*cas*), *bonnie and clyde* (*bon*), and *faust* (*fau*) can be assembled into a genetic pathway, and have been shown to encode transcription factors that are necessary for endoderm formation[7–12]. Embryo transparency, as well as conspicuous heart, blood and blood vessels in the zebrafish have also made it possible to identify cardiovascular system mutants in a manner that is unprecedented in other animal systems. As an example, the gene *jekyll* (*jek*) is necessary for formation of the

Fig. 25-21

Hypothetical vertebrate ancestor (invertebrate) with a single *Hox* cluster

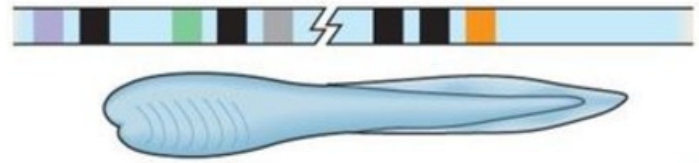

First *Hox* duplication

Duplication of the single *Hox* complex occurs and provides genetic material associated with origin of first vertebrate. Dulpicate set of genes takes on new roles – such as development of backbone.

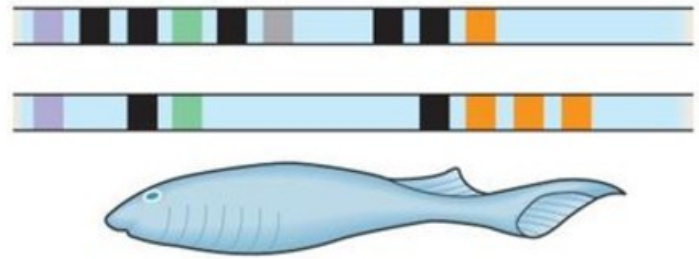

Hypothetical early vertebrates (jawless) with two *Hox* clusters

Second *Hox* duplication

Second duplication of *Hox* complex may have allowed the development of even greater structural complexity – such as jaws and limbs.

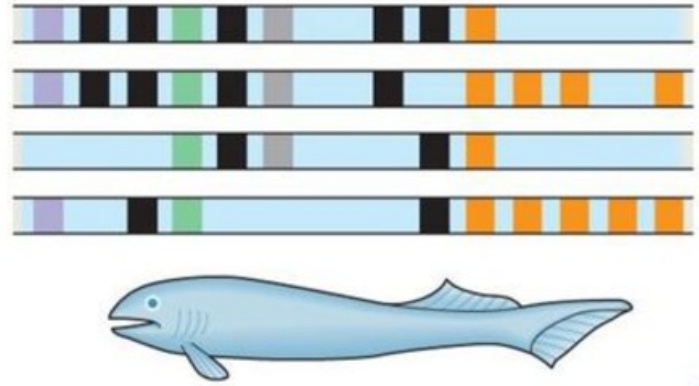

Vertebrates (with jaws) with four *Hox* clusters

Copyright © 2008 Pearson Education, Inc., publishing as Pearson Benjamin Cummings

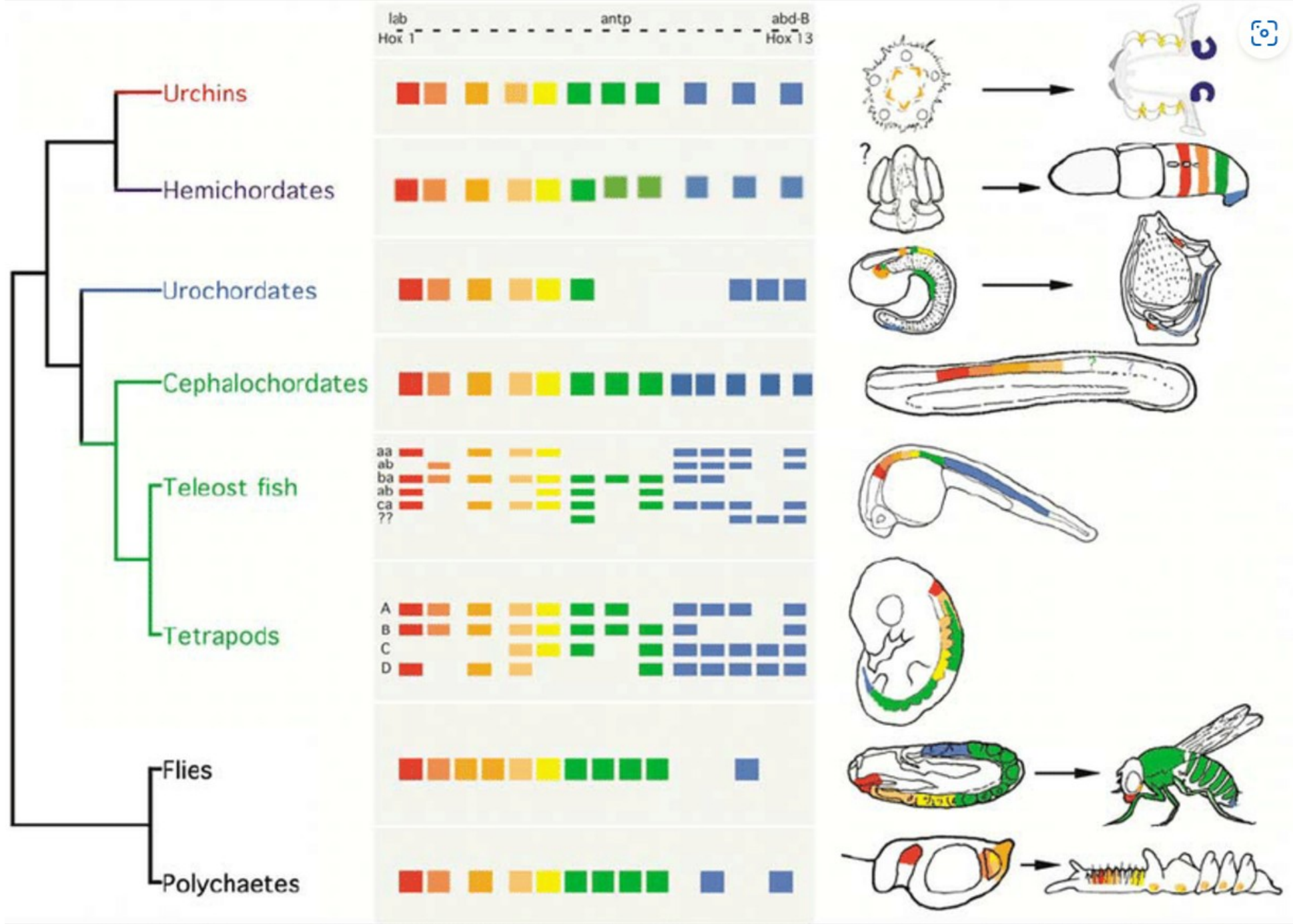

PHYLOGENY GENES FOUND KNOWN EXPRESSION

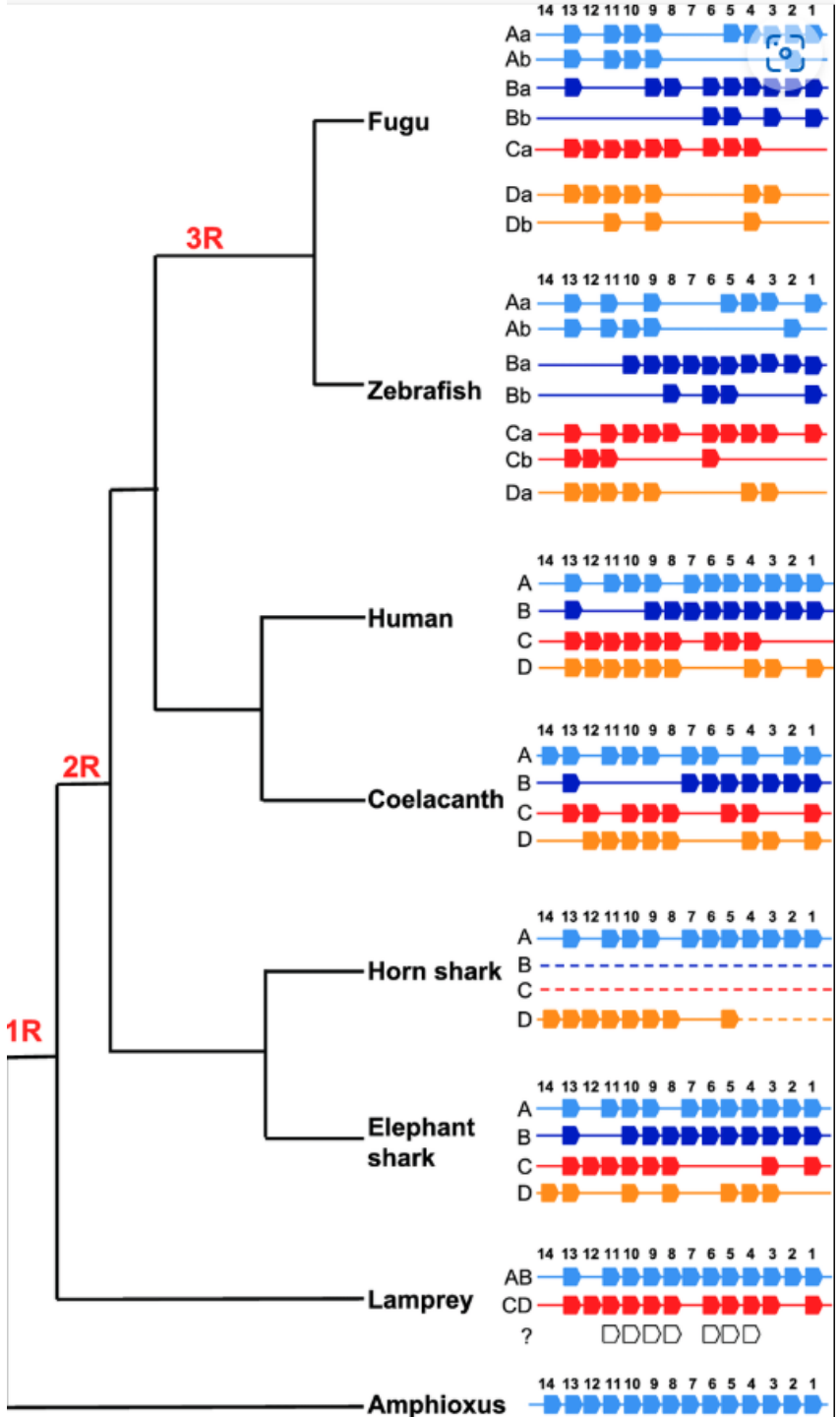
14 13 12 11 10 9 8 7 6 5 4 3 2 1
Aa
Ab
Ba
Bb
Ca
Da
Db
Fugu
3R
Aa
Ab
Ba
Bb
Ca
Cb
Da
Zebrafish
A
B
C
D
Human
2R
Coelacanth
Horn shark
1R
Elephant shark
AB
CD
?
Lamprey
Amphioxus

	Organism	# of protein-coding genes	# of genes naïve estimate: (genome size /1000)	BNID
viruses	HIV 1	9	10	105769
	Influenza A virus	10-11	14	105767
	Bacteriophage λ	66	49	105770
	Epstein Barr virus	80	170	103246
prokaryotes	*Buchnera sp.*	610	640	105757
	T. maritima	1,900	1,900	105766
	S. aureus	2,700	2,900	105500
	V. cholerae	3,900	4,000	105760
	B. subtilis	4,400	4,200	111448
	E. coli	4,300	4,600	105443
eukaryotes	*S. cerevisiae*	6,600	12,000	105444
	C. elegans	20,000	100,000	101364
	A. thaliana	27,000	140,000	111380
	D. melanogaster	14,000	140,000	111379
	F. rubripes	19,000	400,000	111375
	Z. mays	33,000	2,300,000	110565
	M. musculus	20,000	2,800,000	100308
	H. sapiens	21,000	3,200,000	100399, 111378
	T. aestivum (hexaploid)	95,000	16,800,000	105448, 102713

Lecture 12. Early genetic screens and vertebrate genetic screens

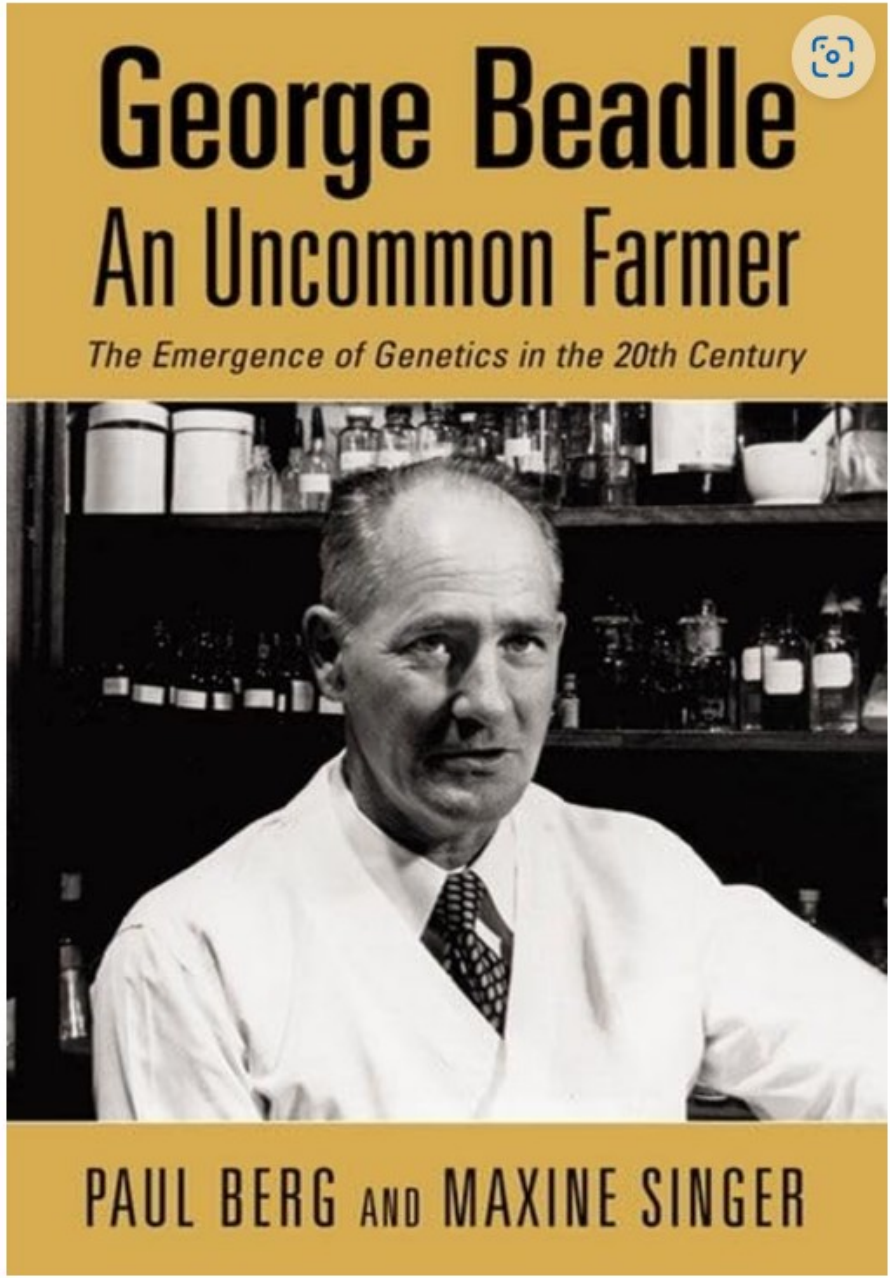

Beadle and Tatum

Using the common bread mold *Neurospora crassa*, in 1941 developed the classic concept of "one gene, one enzyme"
Awarded Nobel Prize in 1945

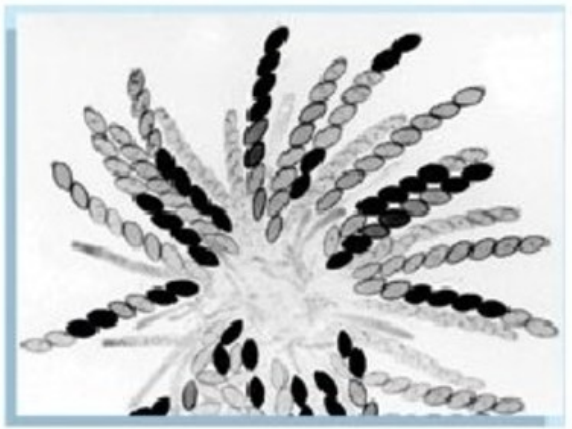

Metabolic mutations in *Drosophila* (Beadle and Ephrussi)

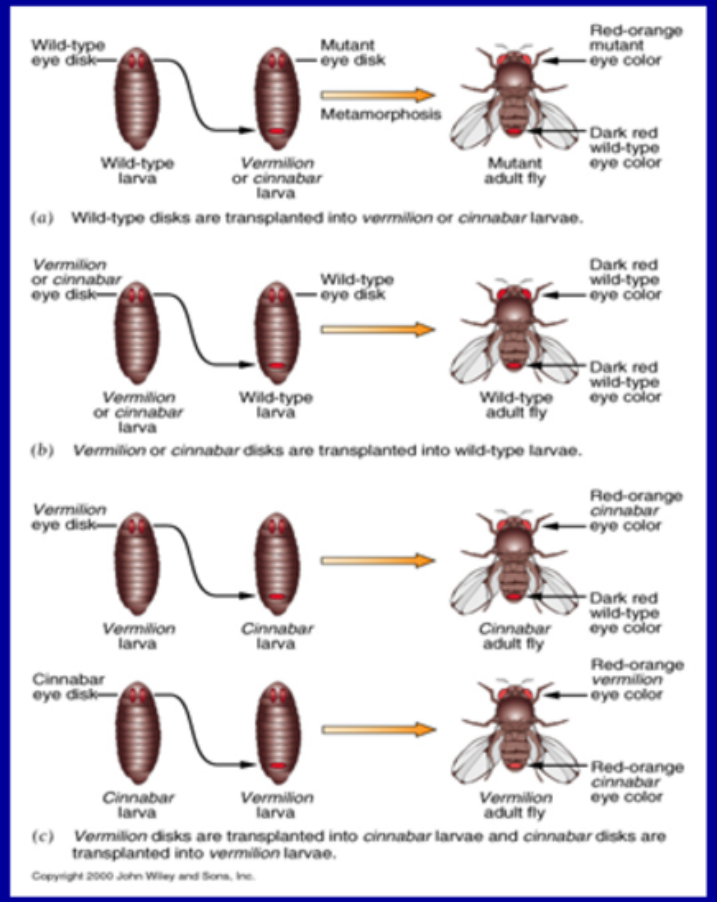

- Fly eyes are normally dark red because of two pigments, one bright red and one brown.
- Mutants in *v* or *cn* have bright red eyes because they lack brown pigment.
- Disk transplantation experiments showed that wild-type hosts produce a diffusible substance than can allow *v* or *cn* disks to form dark red eyes.
- *v* disks transplanted into *cn* hosts also develop normally, but *cn* disks transplanted into *v* hosts still develop bright red eyes!

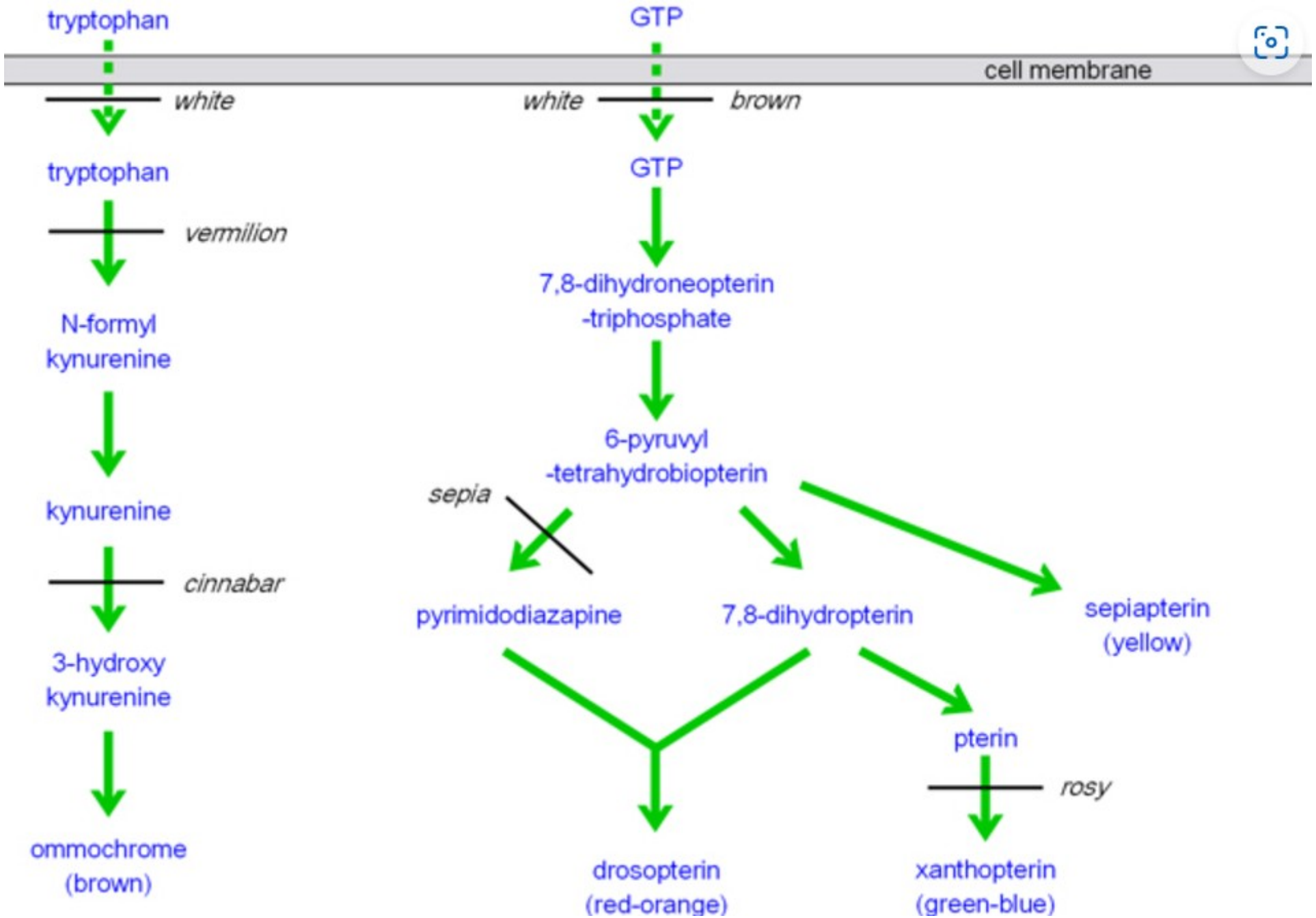
tryptophan
white
tryptophan
vermilion
N-formyl
kynurenine
kynurenine
cinnabar
3-hydroxy
kynurenine
ommochrome
(brown)
GTP
cell membrane
white
brown
GTP
7,8-dihydroneopterin
-triphosphate
6-pyruvyl
-tetrahydrobiopterin
sepia
pyrimidodiazapine
7,8-dihydropterin
sepiapterin
(yellow)
pterin
rosy
drosopterin
(red-orange)
xanthopterin
(green-blue)

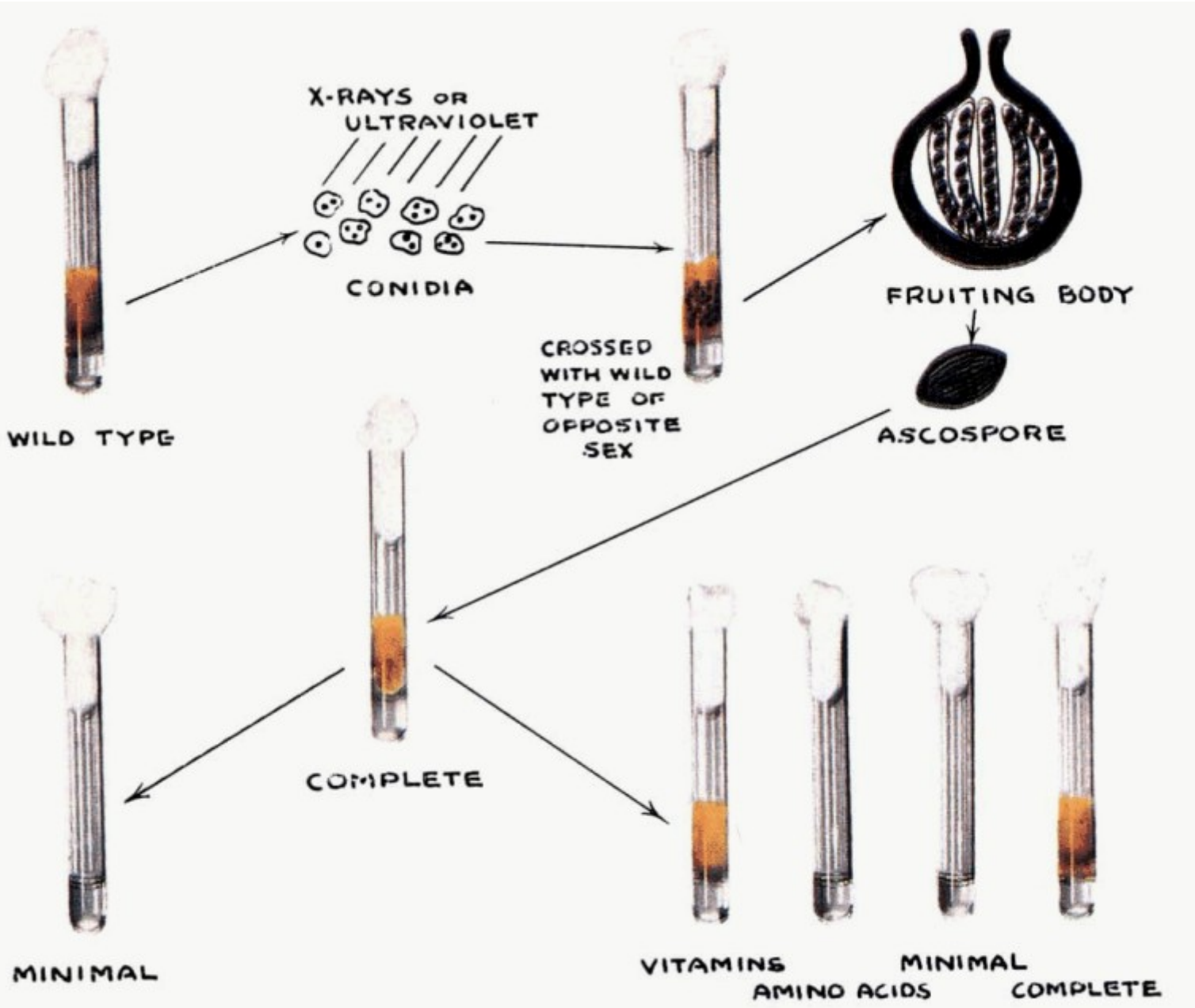

FIGURE 1.—BEADLE's lantern slide explaining the procedure for isolating biochemical mutants of Neurospora.

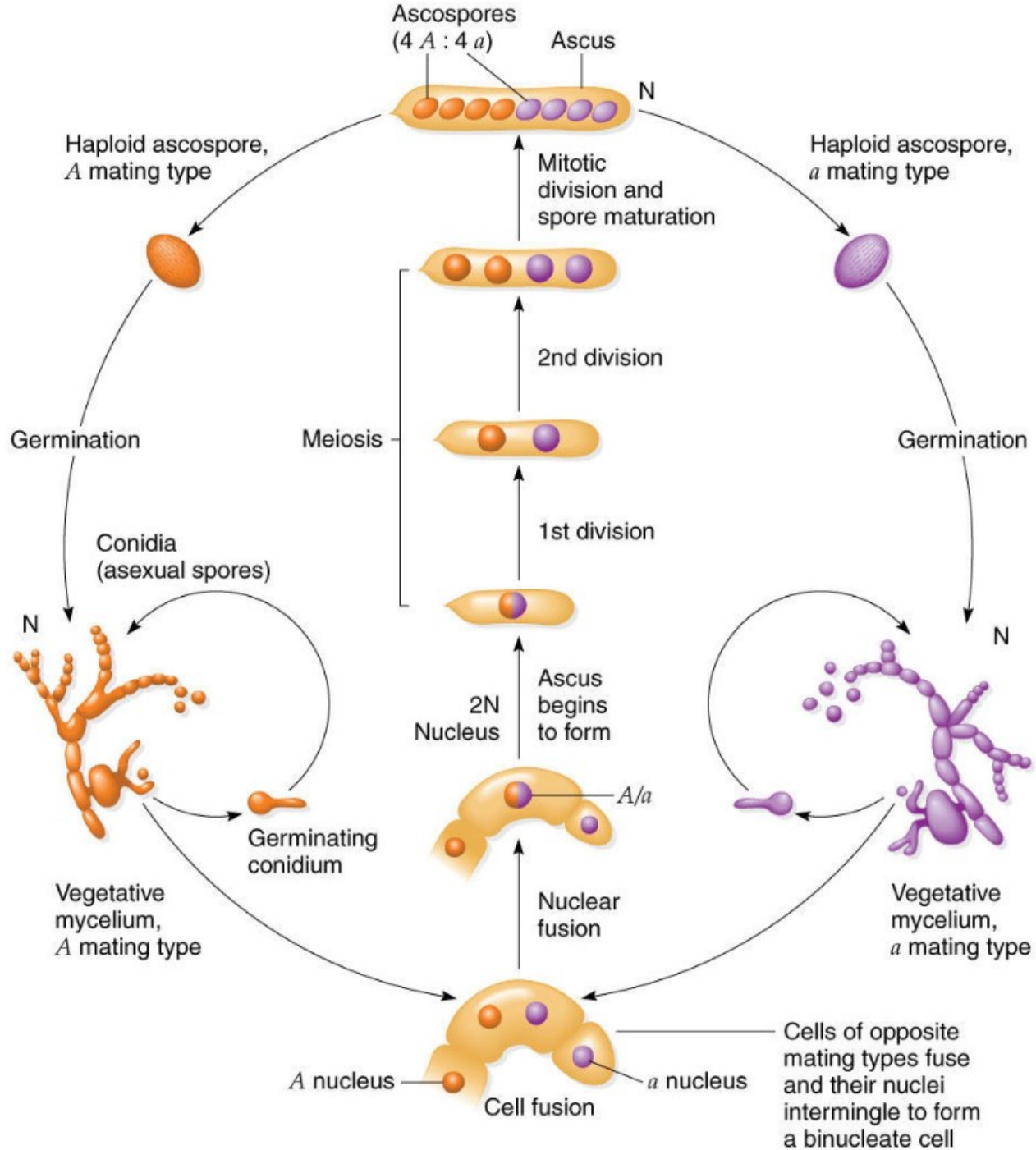

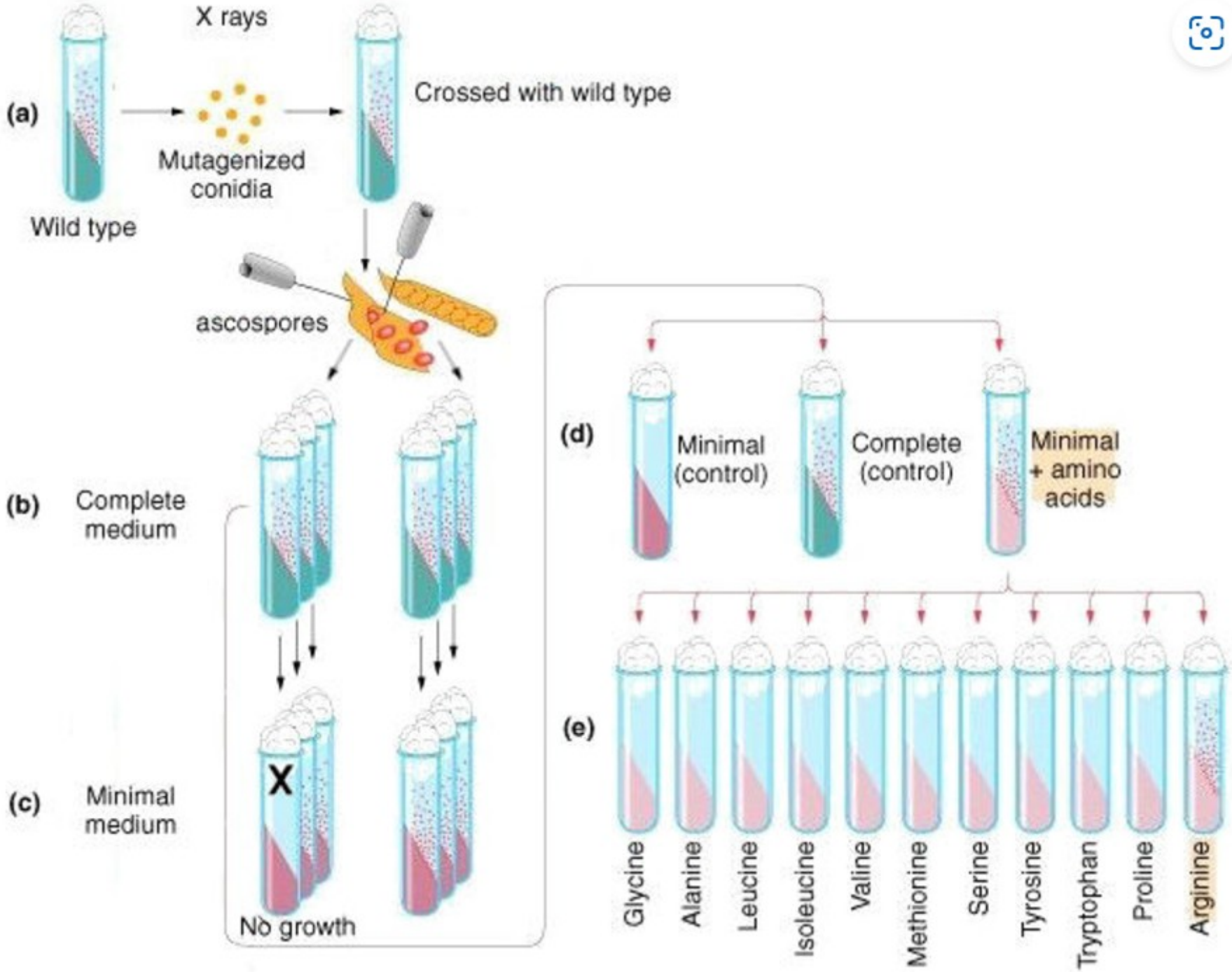
X rays
(a)
Crossed with wild type
Mutagenized conidia
Wild type
ascospores
(b) Complete medium
(c) Minimal medium
X
No growth
(d)
Minimal (control)
Complete (control)
Minimal + amino acids
(e)
Glycine
Alanine
Leucine
Isoleucine
Valine
Methionine
Serine
Tyrosine
Tryptophan
Proline
Arginine

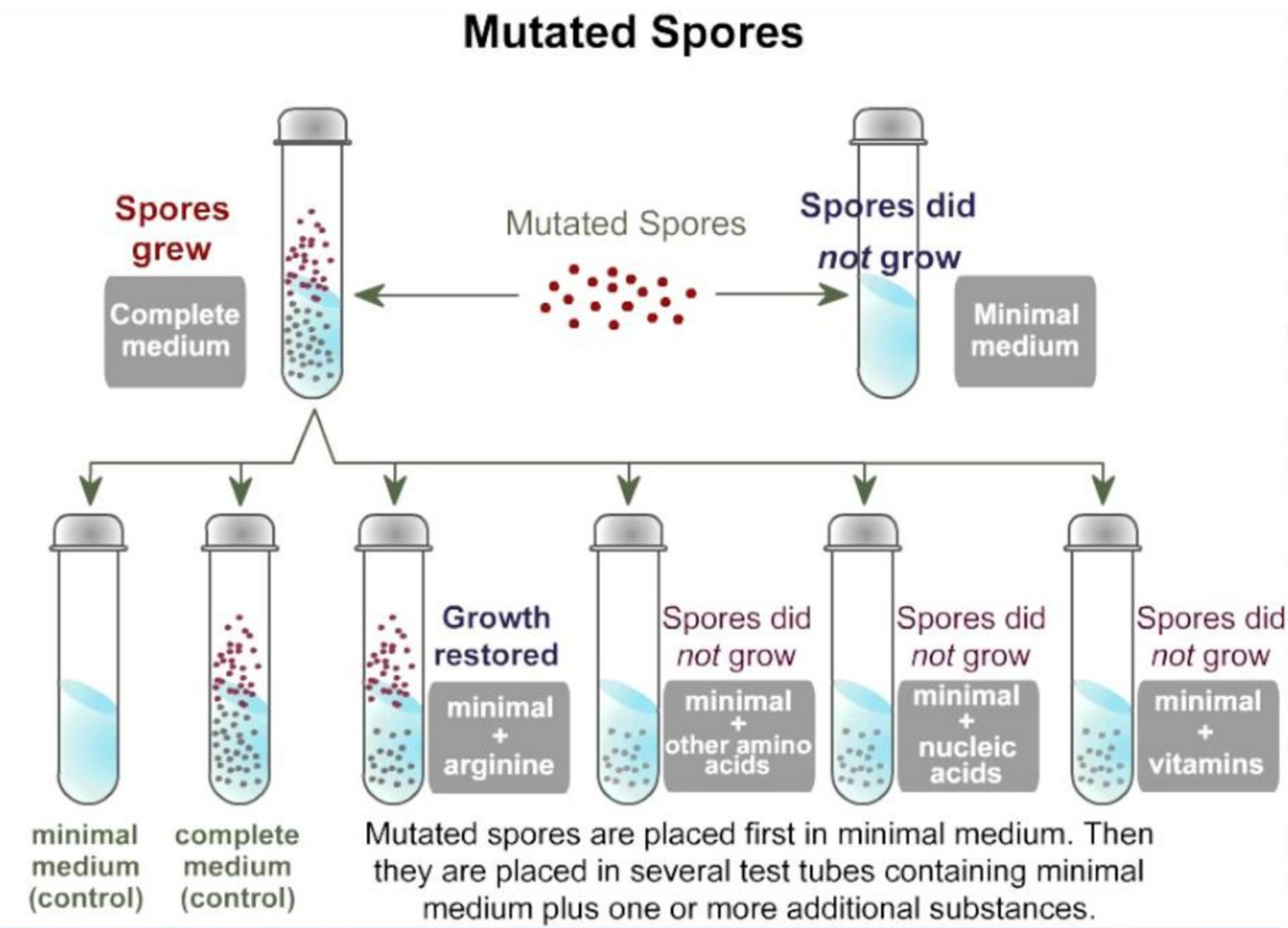

now found that the mutated strains of fungus were unable to grow in the minimal medium. Although they had access to the same basic raw materials used by the wild type, the irradiated fungi were apparently no longer able to produce some of the substances they needed to survive.

Beadle and Tatum then added different substances to different samples of the irradiated spores in minimal medium. In most cases, the mutated fungi still could not grow, but in some cases they could. In this way the

2) The mutated *Neurospora* spores are dissected out of the perithecium and grown separately

3) The *Neurospora* strain with a mutation in nutrient production grows on complete medium but dies on minimal medium

4) The mutant *Neurospora* can grow on minimal media if a vitamin mixture is added but not when amino acids are added

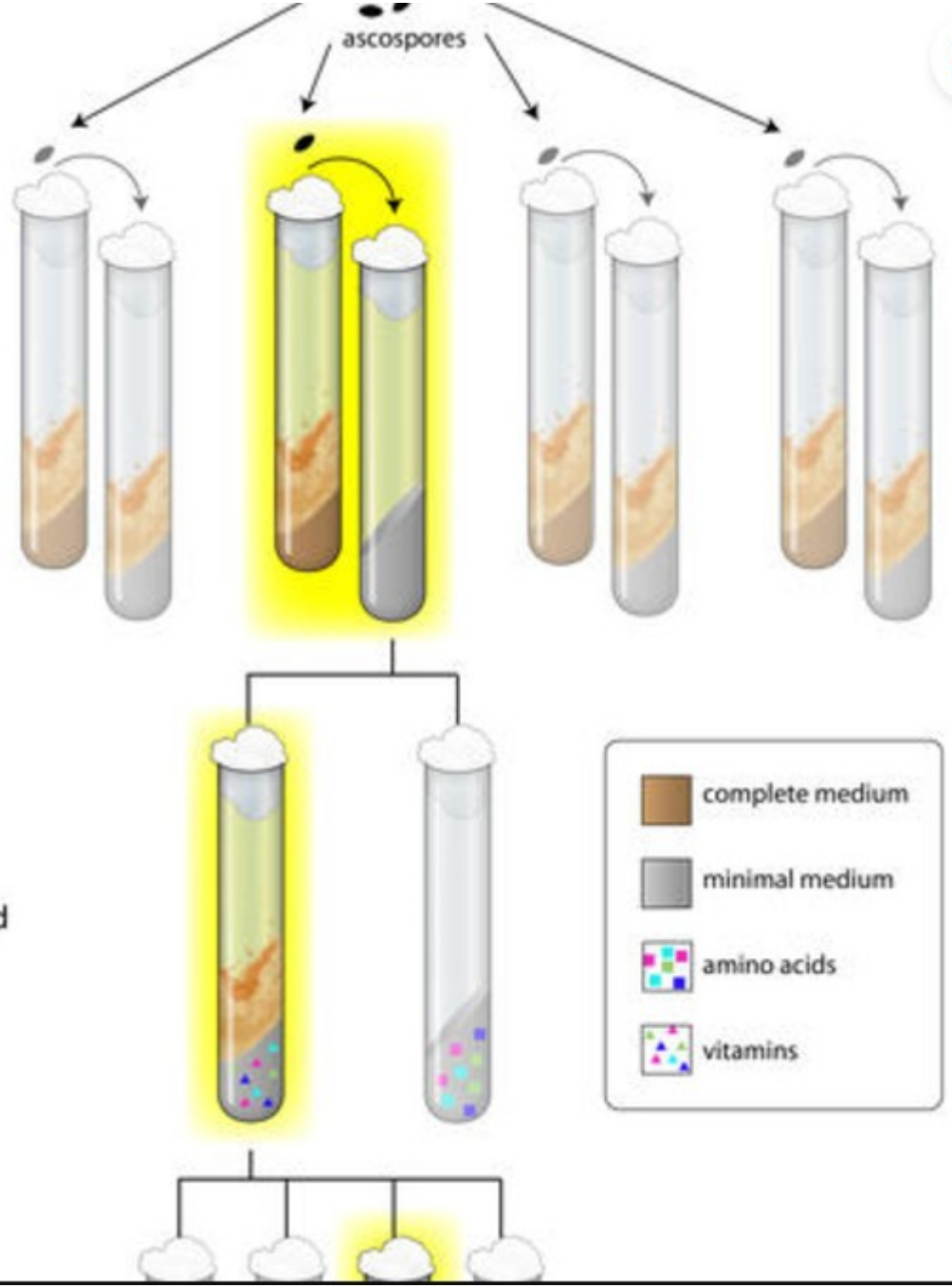

Beadle & Tatum's *Neurospora* experiment

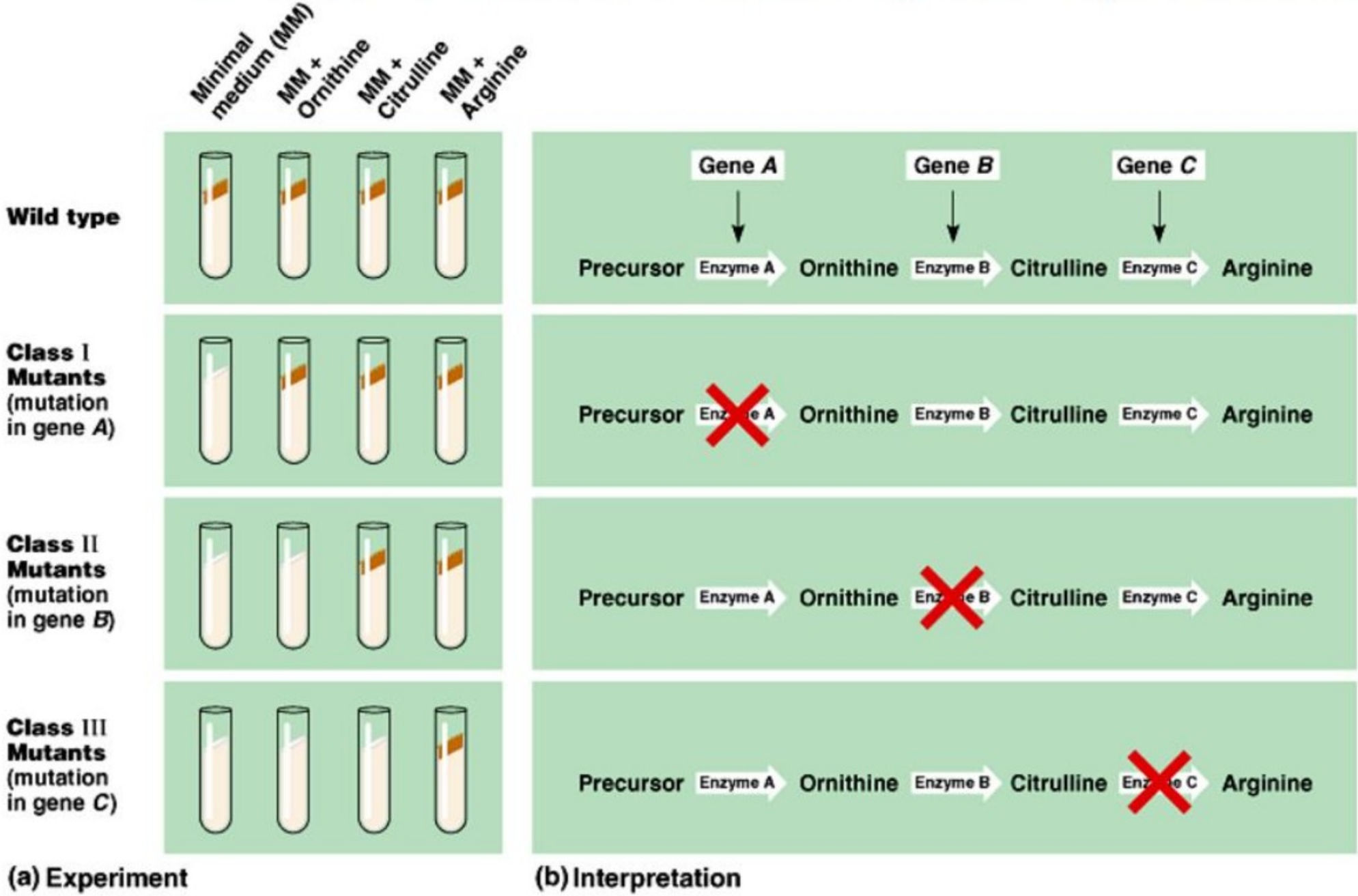

Pioneers of yeast genetics

- **Øjvind Winge** (1886-1964), Carlsberg laboratory, Kopenhagen: http://www.genetics.org/cgi/content/full/158/1/1

  Discovery of alternation of Haplo – and Diplophase in *Saccharomyces sp.* –"Yeast Sex"; development of mechanical yeast manipulation and dissection methods

- **Carl C. Lindegren** (1896-1987), Washington University, St. Louis; University of Southern Illinois, Carbondale, USA
  Isolation of heterothallic yeast strains (= mutant strains with a stable haploid growth phase)

- **Boris Ephrussi** (1901-1979), Institutes Pasteur, Paris; Centre national de la recherche scientifique, Gif-sur-Yvette, France

  Cytoplasmic inheritance (= mitochondrial genetics)

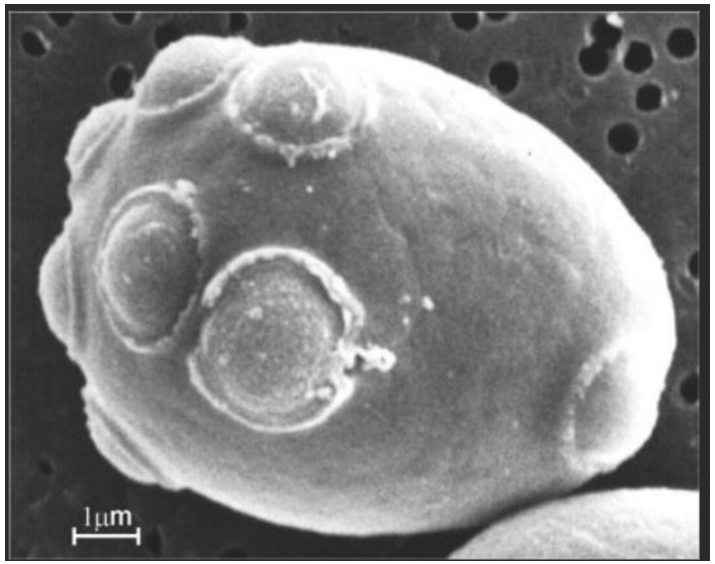

haploid
a cell
mitosis
a cell
a cell
haploid
schmoo
haploid
α cell
schmoo
mating
a/α cell
mitosis
a/α cell
a/α cell
diploid
diploid
meoisis/sporulation
a cell
a cell
α cell
α cell
germination
four haploid spores

Original mother cell is mating type α

Budding produces a daughter cell
and mother and daughter bud again

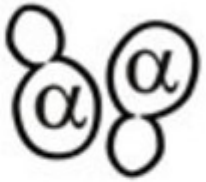

Mother switches to mating type a, but the first
daughter cannot switch until it has budded

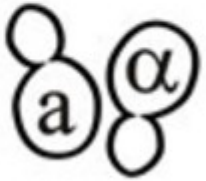

As a result of the switch, mother and second
daughter are both mating type a, first daughter
and its bud are both mating type α

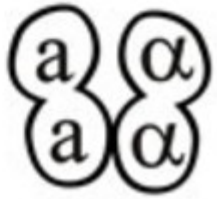

compatible cells mate to form zygotes

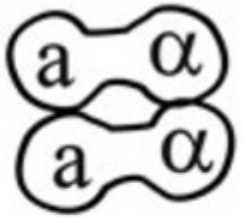

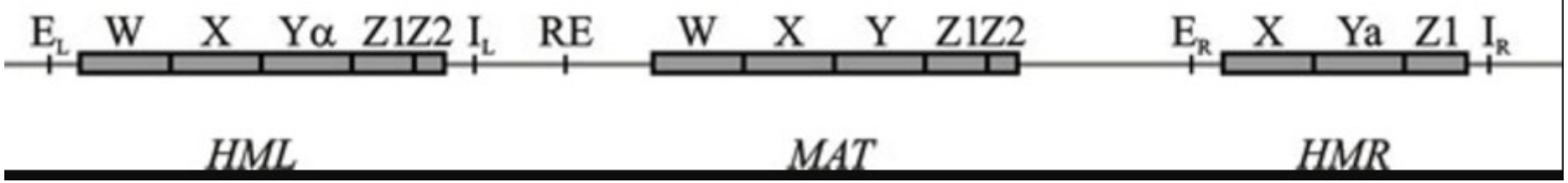

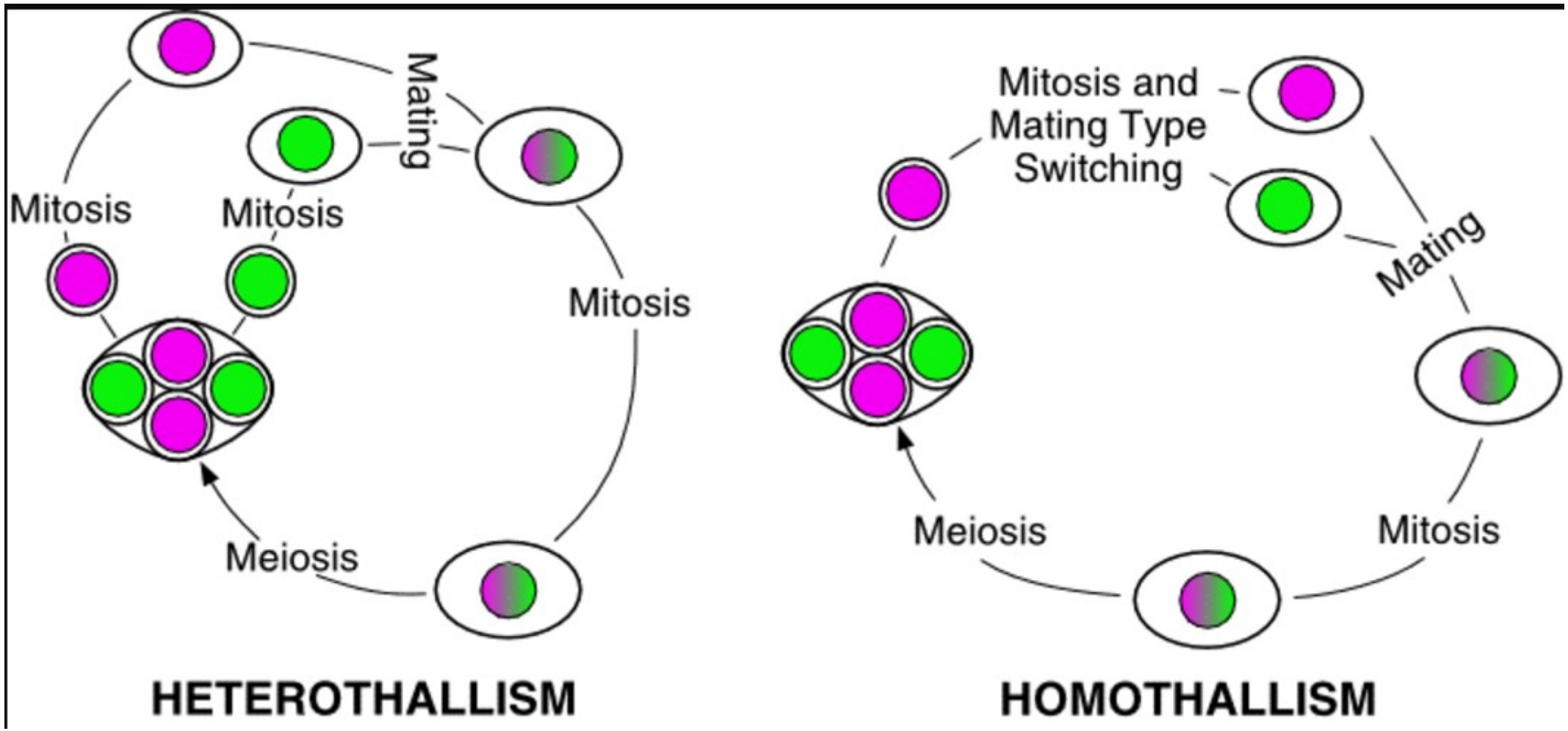
Mating
Mitosis
Mitosis
Mitosis
Meiosis
HETEROTHALLISM
Mitosis and
Mating Type
Switching
Mating
Meiosis
Mitosis
HOMOTHALLISM

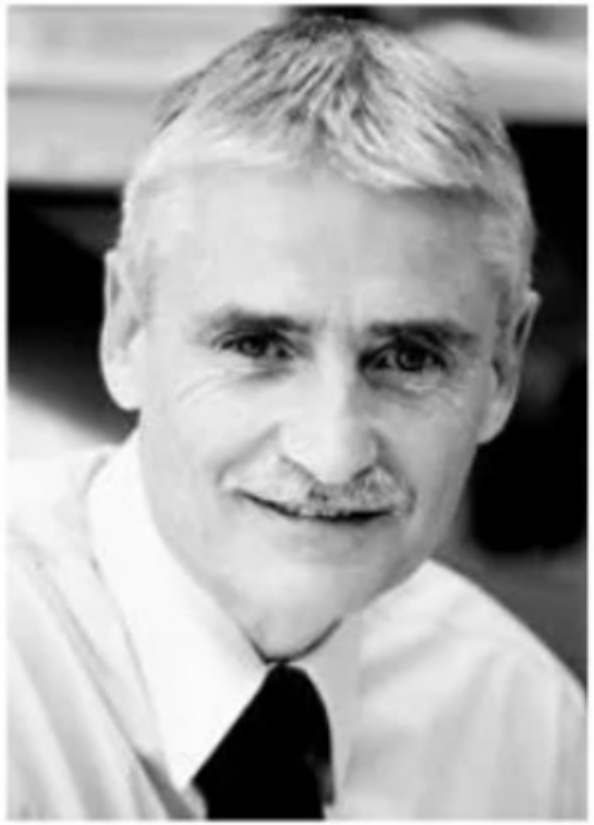

Leland H. Hartwell Tim Hunt Sir Paul M. Nurse

The Nobel Prize in Physiology or Medicine 2001 was awarded jointly to Leland H. Hartwell, Tim Hunt and Sir Paul M. Nurse "for their discoveries of key regulators of the cell cycle".

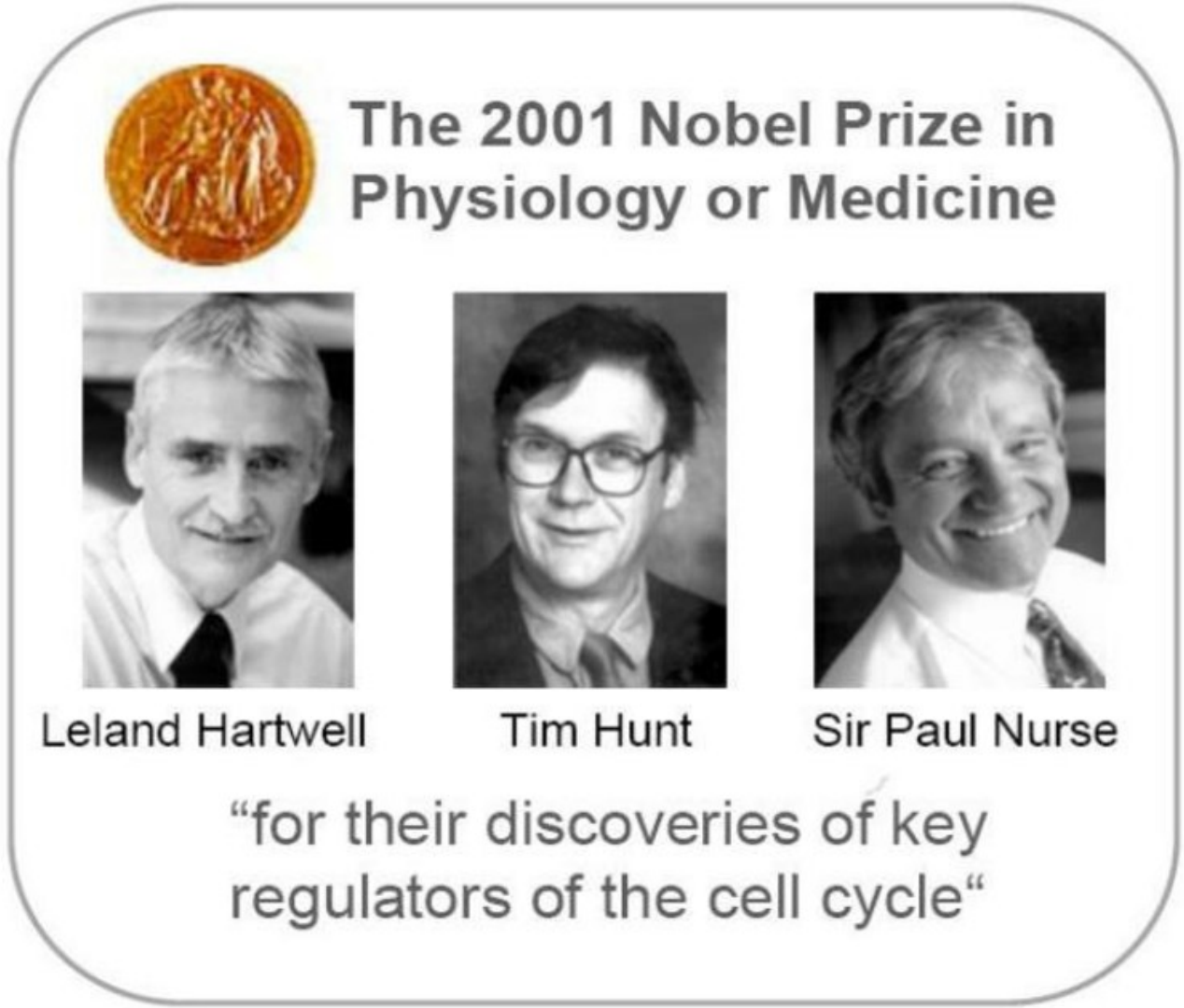

The 2001 Nobel Prize in Physiology or Medicine was awarded to Lee Hartwell, Paul Nurse, and Tim Hunt for their ground-breaking work on cell cycle regulation. Starting in the late 60s, Hartwell used budding yeast to identify mutants that blocked specific stages of cell cycle progression. Nurse, working in fission yeast in the 70s, went on to isolate mutants that could also speed up the cell cycle, thus focussing his attention on the original CDK kinase, cdc2. In the 80s, Hunt identified proteins in sea urchin extracts, the levels of which varied through the cell cycle hence "cyclins". All three have continued to make important advances in cell cycle research including the identification of checkpoints, mechanisms coupling cell morphology to the cell cycle, and identification of additional classes of kinases, cyclins, and inhibitors.

Isolation of temperature sensitive mutants

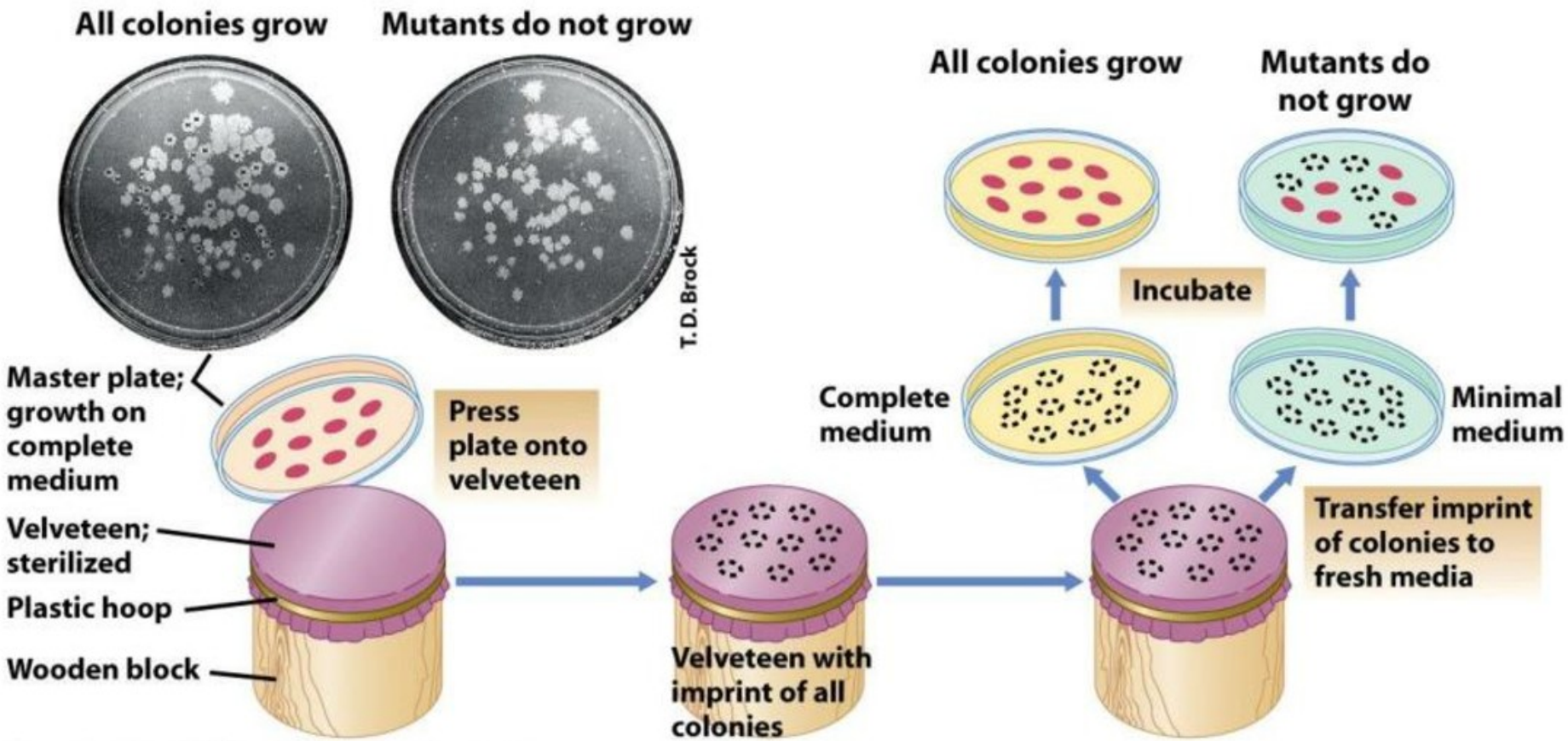

Figure 10-2 Brock Biology of Microorganisms 11/e

1500 ts mutants

146 Cdc- phenotype

32 *cdc* complementation groups

A classical model of inducible gene expression in a eukaryote.

- ***GAL1*** galactokinase (mutant allele is *gal1*)
- ***GAL2*** galactose permease
- ***GAL7*** galactose uridyl transferase
- ***GAL10*** galactose-glucose epimerase

- ***GAL4*** positive regulator (mutant is *gal4*)
- ***GAL80*** negative regulator (mutant is *gal80*)

Yeast *GAL* genes are positively regulated at the level of transcription activation.

- A *gal4*, *gal80* double mutant fails to induce expression of galactose enzymes. (gal4 mutation is epistatic to gal80)

- Interpretation is that GAL4 targets the structural genes to activate transcription.

- GAL80 interacts with GAL4 to control its activity.

Mechanism of transcription activation of the yeast *GAL* genes.

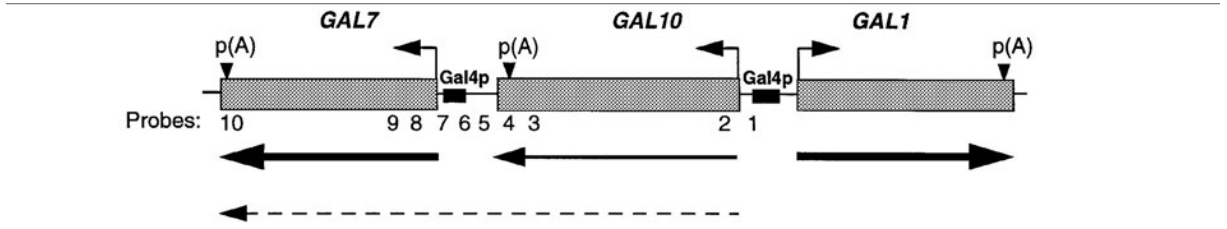

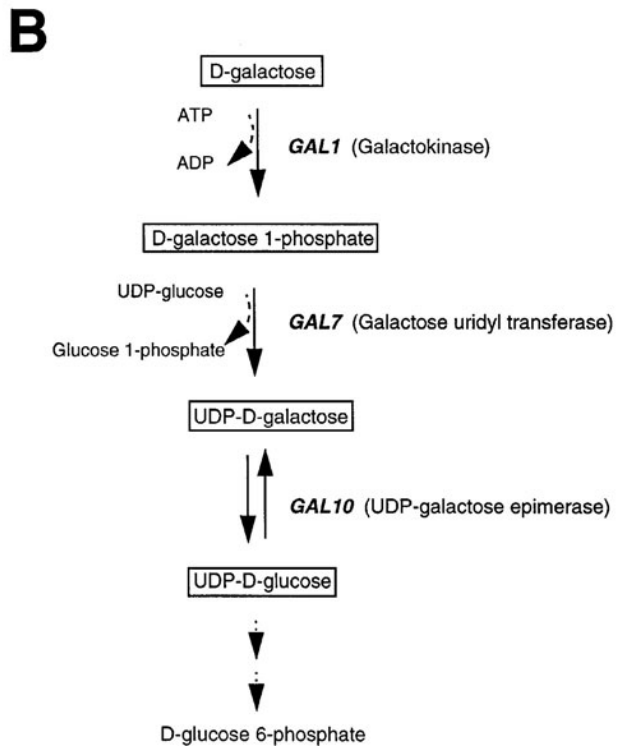

GAL1-lacZ and GAL10-lacZ fusions used for deletion analysis.

lacZ (β-galactosidase)) plate tests and liquid culture assays for beta-gal activity units.

X-gal identifies cells with beta-galactosidase

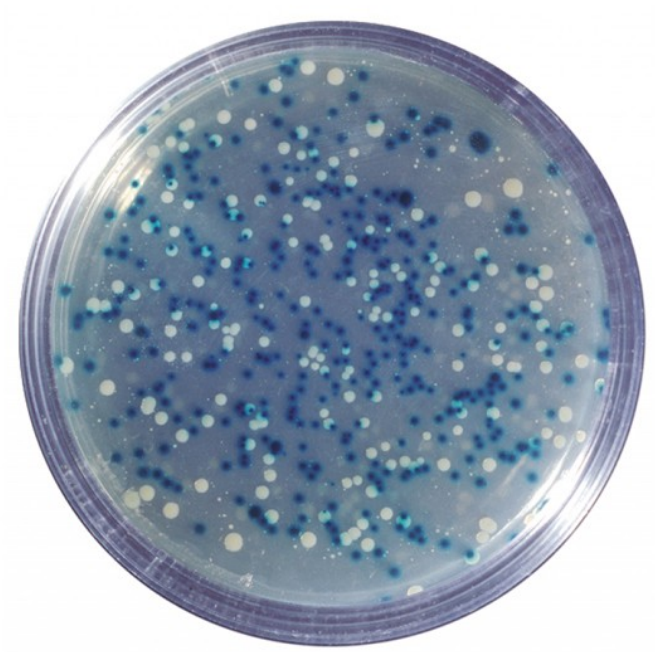

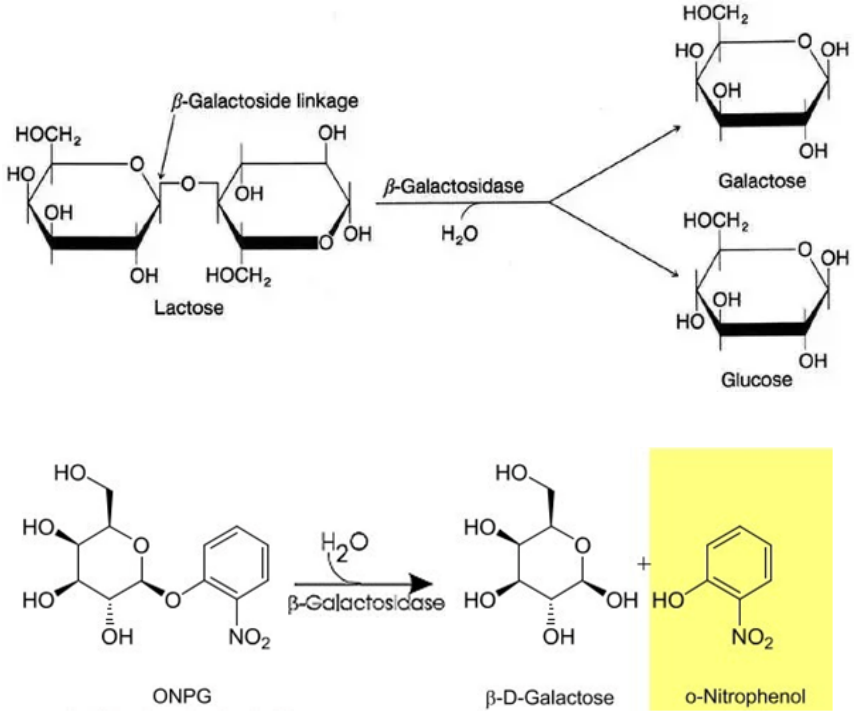

ONPG hydrolysis by cells gives a soluble blue product for spectrophotometric measurement of *lacZ* (β-galactosidase) activity units

Deletion analysis of yeast *GAL1* upstream region defined an Upstream Activating Site (UAS_G).

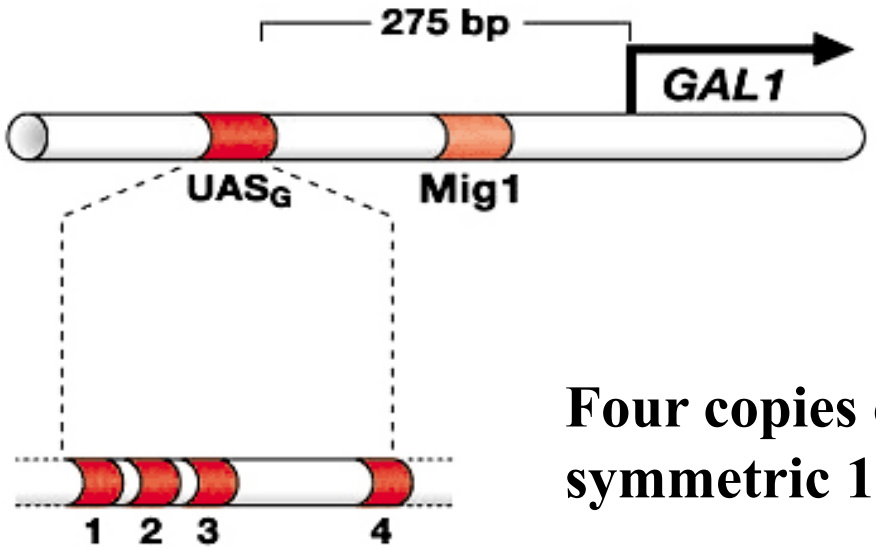

Four copies of a nearly symmetric 17 bp GAL4 site.

GAL1-lacZ and GAL10-lacZ fusions used for deletion analysis.

UAS_G had many properties of the Enhancer defined in SV40.